EFFECTS OF IRON ON BONE MICRO-ARCHITECTURE AND STRENGTH IN FEMALE RATS DURING RAPID GROWTH AND FOLLOWING OVARIECTOMY

By

KAVITHA SANKAVARAM

Bachelor of Science
Acharya N.G. Ranga Agriculture University
Bapatla, Andhra Pradesh
1998

Master of Science
Sri Venkateswara University
Tirupathi, India
2001

Submitted to the Faculty of the
Graduate College of the
Oklahoma State University
in partial fulfillment of
the requirements for
the Degree of
MASTER OF SCIENCE
December, 2005

EFFECTS OF IRON ON BONE MICRO-ARCHITECTURE

AND STRENGTH IN FEMALE RATS DURING

RAPID GROWTH AND FOLLOWING

OVARIECTOMY

Thesis Approved:

Andrea B. Arquitt

Thesis Adviser

Bahram H. Arjmandi

Brenda J. Smith

A. Gordon Emslie

Dean of the Graduate College

ACKNOWLEDGEMENTS

This thesis would not have seen the light of the day if not for the guidance of Dr. Andrea Arquitt. I would like to express my gratitude to Dr. Arquitt for her guidance, whose inspiration and her ceaseless enthusiasm, moral support throughout my masters program, has meant a great deal to me. This research work under her guidance added to my profound interest in pursuing further education in trace minerals. I would like to extend my heart felt thanks to her for sharing her knowledge and understanding in this field. I take this opportunity to sincerely appreciate for her guidance, patience and support during difficult times.

My appreciation also extends to my committee members Dr. Brenda Smith and Dr. Bahram Arjmandi for their suggestions and guidance in completing this thesis. Their thoughtful comments and questions were greatly valued. I also wish to thank Dr. Barbara Stoecker for her time and expertise. I'm thankful to Dr. Doyu Soung for teaching me molecular work. I greatly appreciate the support of my colleagues Ms Shirin and Ms Kiranmayi.

Nothing would have been possible without the constant encouragement and moral support of my husband Mr. Ravichandran in stressful situations. In spite of his work, he ensured that I concentrate on my work and achieve my targets in a timely fashion. I thank him for his love and care.

I extend special thanks to my parents Mr. Shankar and Mrs. Krishnaveni who always taught me to set goals and never stop until I reach them. They have provided me love, constant encouragement and support, without which I am not here today.

No words can explain the appreciation I have for the support of my in laws, Mr. Raja and Mrs. Usha for their consistent support to pursue higher education. I also like to express my thanks to my family members Venu, Chaitu, Sravanth and Vijay if not for this project but for my career development.

TABLE OF CONTENTS

LIST OF TABLES

Table Page

CHAPTER III

CHAPTER IV

CHAPTER V

LIST OF FIGURES

Figure Page

CHAPTER III

NOMENCLATURE

The following terms are used frequently in the text:

1. Bone Remodeling/Bone Turnover - The continuous process in bone that includes bone formation and resorption at the same site.
2. Connectivity Density – numerically indicates the average no of connections present between trabeculae in a specified volume.
3. Cortical Area – numerically explains the amount of cortical bone per square millimeter.
4. Cortical Bone - the compact bone, protective in function that forms the outer layer of the bone as a shell. It is a smooth bone that we can see on the surface of the bone and comprises of 80% of total bone mass.
5. Cortical Bone Thickness – numerically explains the thickness of cortical (the outer layer of) bone.
6. Cortical Porosity - describes the porous or empty spaces in the bone.
7. Degree of Anisotropy - Anisotropy numerically explains the degree of directional organization of bone internal structure when a load is applied in a particular position. A higher DA indicates increasing disorganization when viewed from a given plane.
8. Fatigue – "The failure of a material caused by loading" (1). Fatigue occurs as a result of the degradation of bone strength and a decrease in modulus of elasticity (2-4).

9. Medullary Area – numerically describes the central volume of the bone per square millimeter.
10. Modulus of Elasticity - describes the stiffness and hardness of bone (2). The elastic modulus is the ratio of stress and strain that explains the degree of deformation following loading by providing a value for stiffness. Therefore, bone or any material having higher stiffness subsequently has higher elasticity (1).
11. Osteoblast - a mononucleate cell arising from osteoprogenitor cells (mesenchymal cells), which as it matures, is associated with bone formation.
12. Osteoclast - a large multinuclear cell associated with the resorption of bone.
14. Physiological Force - it is the 30% of total force required to crush the bone at a physiological state by a reasonable force.
15. Stiffness of bone is defined as its rigidity (5).
16. Strain – it is the "fractional or percentage change in length." Strain is calculated as "the amount of deformation divided by the original length of the specimen." Increasing the stress causes bone to break. Before failure or breaking the specimen deforms which is known as strain (4).
17. Stress - defined as the "load per unit area (4)." When an external load is applied, force is developed within the structure. This results in stress, which can be either tensile or compressive stress and usually depends on the way of load application. Normal stress may also occur, which changes the length in a structure. It can also be shear stress that changes the angle in a structure (1).
18. Structural Model Index – numerically describes a bones relative rod like property. A value of zero corresponds to pure plates and a value of three corresponds to

perfect rods. Negative values indicate concave like structure and a value of four indicates sphere. Plate-like properties are considered desirable and rod-like properties are mostly seen in ovariectomized models as cross struts are removed and trabeculae are eroded (6-10).

19. Total Force - describes the force required to crush bone completely (11).
20. Trabeculae - thin strand like structures in cancellous bone.
21. Trabecular (Cancellous) Bone- the lattice like bone, rigid structure but appears spongy. Trabecular bone helps in withstanding dominating loads and strains. Possess honey comb-like structure with spaces in the bone.
22. Trabecular Number – numerically describes the average number of trabeculae present per mm.
23. Trabecular Separation – numerically describes the average separation or air space between trabeculae. Greater trabecular number (Tb. N) would result in less trabecular separation.
24. Trabecular Thickness – numerically describes the average thickness of the trabeculae in a specified region
25. Von Mises Stresses - used as an indicator of the amount of stress within a bone when force is applied (11).

LIST OF ABBREVIATIONS

2D……Two-Dimensional

3D……Three Dimensional

ALP……Alkaline Phosphatase

ALT……Alanine Aminotransferase

AST……Aspartate Aminotransferase

BMC……Bone Mineral Content

BMD……Bone Mineral Density

BS/TV……Bone Surface/Bone Volume

BV……Bone Volume

BV/TV……Bone Volume/TotalVolume

Co. Area……Cortical Area

Co. P……..Cortical Porosity

Co. Th……...Cortical Thickness

CT……Computed Tomography

Conn. D……Connectivity Density

DA……Degree of Anisotropy

DXA……...Dual Energy X-Ray Absorptiometry

FEA……Finite Element Analyses

FEM……..Finite Element Modeling

GHD……...Growth Hormone Deficiency

HB……..Hemoglobin

HCT……Hematocrit

HRT……Hormone Replacement Therapy

IL-1..……...Interleukin-1

IL-6…..…..……..Interleukin-6

LBM……...Lean Body Mass

L_5……Fifth Lumbar Vertebra

M. Area...……..Medullary Area

Micro-CT/μCT……...Micro-Computerized Tomography

Micro FE (μFE)……..Micro- Structural Finite Element

MIL…….Mean Intercept Length

PBM……Peak Bone Mass

Phy_fce……...Physiological Force

PTH…….Parathyroid Hormone

RBC……Red Blood Cell Count

RTC……Reticulocytes

SMI…….Structural Model Index

Tb.N……..Trabecular Number

Tb.Sp……..Trabecular Separation

Tb.Th……..Trabecular Thickness

TNF-α…….Tumor Necrosis Factor-α

TRAP……Tartrate Resistant Acid Phosphatase

OC……Osteocalcin

OVX……..….Ovariectomized

WBC…….White Blood Cell Count

CHAPTER I

RESEARCH PROBLEM

Introduction

Bone, a highly mineralized tissue, is organized into a skeleton and provides mechanical support to the body (12). It constantly maintains a balance between bone formation and bone resorption, which is called bone remodeling. Osteoblasts are the cells involved in bone formation and osteoclasts in bone resorption (12). The volume of bone matrix, the bone micro-architecture, and the degree of bone tissue mineralization determine the strength of the bone (13, 14). In the process of mineralization, minerals are deposited on the calcification front, which is then followed by secondary mineralization that occurs by a slow and progressive increase in mineral deposition (13).

Bone formation is regulated both by local and endocrine factors. Metabolic disturbance in the formation process can result in either excess formation, osteopetrosis, or excess resorption and bone loss, osteoporosis (12). A negative balance between bone resorption and bone formation is observed in osteoporosis as a result of loss of bone mass and micro-architectural deterioration of the trabecular network (13). Studies have also suggested that bone mass is affected by dietary factors and that minerals in addition to calcium may be involved (15). Once the peak bone mass is achieved, a steady loss of bone mass occurs, together with progressive architectural alterations. This process continues throughout life

However, accelerated loss of bone mass occurs in the early postmenopausal period and a slower rate of bone loss in the later years with age (16, 17). Previously, there has been little research investigating the association between bone metabolism and long-term consumption of varying levels of dietary iron. Hence, this study investigates the long-term consumption of varying levels of dietary iron and their effects on bone structure and strength.

Significance of the problem

Approximately one-half of women and one-fourth of men over age 50 are affected by osteoporosis (18). Hence, the diagnosis, treatment, and monitoring of osteoporosis and other skeletal diseases have become prominent health care and research issues (18). Studies have suggested that bone mass is affected by dietary factors and that minerals in addition to calcium may be factors (15, 19). Iron intakes leading to iron deficiency or iron excess and osteoporosis are two major health problems faced by the world today (20, 21). Iron deficiency is a worldwide health problem, and iron excess is increasingly possible with the availability of nutrient supplements as well as with national food fortification policies (15, 19). Very few investigations regarding the association between bone micro-architecture and iron intakes have been done. Hence, it is necessary to take a comprehensive approach to examine the effects of both iron deficiency and iron excess on bone structure and strength.

Study purpose and objectives

The purpose of this study was to examine whether dietary iron affects bone structure and strength during growth and following ovariectomy. The following objectives were developed for this study.

1. To determine the effects of inadequate, adequate, and excessive amounts of iron on bone architecture in three groups of rats: growing, sham-operated or ovariectomized.
2. To determine the effects of inadequate, adequate, and excessive amounts of iron on bone mechanical properties in three groups of rats: growing, sham-operated or ovariectomized.

Study Design

A randomized block design was used in this study. One hundred and twenty-four weanling female Sprague-Dawley rats were randomized into three treatment groups (growing, sham-operated and ovariectomized) and four dietary regimens (6, 12, 35 or 150 ppm iron). After three weeks of acclimatization the rats were fed for 15 (growing) or 27 (sham and ovariectomized) weeks. Growing rats (N=40) were killed at 18 weeks of age and bones were collected. At 18 weeks of age the remaining rats were either ovariectomized to mimic menopause or sham-operated as controls. At 30 weeks these animals were killed and bones were collected. Cleaned fifth lumbar vertebrae (L_5) and right femur stored in -20^{o} C were scanned for micro-architecture (Micro-CT 40, SCANCO MEDICAL AG, Zurich, Switzerland) and strength analyses were performed.

Hypotheses

This study proceeds with the following hypotheses:

1. There will be no statistically significant differences in L_5 trabecular architecture.
    a. There will be no statistically significant effect of iron in growing rats.
    b. There will be no statistically significant effect of iron in sham-operated or ovariectomized rats.

c. There will be no statistically significant differences between sham-operated or ovariectomized rats.

d. There will be no statistically significant diet by treatment interactions in sham-operated or ovariectomized.

2. There will be no statistically significant differences in distal femur trabecular architecture.

   a. There will be no statistically significant effect of iron in growing rats.

   b. There will be no statistically significant effect of iron in sham-operated or ovariectomized rats.

   c. There will be no statistically significant differences between sham-operated or ovariectomized rats.

   d. There will be no statistically significant diet by treatment interactions in sham-operated or ovariectomized rats.

3. There will be no statistically significant differences in femur cortical bone architecture.

   a. There will be no statistically significant effect of iron in growing rats.

   b. There will be no statistically significant effect of iron in sham-operated or ovariectomized rats.

   c. There will be no statistically significant differences between sham-operated or ovariectomized rats.

   d. There will be no statistically significant diet by treatment interactions in sham-operated or ovariectomized rats.

4. There will be no statistically significant differences in L_5 strength.

a. There will be no statistically significant effect of iron in growing rats.
b. There will be no statistically significant effect of iron in sham-operated or ovariectomized rats.
c. There will be no statistically significant differences between sham-operated or ovariectomized rats.
d. There will be no statistically significant diet by treatment interactions in sham-operated or ovariectomized rats.

5. There will be no statistically significant differences in distal femur strength.
    a. There will be no statistically significant effect of iron in growing rats.
    b. There will be no statistically significant effect of iron in sham-operated or ovariectomized rats.
    c. There will be no statistically significant differences between sham-operated or ovariectomized rats.
    d. There will be no statistically significant diet by treatment interactions in sham-operated or ovariectomized rats.

Assumption

It is assumed that long-term storage of bones does not affect the architectural or mechanical properties

Limitation

Rats have minimal Haversian systems in cortical bone. Therefore, the pattern of bone remodeling in rats and humans is different. Although, the ovariectomized rat model is considered acceptable for studies on menopause, the findings of this study are limited to rats due to differences in the bone metabolism between two species

CHAPTER II

REVIEW OF THE LITERATURE

Bone metabolism is affected by multiple factors, including mechanical strain or load bearing, (22) hormonal status (16), nutrition (15), growth factors and disease. In addition, these factors often affect bone in combination. The following sections review literature focusing on some of the factors that affect bone metabolism. Measurements of bone parameters and the appropriateness of using a rat model are also included.

Functions of Bone

Connective tissue is highly specialized. Bone, a connective tissue, provides mechanical support for movement, a "protective cage" for cranial, thoracic and abdominal organs, and is a reservoir for nutrients involved in various metabolic processes. Bone is composed of cells, extracellular matrix, and inorganic minerals. The extracellular matrix contains approximately 85% calcium phosphate and 10% calcium carbonate and provides bone with its structural rigidity (23).

Physiology of Bone Formation and Remodeling

Bone Formation

The skeleton is made up of two tissues (cartilage and bone). Bone, exclusive of marrow, has three types of cells (chondrocytes, osteoblasts, and osteoclasts) (24). Bone exists in two basic types (cortical and cancellous) in the human skeleton,

each having a different role and function. Cortical bone comprises 80% of the skeleton and is well suited for mechanical, structural, and protective functions. Cortical bone is the major component of long bones and comprises the outside protective surfaces of all bones. It is 80-90% calcified and, therefore, dense. Cancellous bone comprises the remaining 20% of skeleton and has high metabolic activity compared to cortical bone. It is less dense being only 5-25% calcified. Cancellous bone consists of trabeculae, the lace-like connective tissue that increases the surface area of bone. Because, bone metabolism occurs at surface sites only, this structure confers high metabolic activity to trabecular bone (18). Bones form through two distinct processes. Endochondreal ossification, a process involving a cartilage intermediate, forms most of the skeleton. Intra-membranous ossification is another process of bone formation in which a small number of skeletal elements such as craniofacial bones are formed (25).

The development of bone begins before birth and formation predominates until approximately the end of the second decade of life (26, 27). Bone is a composite material composed of an organic and inorganic phase. The organic phase is synthesized by osteoblasts, and the inorganic phase is composed of calcium phosphate (28). Osteoblasts, cells present in membranous skeletal elements (25), deposit mineral salts from plasma onto a collagen matrix during this period. Thus, mineral salts are deposited onto a collagen matrix by osteoblasts and increase the bone mass. Osteoclasts are the cells responsible for bone resorption and are the only cell type able to digest the mineralized matrix. The osteoclasts play a crucial role in bone physiology. They foster bone modeling during growth and bone remodeling during adulthood. Thus, defects in osteoclast differentiation or function are associated with multiple genetically inherited or acquired

diseases, all characterized by an arrest of bone resorption (29). Chondrocytes, the cells in endochondreal skeleton, deposit an extra-cellular matrix that is cartilage specific and help in the repair of degraded collagen matrix (25).

Bone Remodeling

One of the most important physiological functions of the skeleton during adulthood is bone remodeling (30). Bone remodeling is the process by which bone mass is maintained at a virtually constant value between the end of skeletal growth and gonadal failure (31). It involves the removal and internal restructuring of previously existing bone and is responsible for the maintenance of tissue mass and architecture in the adult skeleton (32). In young adulthood, bone accumulation is replaced by bone remodeling in which osteoclastic cells resorb and osteoblastic cells secrete bone minerals in response to physiological triggers. In older adulthood, bone remodeling balance changes, and bone resorption exceeds bone formation due to decreased osteoblastic activity resulting in a net loss of bone mass (33). Women experience additional bone loss after menopause as osteoclastic activity increases in response to the decreased production of the bone protective female hormone, estrogen (34).

Findings of van der Linden et al. (24) also suggest that bone remodeling takes place at the surface of trabeculae and results in non-uniform mineral distribution. This will affect the mechanical properties of cancellous bone, because the properties of bone tissue depend on its mineral content (35).

Effects of Growth on Bone Development

The activity of bone formation predominates from infancy through late adolescence, resulting in a steady accumulation of bone mass (36). In the acquisition of

bone mass, puberty plays an important role. Indeed, between the onset of puberty and young adulthood skeletal mass approximately doubles (37, 38). A major determinant of peak bone mass (PBM) is the amount of bone mass accrued during puberty which in turn affects the relative risk of osteoporotic fractures occurring in later life. Therefore, the acquisition of an optimal PBM is a key factor for avoiding osteoporosis (37, 39).

The Saskatchewan Bone Mineral Accrual Study (BMAS) is a longitudinal study of bone growth in Caucasian children (40). In this study, Bailey (40) examined bone mineral accretion in growing children. Findings revealed that peak linear growth was attained at the age of 13.5 years in boys whereas girls attained at the age of 11.6 years. At these ages both boys and girls attained 90% of adult status in height, 70% in bone mineral content (BMC) at the femoral neck, and 60% for the total body and lumbar spine. The rate of bone mineral uptake peaked for males and females, one year after peak linear growth showing dissociation between linear growth and bone mineral accrual. The two-year period before and after peak linear growth is known as the growth spurt and is a critical time for bone mineral accretion. During this four-year period, over 35% of total body and spine bone mineral and over 27% of bone mineral at the femoral neck were deposited. The bone mineral content accumulation during this time is more than the amount most people will lose during adult life. The peak skeletal mass attained during this growth period accounts for 50% of the variability in bone mass in the elderly. Therefore, the growing years determine much of the fracture risk in the elderly (40).

Matkovic et al. (36) found results similar to the Saskatchewan Pediatric Bone Mineral Accrual Study when determining the timing of attainment of PBM. Even after the attainment of skeletal height at the age of 16 years, accumulation of bone minerals

continued to increase at several sites. Attainment of peak height by 16 years of age indicates decrease in longitudinal bone growth (36). The total skeleton mass accumulated between the ages of 11 and 15 years is 37% which is similar to the findings of Bailey's study where it is 35% (40). The average gain in height was 2.4% of the peak adult height for women per year, and the accumulation of total bone mineral was 6% per year, between the ages of 8 and 16 years. The BMC and BMD changed only slightly but insignificantly between the ages of 18 and 50 years. Peak bone mass of the proximal end of the femur appeared to be achieved at about 17 years of age. Findings also indicated that once PBM of the proximal end of the femur is achieved BMD begins declining but not significant (36).

In a study of Koletzko et al. (41) females at the age of 14 had values similar to their mothers' for bone size, mass and density. Longitudinal growth ceased while bone mass continued to increase. Most epiphyses closed by the age of 16. For both male and female, 95-99% of PBM was achieved by the age of 18 (41).

Matkovic et al. reported that the risk of developing osteoporosis was lower for those who had higher bone mass as young adults (36). Low bone mass is also considered a characteristic feature of adult growth hormone deficiency (GHD). Murray et al. examined the relationship between bone mineral density (BMD) and age in 125 severely GHD adults using dual-energy x-ray absorptiometry (DXA) (42). A significant positive correlation was observed between age and BMD (Z scores) at the lumbar spine, femoral neck, total hip, ultra distal (a site distal to the point at which the radius and ulna are 8 mm apart) and distal radius. Young adults were observed to have reduced bone mass, whereas the elderly GHD patients had normal Z scores. The cohort was divided into four age

ranges (<30, 30-45, 45-60, >60). BMD Z scores increased significantly at all five skeletal sites across the age groups from youngest to oldest (P<0.001). When BMD was assessed using absolute values (g/cm^2), BMD at the total hip, ultra distal and distal radius increased with increased age in their grouping of GHD adults (P=0.003, P=0.004, and P=0.002, respectively) in contrast to the decline in BMD observed with aging in the normal population. Also a trend towards an increase in lumbar spine and femoral neck BMD was observed. The authors concluded that, the effect of severe GHD on BMD is dependent on age (42).

Age-related changes on bone

The primary cause of osteoporotic fractures in the elderly is age-related bone loss (43, 44). Bone loss begins approximately at the age of 40 years and progresses linearly at a rate of 0.5 to 1% per year. As a result, by 70 years of age 40 % of bone loss is accrued. This type of bone loss results in increased porosity in cortical and trabecular bone, decrease in mineralization and finally increases the risk of fracture (43, 44). A correlation between decrease in cortical bone strength at the femur with age and an increase in porosity has been reported. Also these porosity changes have shown a strength variance of 76 % (45). In another study, Yeni et al. (46) reported that the toughness in fracture or stiffness of bone differed significantly with cortical porosity. Similarly, Burr et al. (47) suggested that the compact bone stiffness is dependent on its porosity and that the elastic modulus decreases with increases in porosity. Also, bones tend to become more rod-like than plate-like with aging (7, 8, 48).

Most of the studies on age-related bone loss have focused on postmenopausal women since women start losing bone earlier than men. However, changes in bone mass

with age are also observed in the male skeleton. Between the ages of 20-30 years (early adulthood), bone loss begins in women after the growth of long bones is stopped due to a negative balance in the remodeling process (49). Many studies have shown that the onset of menopause has been associated with an increase in turnover and an increase in bone loss. The rate of bone remodeling doubles at perimenopause and triples after menopause. This rate of bone remodeling remains high in osteoporosis (50). A steady increase in bone loss is observed during the perimenopausal period that is independent of chronologic age. As a result, the greatest bone loss occurs in the first five years after menopause (51).

At the onset of menopause estrogen production ceases resulting in increased bone turnover rate (52). Consequently, more resorption cavities on the endosteal surface of bone are produced with the increase in bone turnover. Deficiency of estrogen increases the life span of osteoclasts resulting in the resorption of bone being higher than formation. As a result net bone loss occurs since bone formation occurs at a slower rate than resorption. This increase in resorption leads to increases in the resorption cavities and deeper resorption lacunae causing a net loss of trabecular connectivity. Loss of trabeculae brings changes in the micro-architecture of bone ultimately leading to a decrease in overall strength of the bone (53). This negative balance in bone turnover, where more bone is resorbed than formed is linked to a higher rate of cancellous bone loss in women with osteoporosis (54). Eventually, rapid loss of bone after menopause results in the complete destruction of some structural trabecular elements. The remaining trabecular elements show a reduced thickness due to the continuous loss of trabecular bone leading to further trabecular architecture deterioration (54, 55).

Cortical thinning and an expansion of marrow cavity is another important contributing factor in human osteoporotic fractures at the femoral neck (44, 56). An increase in the cortical area at the femoral midshaft is observed until the seventh decade of life (44). This medullary area triples in females and doubles in males from 21 to 97 years of age. Besides, aging is also associated with marked intra-cortical porosity, which is present in some, but not all femurs (44). A recent study reported by Stein et al. (1999) showed that elderly patients did not have a greater number of pores than younger subjects in the cortical region but elderly subjects showed larger pores. However, this study did not assess the distribution of porosity throughout the cortical width and the porosity changes with age (57).

Age-related bone loss has also been documented in the rat. A significant decrease in osteoid mineralization was observed in male Wistar rats after marrow ablation in femur (58). A decrease in the response of bone cells with age is observed by bone morphometric and structural properties. It is also observed that these rats did not show a significant decrease in femur strength when compared to their peak values as the force required to fracture femurs at midshaft did not change with aging. Conversely, ultimate stress decreased 14% from 12 to 24 months. Ultimate stress is a parameter that normalizes for differences in bone geometry and size. Other biomechanical properties, modulus of elasticity, yield strain and ultimate deformation, were not significant. Although the tissue strength increased with age, the strength of the femur was maintained due to architectural compensations. Based on these findings the authors concluded that bone status was compromised in the aged male rat (59).

Effects of Ovarian Hormone Status on Bone Remodeling

Systemic hormones and local factors produced in bone regulate the activities of bone formation and bone resorption. Systemic hormones involved in stimulating bone formation include insulin, growth hormone (60) and estrogen (60) while hormones involved in bone resorption include parathyroid hormone (PTH) (61) and thyroid hormone (62). Estrogen plays an important role in the growth and maturation of bone as well as in the regulation of bone turnover in adult bone (63). Hence, it is very important to include the effects of estrogen, an ovarian hormone, on bone remodeling.

Estrogen Deficiency

Estrogen plays a very important role in the regulation of bone remodeling (34). Deficiency of estrogen increases bone resorption and reduces trabecular bone mass in humans (64). The increased osteoclastic activity found following estrogen deficiency leads to changes in the trabecular plates resulting in greater perforation of the plates and loss of trabecular continuity (65, 66).

Ovariectomy or estrogen deficiency causes a rapid decrease in the strength of the femoral neck in growing rats as well as in older subjects (67, 68). The most rapid changes due to estrogen deficiency are observed in trabecular bone, particularly in vertebrae (64). Estrogen deficiency leads to increased osteoclastic activity and causes rapid loss of bone mass (63). However, it is not only the general loss of bone but also, even more importantly, the changes in the internal architecture of bone which leads to increased fragility (63, 64). Studies have also suggested that estrogen deficiency increases pro-inflammatory cytokine production IL-1, IL-6 and TNF-α (69, 70). These cytokines may in turn lower the albumin levels thus, affecting the metabolism (71-74).

Deficiency of estrogen has a deleterious effect on trabecular micro-architecture of bone. Ikeda et al. (64) investigated the effect of trabecular bone contour on ultimate strength of lumbar vertebrae after bilateral ovariectomy in female Sprague-Dawley rats (n=190). The rats were divided into 19 groups. Ten rats were killed at day 0, half of the remaining rats underwent bilateral ovariectomy (OVX) and others were subjected to sham surgery. Ten rats from each group were killed at 3, 7, 11, 14, 28, 42, 56, 70, and 84 days post-surgery. Fifth lumbar vertebrae were scanned and analyzed by micro-CT (micro computed tomography) and DXA. Findings reveal that bone mineral content (BMC) and bone mineral density (BMD) of the fifth lumbar body, as indicated by DXA diminished from days 42 (BMC) and 84 (BMD), compared with sham group. Trabecular bone volume fraction (BV/TV), also diminished from day 28 in OVX when compared with both base line control and sham. The authors concluded that changes in trabecular bone contour with increased bone turnover are critical for reducing lumbar bone strength during the early post-ovariectomy period in rats (64).

Dick et al. (75) also reported that deficiency of estrogen affects bone. In this study, 34 Sprague-Dawley rats were randomized into sham or OVX treatment at six months of age. Bone mineral density and bone mineral content, measured by DXA decreased in both ovariectomized and sham-operated animals but significant decreases were observed only in the ovariectomized group of rats (75). Several studies have established that estrogen deficiency is detrimental to bone architecture (76-79).

Osteoporosis

Osteoporosis is characterized by low bone mass and increased fragility of the bones and is often associated with aging. This can lead to increased susceptibility to

fractures from minor trauma (80). Bone mineral density (BMD) is commonly used as an indicator to assess the risk of osteoporosis. The most commonly used tool for the measurement of bone mineral density (BMD) is dual energy X-ray absorptiometry (DXA) at the spine, wrist or proximal femur (81). According to the World Health Organization osteoporosis is defined as, a BMD value (T-score) $\geq$ 2.5 SD below the mean of a young adult (82). In the diagnosis of osteoporosis BMD was used as a preferred substitute marker primarily for 2 reasons: it facilitates in situ measurement, and it provides information on fracture risk, as increased risk of fracture is associated with decrease in BMD. However, fractures do occur in women who have normal BMD (83).

Besides BMD there are several other factors like age, female sex, high bone turnover, low body weight, and life style factors, including risk of falls, smoking and excessive alcohol consumption that can increase the risk of fracture. Also independent risk factors such as medical history of fracture, family history of osteoporosis, and the use of medications such as corticosteroids can also increase the risk of fracture (84).

Studying the factors that affect bone strength and bone quality may provide an insight into the causes of fractures (85, 86). In general, fractures occur when the load on a bone exceeds the ability of the bone to carry that load (87, 88). But this factor cannot be considered alone for fracture risks because bone is a composite material with a number of mechanical properties. Therefore, no single property can adequately describe the strength of the bone. The load carrying capacity of the bone can be better understood by four mechanical terms: ultimate force, resilience, stiffness and toughness (5, 89). The use of finite element modeling in computed tomography helps in estimating the physiological force of the bone i.e., the energy required to break the bone based on computer

reconstructions (90). The strength of the bone is a combination of two main features: bone density and bone quality (91). Therefore, it is important to measure both bone density and bone quality to assess bone strength. DXA provides information on bone mass over a projected area, but it cannot provide information about bone strength. Therefore, computed tomography is used to help explain the components of bone quality in terms of bone architecture (86, 92).

Focusing on the material properties of bone is, therefore, important to understand bone quality and strength of the bone including the structural and material properties. Therefore, understanding the constituents of bone quality and how they can be measured may help identify the predictors of fracture risk. Also this would help to improve the diagnosis, management, treatment, and patient monitoring in osteoporosis (82).

Bone quality and micro-architecture

Bone mass measured by bone mineral density is used as a predictor for assessing the risk of fracture. But significant differences in the bone density of normal individuals and the patients who sustain fractures have been reported in recent clinical studies. Also it is observed that the contribution of bone mass to fracture risk is two fold out of the 13-fold increase in the risk of hip fracture. Because questions still exist in considering BMD as a reliable indicator for fracture prediction, "bone tissue quality" emerged as a new strategy for identifying the risk of fracture (93).

The term bone quality describes a set of characteristics that influence bone strength. These characteristics include structural and material properties that are used as a means to describe the overall quality of bone. Structural and material properties are affected by bone remodeling and modeling which are together referred as bone turnover

(89). The structural properties of bone are best described by the geometry and micro-architecture of bone. Geometry of the bone is understood by the size and shape of the bone and micro-architecture is understood by the trabecular architecture and cortical thickness/porosity of the bone. Similarly, the material properties of the bone can be determined by mineral crystallinity, collagen structure and micro damage in bone (82).

Structural properties

Geometry

Fracture occurs in bone when the stress on bone is higher than the ultimate strength (94, 95). Ultimate strength is "the maximum stress achieved prior to failure of a component on a single application of the load (96)." The stress within a bone is dependent on several factors such as the geometrical arrangement of bone, the material components or the composition of the bone, the direction and size of the force applied (94, 95) and not just its mass (97). However, the stresses are determined by geometry under specified loading conditions (98).

Bone structural or geometrical arrangement is genetically determined and controls the bones' ability to adjust and function accordingly with the existing loads by modeling and remodeling. This process modifies the absolute and relative positions of both the external and internal envelopes of bone. The external envelope is known as periosteum where as the internal envelope is known as endosteum. The endosteal envelope consists of endocortical, trabecular and intracortical regions. These envelopes determine the size and shape of the bone and also the spatial distribution of its mineralized tissue mass. This suggests that together these traits (size, shape and the spatial distribution of mineralized tissue mass) contribute to bone strength (97).

Size and shape: The skeletal system modifies the size and shape of the bone depending upon whether it functions as a lever or spring. For load bearing and leverage, it is necessary to maintain stiffness and lightness rather than flexibility. To serve this purpose bone tissue is designed into long bones such as the femur. The femur contains a medullary canal with the mineralized tissue cortex surrounding it. This tissue cortex is placed away from the center of the medullary canal, the long axis of the bone, which, in turn, enables cortical bone to withstand loads and provides greater resistance to bending. Thus, size of the bone can infer different properties; small bones with a small medullary area have the cortical bone close to the central axis and are more subject to bending than are larger bones with cortical bone at a greater resistance from the medullary center (99).

The bone mass inside the periosteum increases and forms into a cortex while bones grow in length and diameter. During this process the marrow cavity is formed which moves the cortical shell further and further from the neutral or long axis of the long bone. The diameter of the long bone, the mass of cortical bone, its cortical thickness, cross-sectional area (CSA), and the placement of the cortical mass relative to the neutral axis is determined by the absolute and relative movements of the periosteal and endosteal envelops (99).

On the other hand, vertebral bodies function as spring-like shock absorbers where stiffness and peak load bearing are sacrificed for flexibility. The vertebral bodies contain porous and mineralized honeycomb-like interconnections known as spongiosa. This porous structure functions like springs and has the ability to store energy by deforming in compression. The structural adaptation of the vertebral bodies helps to achieve lightness due to its porous network. This feature also provides greater strength to peak strains than

cortical bone despite sacrificing peak stresses (load/area) compared to cortical bone. The cancellous structure of bone helps to withstand larger deformations thus, facilitating flexion, extension, and rotation of the whole vertebral skeleton of the upper body (99).

During growth, vertebral bodies increase in length, width, and depth. As the vertebral body grows, the length and thickness of the trabecular plates also increase proportionately (99). During puberty, both the boys and girls show a similar degree of increase in the apparent trabecular BMD, so that males and females have the same vertebral body, trabecular number, and thickness at peak. Growth builds a bigger vertebral body in males, but not a more dense vertebral body, such that the greater peak load tolerated in males is due to the larger size and not higher density. Also, the load per unit area is not different in young males and females (100).

Two other important factors that play a vital role in determining bone strength are the external diameter of the bone and cortical thickness, together considered as bone dimensions (89, 101). The mechanical strength of the bone increases as the external diameter of bone increases resistance to flexion (5). As a compensatory mechanism, cortical bone adapts to decreasing bone mass in aging by increasing in the diameter (102, 103). It is also observed in men who exhibit greater strength of the long bones and who have greater bone diameter when compared to women (104). This difference is not just due to BMD but also due to differences in bone size and geometry. A recent study in men and women with similar body sizes showed that men had greater BMC and BMD at the hip and distal tibia than women. The differences in BMC and BMD were associated with cortical thickness. This may partly explain the greater rates of fragility fractures in women than in men (105). In another study, Silva and Gibson (55) investigated the age-

related changes in microstructure and mechanical behavior of human vertebral trabecular bone based on idealized two-dimensional model. The study reports that bone strength decreases if the trabecular number is lost, and that it may not be possible to restore the trabeculae that are lost due to resorption. This loss ultimately leads to the reduction in bone volume. Another finding of this study was that the modulus and strength of the vertebrae decreases two to five times more with the random removal of trabeculae rather than uniform reduction with the same loss of bone volume. In another study (106), the vertebral bone size has been found to be smaller in women with spinal fractures with 50% of the deficiency in bone mineral content. This deficiency is a result of a smaller bone size. Similarly, smaller bone size was also observed when patients with spinal fractures were matched with controls with the same areal BMD. Therefore, the size of bone appears to have an effect on overall fragility (106).

The geometry of the bone also affects the distribution of bone mass. The ability of bone to resist bending and torsion can be altered by changing the distribution of bone mass. However this change cannot be seen in BMD measurements (85). The distribution of bone mass is better understood by the architectural properties of bone. Therefore, in addition to geometric properties of bone it is important to understand the quality of the bone in terms of three-dimensional architectural properties.

Micro-architecture

Bone micro-architecture is an important structural property at the tissue level. Micro-architecture describes both the cortical bone and the three dimensional (3D) network of trabeculae in the cancellous bone. Therefore, bone micro-architectural parameters such as trabecular thickness (Tb.Th,) trabecular number (Tb.N), trabecular

separation (Tb.Sp), connectivity of the trabeculae, degree of anisotropy (DA) as well as thickness and porosity of the cortical bone help in understanding the micro-architecture of bone (107). While DA is a architectural property it is more commonly used to help explain mechanical strength.

Trabecular Bone: The trabecular micro-architecture is understood by the thickness (Tb.Th), spacing (Tb.Sp), bone volume fraction (BV/TV) and the extent to which the trabeculae are interconnected. The role of trabecular bone is to transfer loads across joints such as the hip, and to resist compression, as in the spine (94). The ability of bone to withstand the compressive forces and shear or tensile forces depends upon the distribution of the trabecular network. The macroscopic structure of trabecular bone is composed of an interconnected series of osseous plates and struts (rods). The effectiveness of the trabecular network is due to the spacing (trabecular separation), the relative bone volume fraction (BV/TV) and the direction of the osseous plates and struts (108).

Rod-like or plate-like properties of the cancellous bone are described by the term Structural Model Index (SMI). For an ideal plate and rod structure the SMI value is zero and three, respectively. The trabeculae can also possess a true sphere-like structure, which is indicated numerically by a value of four. Healthy cancellous bone is characterized by plate-like elements. Plate-like cancellous bone can transform into rod-like elements due to aging or disease. Hence, the terms "rod-like" and "plate-like" are frequently used for a subjective classification of cancellous bone (6-9). It is also reported that SMI values can be negative when the trabecular bone is dense and possess concave like structure with BV/TV greater than 30%(109). These osseous plates and struts are

arranged three dimensionally within the inner surface of the cortex. The trabeculae that are in a vertical direction reduce the axial forces whereas horizontal plates react to the tensile (shear) stresses (10). When there is a reduction in the trabecular elements (Tb.Th, Tb.Sp, SMI) that are perpendicular to the direction of load it may lead to trabecular failure in terms of bone mechanical strength; i.e., it can lead to buckling or bending of the bone. Therefore, if the cancellous bone architecture is distributed with widely separated and disconnected thick trabeculae the bone is less capable of resisting deformation than an equivalent amount of more numerous connected and thin trabeculae (110).

The cancellous bone architecture varies in different skeletal sites as well as in different disease states (6). Also the effect of bone loss may vary depending upon the directional orientation of the trabeculae. It has been reported that this loss of trabeculae may show different effect on mechanical properties of cancellous bone. It has been reported that in vertebrae, mainly the horizontally placed trabeculae are removed first. This preferential deletion of trabeculae is associated with an increase in the mechanical anisotropy (111). In another study Thomsen et al. reported that the horizontally placed trabecular thickness decrease with aging whereas no changes were observed in the vertically placed trabeculae. However, it is not known if the deletion of rod like trabeculae that are placed in horizontal direction will have the same effect with that of the deletion of plate-like trabeculae or vice versa. Neither of these studies determined the shape of the trabeculae (rod-like or plate–like).

Studies have suggested that the strength of cancellous bone depends upon the three-dimensional architecture and the rod-like or plate-like properties of trabeculae. Hildrebrand et al. proposed a strong correlation between SMI and BV/TV. The study

reported that samples with lower bone mass showed smaller plate to rod ratio (6). In a recent study Van Ruijven et al. suggested that as bone volume fraction decreases, the number of plates also decreases (112). This decrease would also be associated with a 40 % reduction in their thickness with an increase in the proportion of rods. The authors concluded that the effect of bone loss on plate-like trabeculae was opposite to its effect on rod-like trabeculae. Therefore, the strength of the bone depends not only on the thickness of the trabeculae but also on the relative bone volume and plate-like properties (113).

Aaron et al. examined the trabecular architecture in men and postmenopausal women using two dimensional imaging of cancellous bone viewed within its three dimensional context. Both men and women that had similar bone mass as determined by DXA were recruited. Biopsies from 31 osteopenic postmenopausal women with vertebral compression fractures and 22 without vertebral compression fractures were taken. Similarly, biopsies from a group of 16 men with fracture and 11 men without vertebral compression fractures were taken. The study revealed that female patients with fractures had four times the number of broken trabeculae as women without fractures. Men with fractures also showed a higher number of broken trabeculae than who did not have fractures. The authors suggested that the lack of significant differences in men could be due to the smaller group of men and few suitable biopsies, since some of the biopsies from the suitable patients were eliminated due to the fractured trabeculae and displaced fragments while extracting biopsies. The authors concluded that three-dimensional histology of vertebral fractures that has been used in the study is a more sensitive predictor of fracture predisposition and may provide additional benefits in the evaluation

of bone fragility (114). The findings of this study thus, support the concept that trabecular architecture is particularly important to bone quality.

An intact trabecular network appears to be vital in maintaining maximum bone strength. A study in which trabecular bone loss was induced suggested that loss of individual trabeculae has a greater impact on bone strength than the same amount of bone loss attributed to trabecular thinning (115). Therefore, architecture plays a very important role in the prevention as well as in the pathogenesis of fracture because improving the thickness of trabeculae has a very little effect on connectivity. No interventions can benefit existing bone because once the trabeculae are lost they cannot be replaced. Consequently, more emphasis must be given to preventions that can reduce the rate of resorption as well as the rate of remodeling activation (114).

The amount of trabecular bone differs from site to site. The neck of the femur contains 25 % trabecular bone, whereas in a vertebral body the percentage ranges from 66% to 90% (94). Therefore, loss of trabecular bone will primarily be seen first in the spine region or vertebral body. The trabecular deterioration is usually due to excess bone resorption over formation. As a result the densely connected, plate-like trabeculae are transformed to discontinuous rod-like structures. This leads to deterioration in the trabecular architecture (116, 117). It is also reported that, a progressive increase in the amount of cancellous bone occurs in the metaphyses of rat. This is also supported from the study findings of Osterman et al. (118), in which the growing rats that were given 14 C-labeled disodium clodronate subcutaneously showed highest activity of the label in the primary sponigiosa of the distal femur metaphysis and in the cortical bone of the femoral diaphysis when compared to the other parts of femur (118).

The strength of the trabecular bone is in part due to its large surface to volume ratio. Trabecular remodeling occurs on a bone surface by directly removing old bone and then filling in the cavities with new bone. Therefore, remodeling is more active in trabecular bone than in cortical bone due to its large surface. This surface to volume ratio is approximately four times greater than that observed in cortical bone (65). The trabecular bone mass in the vertebral body decreases more rapidly with age and menopause than that of cortical bone mass. Hence, the proportion of cortical bone is higher in the elderly spine than in younger adults. In general, women lose 20% of peak cortical bone mass and 40-50% of trabecular mass by 90 years of age. This leads to a decrease in the load-bearing capacity of the vertebral body (119).

Cortical bone: Cortical bone also plays a very important role in maintaining bone strength. Cortical bone is a dense and compact tissue. It comprises of the diaphyses of long bones and the outer shell of the metaphyses. The macroscopic structure of cortical bone shows osteons (108). Osteons, considered the building blocks of bone, are composed of a series of concentric rings of bone cells and bone matrix. The osteon surrounds a hole filled with blood vessels and nerves (120). These osteons are organized surrounding the Haversian canals in concentric layers, known as lamellae and are placed in interstitial tissue (23, 108). Interstitial tissue is formed from the remnants of old osteons. Osteons contain of space inside them known as lacuna. Osteocytes reside inside this lacuna. Secondary osteons are formed in the process of continuous remodeling of bone where old bone is replaced by new bone. In cortical bone, remodeling occurs at scattered locations on the surface of the bone through resorption and followed by reversal. The cavities thus, formed are refilled by osteoblasts with new bone in new

concentric lamellar pattern. The osteoblasts first synthesize the extracellular matrix composed of collagen and other structural proteins during bone formation. The osteoid is then mineralized. Mineralization occurs in two steps: primary mineralization and secondary mineralization. In the first few days, mineral density of the bone is increased up to a maximum of about 70% due to primary mineralization. But the secondary mineralization shows a gradual increase in the bone density. A maximum of about 90-95% of density is observed after several months. Consequently, recently remodeled bone tissue is less highly mineralized than unremodeled tissue (108).

It is also important to observe the role of cortical bone to assess the risk of osteoporosis as well as to understand the bone biology. Cortical bone parameters such as cortical thickness and porosity help in describing the cortical bone architecture. The loss of cortical bone involves thinning of the cortex and an increase in intracortical porosity (121). McCalden et al. (45) reported that the decrease in the strength of the cortical bone with age at the femur was correlated with an increase in porosity. This porosity changes contributed to a variation in strength of about 76 % (45).

Bell et al. (120) suggested a novel mechanism for induction of increased cortical porosity in cases of intracapsular hip fracture. In this study the investigators studied the relationship between remodeling and bone loss, osteonal diameter, wall thickness, and osteoid width in the femoral neck of patients with hip fracture. These parameters were then compared with age and gender matched healthy controls. Biopsies were taken from 12 female intracapsular hip fracture cases and 11 age- and gender-matched control femoral neck biopsies. Bell et al. suggested that increased cortical porosity in patients with hip fracture appears to depend on the presence of giant canals in the femoral neck.

These canals are related to clusters of remodeling osteons. The study revealed that the osteonal systems were nearly twice as prevalent and had significantly thinner walls in patients with fractures. This study therefore, suggests that the deficits of remodeling in hip fracture are specific to composite osteons, which leads to increased porosity of cortical bone (120).

Most of the bone mass that is lost in postmenopausal women is from the deterioration of trabecular bone (55). This is again due to the rapid rate of bone turnover in trabecular bone when compared with cortical bone (54). This negative effect of remodeling in general can be attributed to hormonal changes. The loss of trabecular horizontal links results in an irreversible loss of structural integrity. Since the amount of trabecular bone in the vertebrae is so high, this deterioration is particularly evident in the spine and revealed as compression fractures (122). Hence, in osteoporosis, more prominent changes are observed in the cortical thickness and trabecular density besides the normal age-related changes leading to a significant decrease of compressive strength in the vertebral body. Thus, these changes increase the likely occurrence of fracture. Therefore, loss of bone, particularly the trabecular bone, will cause a significant decrease in mechanical strength of the vertebral body (123).

On the other hand, studies have also suggested that the strength of the bone varies depending upon the skeletal site and type of bone. Experiments on fatigue resistance of trabecular and cortical bone suggested that cortical bone tissue has higher fatigue resistance than trabecular bone tissue. Findings of Guo et al. (108) suggest that the trabecular tissue is 20-30 % less stiff than cortical bone tissue. The authors proposed that these differences could be due to the differences in tissue morphology (108). In another

study, loads on the rat femoral neck showed more withstanding ability due to cortical bone than cancellous bone (124).

Material properties

Bone is primarily composed of inorganic apatite crystals. These apatite crystals help in the mineralization of organic type I collagen matrix. Several factors such as the degree of mineralization, material properties of collagen matrix, crystal size and the mineral to matrix ratio all contribute to the strength of the bone. However, it is of importance to understand the role of mineralization and collagen, as these are the primary factors that affect the material properties of bone (13, 28, 125).

Mineralization

The degree of mineralization of bone has a significant effect on bone strength (125). The changes in the degree of mineralization and its distribution occur due to changes in turnover. These changes can modify the mechanical properties of bone. Low mineralization leads to reduced stiffness and strength while conversely, stiffness and strength are increased with high mineralization (126, 127). This is also confirmed by a study conducted by Follet and colleagues (125) in which a greater degree of mineralization of cancellous bone led to greater stiffness and compressive strength, while bone matrix volume and micro-architecture remain unchanged. However, a continuous increase in mineralization reduces fracture toughness, making bone more brittle and prone to fracture (14, 28, 126). There may be an optimum level of turnover that is appropriate for a balanced distribution of low- and high-mineralized bone which would increase bone's resistance to fracture (14, 28).

The distribution of bone mineral depends not only on the remodeling activities of bone cells but also on the time course of mineralization of newly formed bone matrix. Ciarelli et al. (127) used back-scattered electron microscopy to study the mineralization levels of human iliac cancellous bone. Findings showed that the newly formed superficial areas of bone in women had a high rate of bone turnover and were significantly less mineralized. The authors concluded that both low and high mineralization may be detrimental to bone mechanical properties, with low mineralization levels causing reduced stiffness and strength and high mineralization leading to reduced fracture toughness due to increased brittleness. Hence, bone mineralization may also be considered as one of the factors influencing bone quality (89, 99).

Collagen

Besides bone mineralization, another factor that is found to affect bone quality is the content and the structure of collagen. The chemistry of cross-links is one of the most distinctive characteristics of type I collagen found in mineralized tissue. Bones from patients with osteoporosis showed a reduced concentration of cross-links (128). This is also supported by another study conducted by Oxlund and colleagues (82, 129). They collected vertebral bones from deceased individuals with osteoporosis and healthy individuals matching there age and gender. The trabecular regions of the vertebral bones from both the groups were observed for cancellous bone collagen. Increased extractability and a significant reduction in the concentration of divalent reducible collagen cross-links were observed in the individuals with osteoporosis when compared to the control group. The extractability of bone collagen depends on molecular packing, non-covalent intermolecular forces, and cross-links between collagen molecules. Also, a

reduced concentration of collagen cross-links was observed in the bones of individuals with osteoporosis. This change in the bone results in a reduction of the material strength of the bone trabeculae. This explains why individuals with osteoporosis had fractures even though they had a similar amount of trabecular bone as the healthy controls. Therefore, cross-links of collagen are considered one of the important factors contributing to bone quality. However, the influence of collagen on the stiffness of bone is less, but it improves bone toughness through intramolecular cross-links (82, 129). Also the collagen fiber orientation shows 71% of variation in bone tensile strength when a linear regression analysis was performed (4). Hence, collagen cross-links also influence bone quality.

Bone Biomechanical Properties

Fractures occur in bone when there are alterations in the distribution of bone mass, bone micro-architecture, and the degree of mineralization (125). These factors together affect the strength of the bone ultimately affecting the load carrying ability. The load carrying behavior of bone is better understood in terms of its biomechanical properties (5, 89). The biomechanical properties of bone are understood by the properties that are associated with elastic and inelastic reactions when a force is applied (2). These properties also involve the relationship between stress and strain (2). The biomechanical properties of bone are understood by all the parameters of strength such as compressive strength, tensile strength, and shear strength. Other parameters like strain, fatigue life, modulus of elasticity also describes the mechanical properties of bone (2, 3).

Bone fatigue may result in fracture. Fatigue occurs as a result of the degradation of bone strength and decrease in modulus of elasticity. This reduction in mechanical

properties or strength of bone occurs when micro-cracks are formed in the bone. These cracks or fractures of bone grow under repetitive stress (2-4). Fatigue may also occur more rapidly as a result of intense exercise when compared to normal activities (4). The modulus of elasticity describes the stiffness and hardness of bone (2). Elastic modulus is the ratio of stress and strain that explains the degree of deformation due to the force or load applied, by providing a value for stiffness. Therefore, bone or any material having higher stiffness subsequently has higher elasticity (1). However, the modulus of elasticity varies depending upon the direction, as the material properties of bone differ in all directions (anisotropic). The mature cortical bone has a modulus of elasticity of 18 gigaPascals (GPa) in longitudinal direction and 12 GPa in transverse direction. Similarly the trabecular bone elasticity ranges from 0.1 to 3.5 GPa. The stiffness of a bone varies depending upon the degree of mineralization as observed in immature or woven bone and porosity as observed in a old bone. Reduced stiffness thus, lowers the modulus of elasticity (4). The ratio of stress to strain at any point in the elastic region of deformation yields a value for stiffness. The stiffer the material, the higher is the modulus. The moduli in compression and tension are different for most biological materials because they are anisotropic.

In other words, the biomechanical properties of bone are those that describe the extrinsic and intrinsic properties of bone. Whole bone properties are called extrinsic properties of bone. Bone tissue properties such as stress and strain are called intrinsic properties of bone (5, 89). In order to understand these biomechanical properties of bone several biomechanical tests are used (5).

Mechanical testing of bone tissue is intended for determining the mechanical properties at the whole-bone, architectural, and bone-tissue level under different loading conditions. Primarily three kinds of biomechanical tests are used for assessing the biomechanical properties of bone: tension, compression, and torsion (130). Bending or flexion tests are also used. A bending test is practical method to measure the mechanical properties of small animal bones. Using this test one can determine both compression and tension of the bone. Tensile stress occurs when the material is stretched whereas when the material is compacted it results in compression stress. Usually fractures occur on the tensile side, as bone is weaker in the tension. To assess the properties of bone either a three-point or four-point bending test can be performed (5). Three-point bending is simple, and, hence, it is preferred when using rodent bones (5). In a three-point bending test the two ends of the bone are supported by fulcra, and then the force is applied at the mid shaft in the perpendicular direction of the long axis of the bone by a crosshead moving at a constant speed (59). In a four point bending test force is applied equally at four loading points: proximal and distal ends, and two points along the longitudinal axis. Applying equal force in all the directions is difficult when using rodent bones because of the irregular shape of the bones. However both types of bending tests have certain disadvantages: 1) they provide information only on a few elastic constants of bone biomechanical properties as the bone is destroyed in this method; and 2) the mechanical loading of the bone can be tested only in one axis while measuring the forces due to axial deformation. This affects the assessment of trabecular bone properties as the trabecular bone displays both anisotropic and visco-elastic properties. Therefore, the reproducibility of single mechanical test at a given orientation of the bone specimen and strain rate is

limited (130, 131). As a complement approach to mechanical testing, micro finite element analyses have been developed to calculate the elastic constants of bone specimens from computer models representing the trabecular micro-architecture (130).

Assessment of Bone Biomechanical Properties Using Finite Element Analyses

Finite element analysis takes into account both the geometric structure and the material properties. A finite element model can be generated using the computed tomography images that provide both three-dimensional geometric details and information about the material properties. Previously, studies have determined the mechanical properties of whole bone, trabecular bone (90, 132), and osteoporotic bone (133) using finite element models derived from the CT images. Studies have also examined the sensitivity of the model to material properties (35, 134, 135), image and mesh resolution, and element type (136, 137) that are important in accurate biomechanical measurements.

In order to understand the biomechanics of bone, it is important to know the terminology that describes the material properties of bone. The total force parameter is used to describe the force required to crush bone completely (11). Physiological force is 30% of total force required to crush the bone at a physiological state. Stress is defined as the "load per unit area" whereas strain is the "fractional or percentage change in length." Strain is calculated as "the amount of deformation divided by the original length of the specimen." Increasing the stress causes bone to break. Before failure or breaking the specimen deforms which is known as strain (4). The Von Mises stresses are used as an indicator of the amount of stress within a bone when force is applied (11). The stiffness of bone is defined as its rigidity (5).

The finite element models are generated from high-resolution images. These images are obtained from the cross-sectional images of a region of interest of the bone specimen. The images thus, obtained from micro-computed tomography (μCT) system are digitized and stacked in order to rebuild the original structure of the specimen as a 3D voxel model. The micro-computed tomography (micro-CT) uses an image resolution of 50 μm or better for specimens of approximately 8 cm in length. Using micro-CT technology has lowered the difficulty of assessing the biomechanical properties of bone specimens. In addition to micro-architecture, the FEA analysis helps to understand the properties of bone at tissue level. Three-dimensional images are developed by building the successive levels or several layers of bone tissue. Bone reconstructions thus developed artificially represent a geometric simulation of the tested specimen. Using these models, the analyses on bone can be performed at the architectural or whole bone level (90, 138-142). This combined approach of experiments and computer modeling has great potential in studying the quality of tissue-engineered trabecular bone (136, 137). However, in addition to finite element analysis it is important to understand the mechanical behavior in the direction of the applied load, since fractures are more prone in that direction. This mechanical behavior of bone can be understood by degree of anisotropy.

Degree of Anisotropy

Similar to other biological structures, bone has a certain grain or a preferred direction associated with the structure known as anisotropy (5, 143). "Anisotropy is constituted under the influence of preferential-oriented force applied to bone and permits [bone] to establish resistance to these strengths in a given preferential direction (144)." In other words,

anisotropy characterizes the degree of directional organization of a material. The more preferential direction the structural organization has, the more important is the degree of anisotropy (DA). The anisotropy of trabecular bone depends on the skeletal site. Anisotropy was assessed in several bones such as the calcaneus, hip, vertebrae and radius. The results have shown that the main direction of force applied to the bone influences anisotropy (145-147).

In a study, Sugita et al. (143) investigated the anisotropy of femur bones to examine the mechanism underlying femoral neck fracture. This study utilized twenty-three femoral heads from 20 female and three male patients with femoral neck fracture and with a mean age of 79.9 ± SD years. The femoral heads were removed during endoprosthetic replacement and stored at −20°C. They were defrosted in physiological saline at room temperature. The specimens obtained from each femoral head were randomly assigned for testing into two groups: parallel and perpendicular. The parallel group included 43 specimens, and the perpendicular group included 39 specimens. A compressive load was applied either parallel or perpendicular to the primary compressive group of the specimens in each respective group. Three parameters were obtained: compressive stiffness, maximum stress, and maximum energy. Each wet trabecular bone specimen was subjected to a stress-strain test in which compressive stress was applied either parallel or perpendicular to the primary compressive group. The compressive stress load was produced by displacement of the upper and lower plates of a servo-drive compression test machine (1356, Aiko, Kyoto, Japan) at a speed of 0.065 mm/sec. The magnitude of the applied load was measured by a strain force transducer (LU-200KE; Kyowadengyou, Japan) attached to the upper plates. Deformation of the specimen was measured by the displacement transducer (DT-20D; Kyowadengyou,

Kyoto, Japan) attached to the lower plate. The study confirmed that mechanical behavior of cancellous bone changed with subsequent changes in the testing direction. These variations were interpreted as an anisotropic feature of bone stress. Also it is observed that the trabecular bone anisotropy corresponds to the preferential orientation of trabeculae. The authors concluded that anisotropy of the cancellous bone should be considered in predicting the fracture risk (143).

The anisotropy evaluation can be done either on three-dimensional (3D) or on two-dimensional (2D) images. The most currently used method to assess anisotropy is the mean intercept length (MIL) using three-dimensional (3D) images. The principle behind this method is to fit an ellipsoid to a polar diagram plotted with the values of the MIL obtained in several directions. The MIL for each direction is calculated as the total line length divided by the number of intersections between the bone-marrow interfaces. The magnitude and the vector orientations of three main MILs are determined from this ellipsoid. Based on these MILs, the DA can be defined as the ratio of the longest MIL vector magnitude to the smallest one. The MIL method is also used on 2D images where an ellipse is generated instead of an ellipsoid. Using MIL method for the evaluation of the degree of anisotropy is generally considered accurate (133, 147-149).

Micro-CT generates data on DA using MIL method and three-dimensional images. It is suggested that poor bones have higher DA values (150). When an analysis was performed for the bone graft market, it was observed that the porous hydroxyapatites with anisotropic characteristics showed lower compressive moduli than the isotropic specimens with the same apparent densities (151, 152). Similar findings were suggested by Chappard and colleagues (147) from their study. They found higher DA values in the bones of subjects with vertebral

fractures than in control subjects. Furthermore, the L1 and L2 vertebra of dogs that showed an improvement in the structural properties following alendronate treatment also showed a decreased degree of anisotropy in the bone specimens (153).

Assessment of Bone Structural Properties Using Micro-Computed Tomography

Advanced non-invasive techniques are essential for obtaining information on bone microstructure of specific parts of the skeleton and for determining its evolution with age and progression of disease. Specifically, to estimate mass losses and density variation, the key elements are microanalysis and classification of cortical and cancellous parts of bone. The commonly used techniques for diagnosis are radiography and laboratory tests such as biopsy, but the results are limited to two dimensional (2D) image measurements. These do not assess completely the complex three-dimensional structure of bone. Computed tomography (CT) offers the opportunity to obtain three-dimensional (3D) mapping of bone structure (154). Recent studies demonstrated that micro-CT can produce images from a variety of species at whole bone level (155). However, creating images from larger species using micro- CT is difficult, but possible if higher computing resources are used. Therefore, whole bone micro-CT is currently used for only small bones like rats and mice due to practical constraints (156).

Micro-computed tomography thus, can be used as a tool to understand the structure of bone at the whole bone level. For example, in a study conducted by Bonadio et al. (156) the images of mouse bones were used to measure the cross-sectional properties. This is achieved by using micro-CT at 20µm resolution. The authors were able to demonstrate a compensatory increase in the amount and distribution of cortical bone tissue, while maintaining whole-bone properties in spite of a decrease in the tissue

properties observed in another similar study conducted on MOV-13 transgenic mice (157). Also, this study revealed that it is possible to estimate a combined effect of mechanical testing based on the descriptions of the structure obtained from micro–CT images. Thus, based on the information obtained by measurements made from whole-bone micro-CT images and whole-bone mechanical testing the authors were able to hypothesize that there was degradation in the mechanical properties of the tissue. The authors later confirmed this by performing mechanical testing at the tissue level (156).

In recent years the use of micro-computed tomography (μCT) has become very popular in measuring the bone samples, because of its relative rapidity compared with conventional histology and its potentiality as a nondestructive method (158). Also, since bone mineral density alone is not enough to assess the risk of fracture, the distribution of bone mass is used as a predictor of fracture risk. Bone architecture assessed by micro-CT explains the distribution of bone mass in three-dimensional space. Bone architecture contributes to the tissue's biomechanical integrity and, therefore, to fracture risk (24, 115). Increased bone fragility with age could also be caused by a change in material properties of the tissue (159). Hence, it is very important to assess the changes in trabceular architecture, which is thus, made easy and possible by micro-computed tomography. It is observed in osteoporosis there is a decline in bone tissue, especially trabecular bone (160, 161). Skeletal fractures are the major complications of osteoporosis leading to increased morbidity and mortality in patients affected by this disease. Hence, micro-CT is increasingly used for the study of osteoporosis and other bone related disorders in animal models.

Connectivity, a property described by μCT analysis, decreases as bone mass decreases (162, 163). Although connectivity is not related to bone mass, it is very important to consider as a structural component contributing fracture risk (164). In a study conducted by Ulrich et al. (165) human cancellous bone (N=237) from different skeletal sites (iliac crest, lumbar spine, femoral head, and calcaneus) was used to calculate structural indices and elastic constants. These values were used to explore the predictive value of various three dimensional structural indices (3D) for understanding the elastic properties of bone. These 3D images were used to calculate bone volume over total volume (BV/TV), bone surface volume over total volume (BS/TV), trabecular thickness (Tb.Th), trabecular separation or spacing (Tb.Sp), trabecular number (Tb.N), and MIL ratio and for micro structural finite-element (micro-FE) analysis. These values were used to calculate Young's moduli, Shear moduli, and Poisson's ratios. A group of critical specimens was selected to represent specimens that could not be identified as osteoporotic or normal based on the BMD measurement alone. Using linear multivariate regression analysis the critical specimens, structural indices and elastic constants were correlated. When one of the 3D structural indices was included as an independent variable it was found that the elastic constants correlated better than when BV/TV was used as an independent variable. The correlation coefficients (r^2 values) increased from 53% (BV/TV alone) to 82% (BV/TV and MIL ratio) suggesting that including these structural indices in the model improved the correlation values. However, these indices that were identified as more significant were not the same for the different skeletal sites. The elastic constants for cancellous bone samples demonstrated an improvement when BV/TV is supplemented with structural indices. The authors concluded that the diagnosis

of osteoporosis and the mechanical properties of bone assessment could be improved if 3D bone micro-architecture is used in addition to BMD (165). Thus, micro-computed tomography (μCT) enables analysis of three-dimensional bone architecture in relation to bone strength by using high-resolution imaging technique (166, 167). A complete data set of three-dimensional bone architecture images forms the basis for finite element modeling (FEM) that helps to predict the mechanical properties of bone (22, 90)

Rat as animal model for studying bone

For many women today, a major health problem is postmenopausal osteoporosis. Understanding osteoporosis is hindered by the complexity of studying the disease, as it is restricted to humans. Osteoporosis is characterized by a slow progression of disease (16), and, hence, it requires several years of study duration in response to a therapy. Since the results come slowly, gathering data is time consuming. Also, it is difficult to maintain a study group for reasons of natural attrition either due to relocation or death. Hence, it is very helpful to choose an animal model that can provide more uniform experimental material, which allows for wide testing of future therapies. An appropriate experimental animal model that is selected carefully for the study of osteoporosis minimizes the limitations associated with studying the disease in humans such as time and behavioral variability among test subjects (168, 169). The selection of any animal model should be based on appropriateness, convenience, and relevance (170).

Appropriateness

All the factors that are acceptable as well as that facilitate studying a particular condition in an animal model are known as appropriateness (169). The rat is an appropriate animal model for studying factors related to bone development and

osteoporosis because growth patterns in a rat model is similar to humans. Rapid increase in length, weight, density and calcium content of femurs occur from one to three months of age in rats, which is similar to humans during rapid growth periods. There is an enormous modeling, remodeling, and growth occurring in this period. Hence, this age group can be opted for studying childhood and adolescence in humans. A gradual increase is observed from the age six months in rats (169). At 12 months of age all bone parameters in rats reach stability and no further changes up to 24 months of age occur.

A second factor that should be considered in selecting an animal model is that the anatomy and physiology should be similar to humans (168). Researchers should consider the following aspects to determine an appropriate animal model: "1) appropriateness as an analog, 2) transferability of information, 3) genetic uniformity of organisms where applicable, 4) background knowledge of biological properties, 5) cost and availability, 6) generalizability of the results, 7) ease and adaptability to experimental manipulation, 8) ecological considerations, and 9) ethical and societal implication (171)."

The effects of ovariectomy have been studied in rats at different ages. Kalu suggested two ideal age groups that were especially appropriate for studying postmenopausal osteoporosis: mature rats (approximately three months of age) and aged rats (12 months old). At 3 months of age bone growth in the rats slows drastically and plateaus by 12 months (172). A high degree of genetic homology is observed between humans and rats (93%). Hence, the adult rat skeleton has many similarities to the human skeleton and is appropriate for studying bone and related problems. The size of bone in both humans and rats increases by epiphyseal and periosteal growth (5, 173). Rats also experience the remodeling process of the secondary spongiosa like humans (174). Also

male rats undergo epiphyseal closure at the proximal tibia at about eight months of age whereas female rats undergo closure at about 10 months of age by bony bridging (175), leading to a slowing of the rate of bone growth.

Acheson et al. (176) studied female (N=13) and male (N=10) Sprague Dawley rats for skeletal development and compared rats for similarities to human skeletal development. Starting from 20th day the rats were weaned and fed ad libitum. The rats were separated by sex. Using radiography techniques based on the principles of Oxford method, the skeletal maturation of rats was assessed. The changes that occur in the epiphyses of both long and round bones and irreversible processes during maturation were observed. These changes, which are otherwise called as maturity indicators, indicated that there are similarities between rat model and human skeletal system. Female rats matured more quickly than male rats, but at all stages of growth male rats were heavier and longer than the female rats. It is also observed that in male rats, the body length increased at a higher rate whereas it decreased in female rats between 70th and 80th day of life. At birth both the rat and human skeletons are immature and incompletely mineralized. Hence, the rat is an appropriate model to study the skeletal development as most of the changes to cartilage bone occur outside the uterus facilitating the study of stress as well as and other environmental factors.

Convenience

The simplicity in using an animal model is known as convenience (169). It is convenient to maintain and work with rat model. Rats are relatively economical with fewer ethical constraints when compared to other animal models such as dogs and non-human primates. They are widely available with a well-characterized skeleton and they

grow rapidly. The shorter life span of rats also facilitates studies on the effects of aging on bone (177).

Relevance

Comparisons made between animals and humans with reference to a particular event or aspects that are being studied are considered as relevance (169). There are many skeletal similarities between rats and humans. Similar to postmenopausal women, aged ovariectomized female rats also showed higher levels of bone loss in vertebrae than in femur i.e., the loss of cancellous bone was higher than cortical bone loss (169, 178). A similar pattern was observed in bone resorption exceeding the bone formation with an increase in the levels of biochemical markers of bone turnover (169). The ovariectomized rat model and postmenopausal women showed similar characteristics like rapid loss of cancellous bone, decreased intestinal calcium absorption, and a positive response to treatment. The response to treatment in ovariectomized rats given estrogen, biophosphonates, calcitonin, vitamin D and its analogs, tamoxifen, parathyroid hormone, and exercise showed similar preventive effects on bone loss as found for postmenopausal women. These similarities thus, confirm that the rat model is suitable for studying osteoporosis. Rat bones also show a similar skeletal composition of humans. The skeletal system in humans and rats consists of 80% cortical bone and 20% trabecular bone (179).

Wang et al. (180) reported that Sprague-Dawley rats show a significant age-related bone loss in the cortical and trabecular bone. The loss of bone started from nine months of age when bone growth had been completed. The authors suggested that the vertebra and femoral neck are the relevant bone sites to determine the cause of the loss of bone, and Sprague-Dawley rats are appropriate animal models to study for age-related

bone loss. No significant age-related changes are observed in F344 rats (80). Therefore, not all strains of rats are suitable animal models for studying age-related bone disorders.

Associated problems with rat model

Osteoporosis is a widespread disease, and numerous human subjects are available to conduct research. The rat model is preferred by researchers, however, due to ethical constraints that confine their ability to test new hypothesis or potential therapies in human beings (169). While the rat model has several advantages, there are certain disadvantages like the small blood volume for multiple biochemical measures and small total amount of bone available, minimal intra-cortical bone remodeling, and size related difficulty of performing surgical procedures.

It is well known that the aging rat shows increased bone fragility and a reduction in cortical bone, but it is unclear if this results in the higher incidence of fractures. Another problem is that rodents do not experience a natural menopause. As a result, a stable skeletal mass is maintained throughout the life span (169). Rats show a continuous estrus cycle for most of the life span (about 19 months of age). During this period, the bone mass is maintained due to the secretion of sex hormones by the ovaries. Ovariectomy has been used to produce an artificial menopause. In spite of having Haversian systems, although minimal in aged rats, and a significant loss of bone mass after ovariectomy, rats have a very limited naturally occurring multicellular unit-based remodeling (169, 172, 181, 182). They also have a fine-fibered lamellar bone trabecular remodeling and no intracortical remodeling. A rapid growth of longitudinal bone is observed in the long bones of rats after ovariectomy. However, this can be minimized by

using aged rats (9-12 months old) or by studying the skeletal sites where reduced longitudinal growth is seen such as lumbar vertebrae (181).

Rats exhibited continuous growth including increased body weight when they were fed ad libitum. However, this increase in weight is due to the high deposition of body fat rather than to increases in lean body mass. Rats showed a decrease in body weight as well as lean body mass once they started aging. A decrease in osteogenesis and epiphyseal growth plates of rats between six to 18 months of age has been indicated in several studies. If rats live long, then they may suffer from senile bone loss (175).

Rats show a very minimal Haversian remodeling of cortical bone (169, 183). This contributes to less bone remodeling in cortical bone (184-186). As a result there will be a reduced accessibility to study the ovariectomy-induced changes in regions that contain higher amounts of cortical bone such as femoral diaphysis. It is very important to study the cortical bone changes in humans, such as the perimeter of the femoral neck as they can be clinically very important. This suggests that a careful approach is required in determining the various sites to be studied in rat, as there are differences in certain locations of human bone growth (183). However, the cancellous bone of rats is similar to humans in the remodeling activities of activation, resorption, and formation at several sites (23). Hence, it can be concluded that in spite of their differences, rats exhibit a similar mechanism of bone turnover as seen in humans and can be considered a good model for studying bone.

Rat model and iron absorption

Growing rats are extensively used for studying mineral metabolism. However, it is important to consider the differences between rat and human metabolism when using

rats for the assessment of dietary iron absorption as they have serious limitations. It has been revealed that rats have higher iron absorption rate than humans. Though the actual cause is unclear the possible reason is predicted as the ability of rats to synthesize ascorbic acid. Since studies on humans have established that iron absorption is enhanced by ascorbic acid, the differences in iron absorption of rats and human could be due to the effective absorption of iron facilitated by ascorbic acid (187)

Effects of iron on bone

Tuderman et al. proposed that iron is a cofactor for prolyl and lysyl hydroxylases. These enzymes act as catalysts in the ascorbate dependent hydroxylation of prolyl and lysyl residues which is an essential step in cross linking of lysyl oxidase (188). A similar but detailed mechanism of iron and its role in collagen formation has been explained by O' Dell (21).

There are at least 4 types of collagen but 90 % of bone collagen consists of Type I collagen. This collagen molecule is made up of three polypeptide units that are in the form of a coil known as α-chains. During the biosynthesis of collagen, procollagen is produced. From the α-chains, these peptide extensions are removed from the amino and carboxyl ends by a process known as hydroxylation. The amino acids in type I collagen include hydroxyproline and hydroxylysine, but hydroxyproline is present in higher amounts. Both of these should be incorporated into peptides of collagen. This is done by post-translational hydroxylation. Three enzymes namely prolyl-4-hydroxylase, prolyl-3-hydroxylase and lysyl hydroxylase are required for this process. All these enzymes require ferrous iron as a cofactor. Proline hydroxylation is necessary for triple helix

formation, which is necessary for cellular secretion of collagen. Therefore, iron plays a very important role in the collagen synthesis of bone (21).

Effects of iron deficiency on bone

Iron acts as a co-factor in collagen synthesis and, thus, play a very important role in bone formation (21, 188). There are only a few studies to support the hypothesis that iron deficiency affects collagen metabolism. This could be due to the fact that anemia and other pathologic signs are observed initially before any changes could be seen in collagen hydroxylation (21).

Rothman et al. conducted a study to see the effects of iron deficiency anemia on fracture healing. For the purpose of the study, 120 Sprague Dawley rats weighing 300g were randomized into two groups: a control group fed a diet of powdered milk with a multiple vitamin supplement with adequate iron and an experimental group fed with the same type of diet as control except for iron. Anemia was induced by withdrawing four milliliters of blood once a week for four weeks. Iron deficiency anemia in the experimental rats was confirmed by hematocrit and serum iron measures. Fracture was induced by surgical procedures in the midshaft of the right fibula of both the experimental and control rats. Rats were sacrificed after the fracture at 3, 6, and 8 weeks. At each time period forty rats were sacrificed. To evaluate the fracture healing, tensile strength and microscopic examination of histologic serial sections of the site of fracture were used (189).

Tensile strength at three weeks, six weeks and eight weeks were compared between the control and experimental rats. Significant differences were observed between the treatment group and control group. The treatment group showed lower

fibular tensile strength as well as fracture non-union and retardation of fracture healing when compared to the control group rats after fracture. No differences were noticed between anemic and control rats in serum calcium, phosphorus, alkaline phosphatase (ALP), serum glutamic-oxaloacetic transaminase (aspartate aminotransferase or AST), albumin or uric acid (189).

In another study Heppenstall and Brighton observed fracture healing in the presence of anemia in 30 male white New Zealand rabbits (weighing 2-3 kg). Animals were randomized in three groups: control group, normovolemic treatment group and hypovolemic treatment group. Blood was withdrawn (20 mL) from the control group and then the whole blood was re-injected. In normovolemic treatment group 20 mL of blood was withdrawn, red cells discarded, and then an equal volume of plasma was re-injected. Phlebotomy (20 ml of blood) was performed in the hypovolemic treatment group. Fracture was induced in the fibula of all the animals through surgical procedures. The animals were sacrificed 21 days following fracture. A three point bending test was performed on the fibulae. Roentgenograms and histology was also performed (190).

The results of the control group were compared to other two treatment groups. Both the treatment groups, normovolemic and hypovolemic, showed a lower serum hematocrit values when compared to control group. The fibular strength and fracture healing was assessed by roentgenogram and histological testing. Findings revealed healing in control group and normovolemic group whereas a delay was observed in hypovolemic group. Also strength of the fibula in control and normovolemic groups was similar but very low strength was seen in normovolemic group. In spite of anemia, the normovolemic group exhibited fracture healing similar to the control group. This could

be due to the increased cardiac output and normalized tissue oxygen delivery since proper blood volume is maintained. But the hypovolemic rats were unable to repair the fracture due to decreased oxygen delivery secondary to blood loss as well as to loss of plasma constituents (190).

Deficiency of iron can cause alterations in the metabolism of other nutrients like calcium, phosphorus and magnesium. Campos et al. (191) conducted a study using 94 weanling male albino Wistar rats to observe the possible interactions between calcium, phosphorus and magnesium after inducing nutritional iron deficiency. Animals were randomized into two groups: control group and iron deficient rats. All animals were fed a diet according to AIN-76 recommendations for all nutrients except iron. An aliquot of blood was obtained at different time points (0, 10, 20, 30 and 40 days). The levels of iron in the treatment group was lower in liver, spleen, sternum, and femur when compared to control group at all time points. But an increase in the intestinal calcium, phosphorous, and magnesium absorption was observed in treatment group. However, the phosphorous and magnesium balance decreased and that of calcium levels remained unchanged as the treatment progressed (191).

In the treatment group, serum calcium concentration was low at all time periods. Similarly, calcium, phosphorous and magnesium content also decreased in the femur at all time periods compared to control rats. Besides bone mineral content no other bone measures were taken. Significant increases in serum cortisol and parathyroid hormone (PTH) were observed in iron deficient animals when compared to control group after 40 days of dietary treatment. The authors concluded that mineral metabolism of calcium, phosphorous, and magnesium was altered with iron deficiency anemia (191).

Yokoi et al. (192) used male Wistar rats to study the effects of dietary iron deficiency on mineral levels in tissues of rats. The rats were fed with either 128 micrograms iron/g (control) or an iron-deficient diet containing 5.9 micrograms iron/g (treatment). Iron concentrations in different tissues of the body i.e., blood, brain, lung, heart, liver, spleen, kidney, testis, femoral muscle, and tibia were lower in rats fed with iron deficient diet when compared to control group. Similarly, magnesium and zinc levels in blood were also lower in treatment versus control groups. However, calcium and copper in blood and liver were significantly higher in treatment versus control animals.

Significantly higher manganese concentrations were found in iron deficient animals as compared to the controls in brain, heart, spleen, kidney, testis, femoral muscle and tibia. Based on these results it can be concluded that iron deficiency affects mineral status (iron, calcium, magnesium, copper, zinc, and manganese) in rats (192).

The influence of copper and iron deficiencies on the femoral mineral content and biomechanical properties was examined in 3-week-old male weanling Long-Evans rats. The rats were randomly assigned to one of three dietary treatments: control (n = 5), copper-deficient (n = 6) and iron-deficient (n =7) groups until 9 weeks of age. Femur bone mass was assessed using radiography and single photon absorptiometry. A significant decrease in the breaking strength of femur was observed in rats fed both copper and iron deficient diets. Also rats fed both of these diets (copper and iron deficient) showed smaller cortical area, but larger medullary area in femur one fourth from the distal end but no differences were found in the midshaft and proximal end of the femur when examined by radiography. However, no significant differences were observed in BMD and BMC. The authors concluded that iron deficiency significantly

influences bone biomechanical strength and hence, further research is required as iron deficiency anemia is one of the major public health concern (193).

Medeiros et al. (15) studied the impact of iron deficiency on the morphology and density of rats' femur and tibia. Thirty-two weanling Long-Evans male rats were assigned to one of four dietary regimens: control diet as per the recommendations of AIN in 1980, an iron-deficient diet (5-8 mg/kg or 89-143 μmol/kg diet), a calcium restricted diet (1.0 g/kg Ca or 0.025 mol/kg diet) and an iron–deficient and calcium restricted diet with a sample size of eight in each group. The diet was continued for five weeks. Rats fed low calcium and iron diets showed significant changes in bone density and morphometry. All the three experimental groups showed a decrease in the tibia, cortical and total femoral width compared to the control group. Iron-deficient diet fed rats also showed a significant decrease in medullary widths compared to the other three groups. Similarly, total cortical bone area also decreased in all the three experimental groups compared to controls. However, the tibia cortical area in the iron-deficient rats was greater than that of calcium restricted or calcium and iron restricted groups. Also DXA analysis on bone density showed a significant reduction in iron-deficient, calcium restricted, iron and calcium deficient groups when compared to control group. It appears from this study that iron deficiency decreases bone mass and increased bone fragility. The authors suggested that iron deficiency has a negative impact on bone health and this is aggravated by a calcium-restricted diet (15).

In another recent study, Medeiros et al. (11) observed the effect of iron deficiency on bone micro-architectural parameters. Thirty-two weanling female Long-Evans rats were randomly assigned to one of the four groups of diet: control, calcium restricted (1.0

g Ca/kg diet), iron deficient (<8 mg Fe/kg diet) and control, pair-fed to the iron-deficient group. The study examined if iron deficiency has direct adverse effects on femur and vertebral trabecular bone. Both BMD and BMC were lower in the calcium-restricted and iron-deficient rats than pair-fed and control rats when DXA analysis was performed on the whole body and femur. However, pair-fed rats also showed a decrease in the femur BMD and BMC when compared to control rats. Bone strength measured by finite element modeling was compromised in femurs from rats fed calcium-restricted and then in iron-deficient diets compared to pair-fed and control groups. Analyses by micro-computed tomography (Micro-CT) on the third lumbar vertebrae revealed that bone volume fraction (BV/TV), trabecular number (Tb. N) and trabecular thickness (Tb. Th) decreased in both calcium and iron deficient groups with an increase in the trabecular separation (Tb. Sp). Also the architectural parameters affected the structural model index (SMI) and exhibited rod-like properties in both the deficient diet groups. The control and pair-fed groups did not differ from one another, suggesting that iron deficiency and calcium restriction affected vertebrae independently of food intake and body weight (11).

Finite element analysis (FEA) revealed that the trabecular bone of vertebrae in calcium-restricted rats required less total force than all the other groups, while iron deficient rats required less force than pair-fed and control groups, respectively. A similar trend was observed in bone stiffness and Von Mises stress with the calcium restricted group having the lowest values and then followed by iron deficient group. However, no significant differences were observed between control and pair-fed animals. An increase in urinary deoxypyridinium cross links, serum osteocalcin, and cholcalciferol were observed in calcium-restricted rats when compared to the other three groups. The

analyses by micro-CT in this study demonstrated that iron deficiency has an effect on micro-architectural parameters of vertebral trabecular bone but not as severe as the calcium restriction (11).

Effects of iron excess on bone

Iron, on the other hand, may act as a toxin to bone cells and contribute to osteoporosis or other bone diseases in people with impaired iron metabolism and iron overload. Schnitzler et al. (194) examined the role of alcohol, iron overload and hypovitaminosis C to the osteoporosis associated African hemosiderosis in 53 African males diagnosed with skeletal disorders (vertebral osteoporosis, femoral neck fracture, and osteonecrosis of the femoral head). Forty-three age-matched black males were the control group out of which nine were limb surgery patients and the rest (n= 34) had died suddenly but previously had been healthy. Double-tetracycline-labeled iliac crest bone biopsies and serum biochemistry were performed on patients with (+ Fe, n= 38) and without iron (-Fe, n=15) overload and also on controls. Bone biopsy on both –Fe group and the + Fe group showed less trabecular thickness and greater trabecular separation than controls. The trabecular number also was lower in + Fe group than in controls. The +Fe group had significantly higher serum ferritin, transferrin and serum iron but lower levels of ascorbic acid than the –Fe and control groups. The erosion depth was significantly higher in + Fe group, followed by –Fe and control groups, respectively. The iron granules in the marrow showed a positive correlation with trabecular separation and erosion depth while a negative correlation was observed on trabecular number. The authors concluded that osteoporosis was associated with dietary iron overload and

resulted from a combination of alcohol abuse, iron overload, and hypovitaminosis C (194).

Conte et al. (195) compared BMD and bone histomorphometric analyses among six human males (mean age 48.8 ± 5.5 years) with primary hemachromatosis (PH) to eight human males (mean age 49.5 ± 7.9 years) with alcoholic cirrhosis (AC) and thirty healthy male subjects (control). Densitometric and histomorphometric results indicated impairment of trabecular bone in both patient groups as compared to controls. Cortical impairments were observed only in hemosiderosis patients. Plasma alkaline phosphatase activity (ALP) was greater in patients with alcoholic cirrhosis. However, no significant differences were observed between primary hemachromatosis and alcoholic cirrhosis patients in the plasma or in urine calcium and phosphate. Elevated levels of creatinine-corrected urinary hydroxyproline excretion were observed in PH and AC groups compared to the control group. Densitometric and histomorphometric findings suggested a decrease in BMD and a derangement of trabecular bone in both alcoholic and hemochromatotic cirrhosis. Cortical porosity was observed only in hemochromatotic patients (195).

The effect of iron overload on bone remodeling has been studied in ten female pigs of age 76-91 days. In this study, five control pigs were compared to five pigs treated with 300 mg of iron dextran for 35 days. Animals were sacrificed after 36 days. Bone histomorphometric analyses revealed that treated pigs showed a decrease in osteoblast cell surfaces, double and total labeled surfaces, appositional rate, and tissue formation. Whereas, an increase in reversal surfaces were observed. No significant changes were observed in mineralization since no changes were observed in osteoid thickness. Also the

treatment group showed no changes in urinary calcium, phosphate and hydroxyproline, or on serum 25-OHD and serum 1,25(OH) 2D levels. No differences were observed in bone calcium, phosphate, magnesium or ash content. However, the iron content in the metatarsal bone was significantly higher in treated animals when compared to control animals. A significant correlation was seen between liver and bone iron. Although an imbalance is observed between bone formation and resorption, no changes were observed in bone mass as indicated by trabecular bone volume and bone ash content. The authors hypothesized that this could be due to short duration of the study (196).

Twenty-two men with idiopathic hemochromatosis aged 35 to 62 years (5 hypogonadol (H), 9 eugonadal non-venesected (EN), and 8 eugonadol vennesected (EV)) and 20 age-matched controls were recruited to study the prevalence, severity, type and pathogenesis of osteopenia. Spinal radiography, spinal and forearm bone mineral density estimations, skeletal histomorphometry, and serum biochemistry was performed on all participants. Findings of this study revealed that serum ferritin, aspartate aminotransferase (AST), alanine aminotransferase (ALT), serum inorganic phosphate and urinary hydroxyproline were higher in the hypogonadol group than all other groups. However, serum ferritin, AST and ALT were higher in eugonadal when compared to eugonadal vennesected and control. The radial bone density, vertebral bone density and trabecular bone volume were significantly decreased in hypogonadol compared to other groups. The mineral apposition rates were significantly lower in all groups when compared to controls and significantly lower in EN than EV. The iliac crest bone biopsy showed that the osteoclast surface and number were significantly greater in H compared to all other groups. The authors concluded that bone density was significantly lower in

patients with idiopathic hemochromatosis and that bone density is significantly lowered in patients associated with hypogonadism (197).

Diamond et al. (198) conducted another study with106 men and women who were diagnosed with chronic liver disease (39 with alcoholic liver disease, 23 with hemochromatosis, 25 with chronic active hepatitis, and 19 with cholestatic liver diseases). The subjects were divided into two groups: cirrhotic and non-cirrhotic. Data were collected on BMD from 113 healthy volunteers (Control) who were matched for age, sex, and menopausal status. Bone biopsy was conducted on forty subjects of the control group as well as 106 subjects in the experimental group. The cancellous bone area was significantly lower in all subjects when compared to control group. All the patients had mean concentration of bone iron 2.5 times greater than controls, but 80% of the patients were within the normal range. No significant differences were observed in bone aluminum and copper levels in any of the groups. Bone biopsy in cirrhotic and non-cirrhotic patients revealed that 40 of them were osteoporotic and 23 of these 40 participants showed low bone formation rates. A negative correlation was observed between bone iron and bone formation. The analysis of forearm mineral content by single photon absorptiometry was significantly lower in cirrhotic patients when compared to non-cirrhotic patients. Similar results were found when the BMD of vertebrae was measured using single energy computed tomography. When in vitro experiments were conducted using rat osteoblast-like osteosarcoma cells, diminished cellular proliferation and function was observed at high iron concentrations (400 μmol/liter). Elevated levels of iron were observed in patients with chronic liver disease. The authors concluded that the

results of these studies were insufficient to support that iron was responsible for the osteoblast dysfunction observed among these patients (198).

Duquenne et al. (199) conducted a study using a French Caucasian male (age 48 years), diagnosed with primary heamachromatosis but who initially presented for the treatment of multiple spontaneous vertebral fractures. Elevated levels of ALP but lower levels of testosterone and reduced osteoblast, osteoclast activity was observed. A remarkable decrease in trabecular bone volume associated with a decrease in cortical bone thickness was observed. Urinary hydroxyproline excretion corrected for creatinine was elevated. However normal thyroid status is observed. Assessment by DXA at the lumbar spine and femoral neck showed very low bone mineral content. The authors concluded that although the exact mechanism is not known, osteoporosis in hemachromatosis might be due to excessive bone resorption and inadequate bone formation (199).

Dietary iron overload also was found to alter the metabolism of nutrients. Storey and Greger (200) examined the interactions of iron, zinc and copper on 96 male Sprague-Dawley rats. Rats were fed with adequate levels of iron (33-35 micrograms Fe/g diet) and zinc (15-25 micrograms Zn/g diet) and diets with excessive levels of zinc (2441-2470 micrograms Zn/g diet) or iron (1408-3042 micrograms Fe/g diet). Decreased tibial zinc retention was found in animals fed excess iron diets when compared to animals fed excess iron in only one meal. Also excess iron diet fed rats (3042 micrograms Fe/g diet) showed significantly lowered daily food intake, final body weight and higher ratio of liver to body weight. Elevated levels of iron were observed in kidney and liver of rats fed excess iron diet than all the other groups. Similarly, tibia copper levels were higher in the

excess iron group fed for several weeks when compared to control group while copper levels were significantly lower in rats fed excess iron in only one meal. Although not significant, kidney and tibia zinc levels were also found low in excess iron group compared to the control group (200). The authors concluded that animal or human studies on nutrition interactions given a single dose of test substances might not be reliable because acute responses do not reflect all the changes induced due to chronic feeding.

Association between iron and bone mass

Studies on animals have suggested that both iron overload and iron deficiency are associated with low bone mass. In a study conducted by Medeiros et al.(193) using Long-Evans male rats revealed that the strength for breaking the bone was lower in iron deficient rats than control and pair fed groups, suggesting that iron deficiency may play a role in bone fragility. The study of Kipp et al. (201) also revealed that iron deficiency resulted in low bone mass and bone volume. Another study conducted more recently by the same author suggested that long-term iron deficiency altered bone mass and bone structure in growing female rats (202). Iron overload has also been associated with low bone density (194, 197). Thus, the association between bone mass and iron has been supported by animal studies. However, very few clinical trials have been conducted to see the association between iron and bone mass.

The relationship between bone mass and ferritin was studied in a four year clinical trial of calcium supplementation in adolescent girls. Adolescent girls (n=354) in pubertal stage 2 who were premenarcheal at baseline (x+/-SD age: 10.8+/-0.8 y) were recruited to study the effects of growth, menstrual status, and calcium supplementation on iron status. Girls were randomly assigned to either placebo or treatment group. The

treatment group was given 1000 mg Ca/d as calcium citrate malate. Physical examinations, anthropometric measurements, bone mass measurements, and nutritional status were measured. Ferritin and red blood cell indexes were also assessed . The effect of menarche on serum ferritin concentration was evaluated after adjusting for changes in lean body mass (LBM). A significant negative association between changes in LBM and serum ferritin was observed. A trend for a positive association was observed between BMD of forearm and serum ferritin at baseline. A similar trend was noticed between the total body bone mineral density and content and serum ferritin in the fourth year of the study but only in the placebo group. No significant differences were observed in serum ferritin concentrations and red blood cell indexes between menstruating girls with higher iron and low iron intakes. The authors concluded that growth spurt and menstrual status had adverse effects on iron stores in adolescent girls with low iron intakes. Nevertheless, long-term supplementation with calcium (total intake: approximately 1500 mg/d) did not affect iron status (203).

The study of Harris et al. (204) on healthy, non-smoking postmenopausal women (n = 242; 40-66y) also confirmed an association between dietary iron and bone mineral density (BMD). Postmenopausal women who satisfied the inclusion criteria in terms of diet (iron intake < 40mg/d) and mean energy intake (± 40% of the RDA) were included in the study. A three day diet record was used to assess the mean nutrient intake. Bone mineral density (BMD) at different sites (lumbar spine L2-L4, trochanter, femur neck, Ward's triangle and total body) was measured using dual energy X-ray absorptiometry (DXA). The BMD measured at each site is taken as a dependent variable and iron as an independent variable to calculate the regression models. Besides adjusting for protein

and/or calcium it was found that high iron was associated with greater BMD at all sites. Women who had a mean consumption of calcium between 800-1200 mg/d and with higher levels of iron intake showed greater BMD at several bone sites. But higher levels of iron intake in women with higher (>1200 mg/d) or lower calcium intakes (<800 mg/d) did not show a distinct effect on BMD. The authors concluded that dietary iron may play more important role in bone mineralization than originally thought and suggested for future studies on the combined effect of dietary iron and calcium on BMD (204).

Maurer et al. (205) observed an association between bone mineral density (BMD) and dietary intakes of iron and calcium. The study was conducted over a period of one year on healthy non-smoking postmenopausal women (mean age 55.6 +/- 4.6 y) undergoing hormone replacement therapy (HRT, n= 116) or those who had not used HRT (n=112). Dietary assessment was performed at 8 randomly assigned days and at different time periods: baseline (3 days), 6^{th} month (2 days) and 12^{th} month (3 days). Mean nutrient intake was recorded. All women were given elemental calcium supplements in the form of calcium citrate. BMD was measured at 5 different sites of the body (Lumbar spine L2-L4, femur trochanter, femur neck, Wards triangle, and total body) using DXA. The effects of iron and calcium intakes on BMD change versus baseline BMD, weight change, exercise, and energy intake was examined by regression analyses. Women were grouped by HRT status and then the interaction of calcium with iron on change in BMD was assessed using tertiles of iron and calcium intake and estimated marginal mean change in BMD. A positive association between iron and BMD was observed in women using HRT at the trochanter and Ward's triangle but not in women who were not on HRT. However, the association between calcium with BMD change was observed at the

trochanter and femur neck. Women on HRT with lowest intake of calcium showed an increase in BMD with the increased iron intake. But in contrast BMD increased with highest calcium intake in women who were not on HRT. The authors concluded that the association between iron and calcium on change in BMD might be influenced by the use of HRT (205).

CHAPTER III

MATERIALS AND METHODS

The experimental design, diet, housing, feeding and necessary protocols are included in this chapter. The protocol for micro computed tomographical analysis of L_5 vertebrae and femora are also included. The statistical analyses for assessing the results are described.

Experimental Design

We received one hundred and twenty-four female Sprague-Dawley weanling rats (SASCO, Kingston, NY) at 21 days of age. Immediately upon arrival the animals were randomized into 4 x 3 diet by treatment groups with 40 rats per treatment and 10 rats per diet except that the extra rats were randomized to the 6 or 150 ppm iron diet in the ovariectomized treatment group. The treatment groups were growing and two ovarian hormone status groups: sham-operated and ovariectomized, respectively. The rats were maintained on commercial rat chow (AIN-93-G diet, Teklad, Madison, WI) and deionized water for three days after arrival. Dietary iron levels were set at 6, 12, 35 and 150 ppm. Animals were maintained on the assigned diet throughout the treatment period. At 18 weeks of age growing rats were killed and bones were collected: ovariectomy was performed to mimic menopause or sham-operated as a control at 18 weeks in the other two groups. After 30 weeks of age both sham-operated and ovariectomized rats were

killed and bones were collected. The experimental design is illustrated in Figure 1. Right femur and fifth lumbar vertebrae were collected and stored in -20^{o} C for analyzing the bone micro-architecture. The study was approved by the Institutional Animal Care and Use Committee (IACUC) at Oklahoma State University (see the approval form in Appendix A).

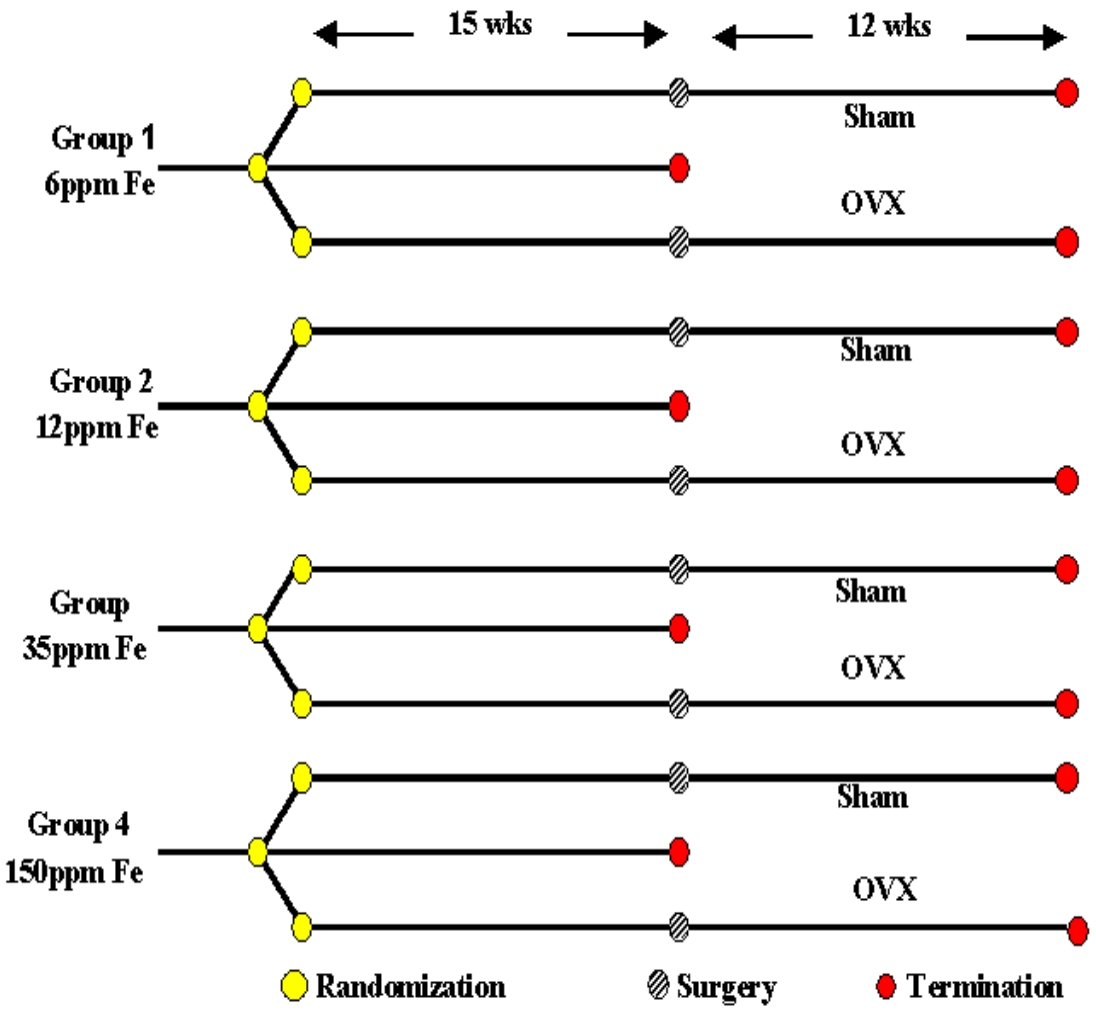

Figure 1: Experimental design

Treatment Protocol

Housing

All the animals were housed in Oklahoma State University Laboratory Animal Resources (LAR) facility in light, temperature and humidity controlled conditions under the supervision of a veterinarian. The animals were maintained under a 12-hour light/dark cycle. The rats were placed in individual plastic cages with raised plastic flour grids. Below the grids a small amount of ground cornhusk bedding was used for waste absorption. Every week all the cages, feed dishes and water bottles were changed.

Diet

For the purpose of this study, all the organic diet components were purchased from Teklad (Madison, WI). Researchers prepared the diet and mineral mixes as per AIN-93G and AIN-93M standards (206) with the exception of iron concentration. The diet composition for the growth and maintenance diets is given in Table 1. Mineral mixes were prepared in one-kilogram batches but a total of 2.5 kg was prepared and mixed from single lots of ingredients, sufficient for the entire experiment. First the macro and micronutrients were weighed and then a burundum fortified porcelain jar was used for combining and mixing the mineral mixes. Four dietary regimens were prepared with two groups containing iron inadequate diets calculated at 6 ppm, 12 ppm, one control group calculated at 35 ppm and one excess level of iron calculated at 150 ppm. But for the purpose of this research, only samples from 6 ppm, 35 ppm and 150 ppm iron fed animals were used. The ingredients and the amount of mineral mixes used for growth and maintenance diets are given in Tables 2 and 3 respectively.

Feeding

To minimize spilling of the diet, animals were fed late in the afternoon. Animals and the remaining diet were weighed twice a week. The diet was weighed and adjusted biweekly based on feed consumption of animals that gained the least weight. Two plastic cups were used for each rat labeled with rat number, diet and treatment. The feed was weighed into the cups twice a week, and the cups were taken to the LAR and stored in the refrigerator until feeding time.

TABLE 1

American Institute of Nutrition 1993 Purified Diet Components for Laboratory Rodents[1]

	Diet Composition	
Component	Growth (AIN-93G, g/kg)	Maintenance (AIN-93M, g/kg)
Corn Starch	397.5	582.10
Casein	200.0	140.0
Dextrinized Corn Starch	132.0	155.0
Sucrose	100.0	100.0
Soybean Oil	70.0	40.0
Cellulose	50.0	50.0
Mineral Mix	35.0	35.0
Vitamin Mix	10.0	10.0
L-Cystine	3.0	1.8
Choline	2.5	2.5

[1]Reeves, et al. (206)d}

TABLE 2

American Institute of Nutrition 1993 Growth Mineral Mix

Component		Growth (AIN-93G, g/kg)
Calcium Carbonate	40.04% Ca	357.00
Potassium Phosphate	22.76 P, 28.73% K	196.0
Potassium Citrate	36.16% K	70.78
NaCl	39.34% Na, 60.66% Cl	73.275
Potassium Sulfate	44.87% K, 18.39% S	46.6
Magnesium Oxide	60.32% Mg	24.0
Zinc Carbonate	52.14% Zn	1.65
Manganous Carbonate	47.79% Mn	0.63
Cupric Carbonate	57.47% Cu	0.30
Potassium Iodate	59.3% I	0.01
Sodium Selenate	41.79% Se	0.01025
Ammonium Paramolybdate	54.34% Mo	0.00795
Sodium Meta-Silicate	9.88% Si	1.45
Chromium Potassium Sulfate	10.42% Cr	0.275
Lithium Chloride	16.38% Li	0.0174
Boric Acid	17.5% B	0.0815
Sodium Fluoride	45.24% F	0.0635
Nickel Carbonate	45% Ni	0.0318
Ammonium Vanadate	43.55% V	0.0066
Levels of Dietary Iron for AIN-93G (Corrected for Amount of Iron in Cellulose)		
	6 ppm	35 ppm	150 ppm
Ferric Citrate g/kg	0.88	5.8883	25.8126
Powdered Sucrose for AIN-93G (Corrected for Amount in Titrated Minerals)		
Sucrose g/kg	217.37	212.36	191.98

TABLE 3

American Institute of Nutrition 1993 Maintenance Mineral Mix

Component		Maintenance (AIN-93M, g/kg)
Calcium Carbonate	40.04% Ca	357.00
Potassium Phosphate	22.76 P, 28.73% K	250.0
Potassium Citrate	36.16% K	28.00
NaCl	39.34% Na, 60.66% Cl	73.275
Potassium Sulfate	44.87% K, 18.39% S	46.6
Magnesium Oxide	60.32% Mg	24.0
Zinc Carbonate	52.14% Zn	1.65
Manganous Carbonate	47.79% Mn	0.63
Cupric Carbonate	57.47% Cu	0.30
Potassium Iodate	59.3% I	0.01
Sodium Selenate	41.79% Se	0.01025
Ammonium Paramolybdate	54.34% Mo	0.00795
Sodium Meta-Silicate	9.88% Si	1.45
Chromium Potassium Sulfate	10.42% Cr	0.275
Lithium Chloride	16.38% Li	0.0174
Boric Acid	17.5% B	0.0815
Sodium Fluoride	45.24% F	0.0635
Nickel Carbonate	45% Ni	0.0318
Ammonium Vanadate	43.55% V	0.0066

Levels of Dietary Iron for AIN-93M (Corrected for Amount of Iron in Cellulose)

	6 ppm	35 ppm	150 ppm
Ferric Citrate g/kg	0.88	5.8883	25.8126

Powdered Sucrose for AIN-93M (Corrected for Amount in Titrated Minerals)

Sucrose g/kg	217.37	212.36	191.98

Water

Rats were given deionized water ad libitum to ensure adequate hydration. Glass bottles with straight stainless steel sipper tubes were used to provide water to animals. Animals were given fresh water thrice a week.

Surgery

At 18 weeks of age rats that were randomized into sham or ovariectomy group were subjected to surgery. Food was with held for 12 hours and water withheld for 6 hours prior to surgery. Animals were anaesthetized by halothane inhalation. Ovaries were removed by ligation in ovariectomized animals. Ovaries were lifted from and then replaced in the body in sham-operated animals. After surgery the animals were continued on their respective dietary regimen.

Necropsy

Necropsy was performed on growing rats when they were 18 weeks of age and bones were collected. Food was withheld prior to killing but deionized water was given. Animals were anesthetized by intraperitoneal injection with 50mg of ketamine and 2.5mg/kg body weight of xylazine. Femur and L_5 vertebrae were collected and stored at -20^0C. Calvarias were collected and stored at-80^0C. The same procedure was adopted for the necropsy and tissue collection of sham-operated and ovariectomized rats at 30 weeks of age.

Analyses

Micro Computed Tomography

Cleaned fifth lumbar vertebrae and right femora were scanned for micro-architecture (Micro-CT 40, SCANCO MEDICAL AG, Zurich, Switzerland, 2001) and

strength analyses were performed. Fifth lumbar vertebrae and right femur of three groups of rats (growing, sham operated and ovariectomized) and three dietary treatments (6ppm, 35ppm and 150ppm of iron as the ferric citrate) were imaged with a desktop μCT, with a voxel size of 16×16×16.5μm and a slice thickness of 0.016mm. CT images were reconstructed in 1024×1024 pixels using a medium resolution. A low pass gaussian filter was applied to remove noise and a fixed threshold was used to extract the structure of mineralized tissue. The apparatus consists of x-ray gun/tube through which the x-rays were generated. These generated x-rays detect a two dimensional charge coupled device (CCD) array with 512/1024/2048 elements. In micro-CT the object is placed in a plastic holder, which is attached to the turntable, and placed in between the x-ray source and CCD camera. After acquiring the data, the object/specimen is rotated a very small angle and is scanned again. This process continues until the table rotates to 360^{o}. The scanned 2D images were stacked and rebuild in the computer to obtain a 3D image. The scout view scan, which measures the overview image, is obtained for selecting the region of bone to scan for 3D imaging. Region / Volume of interest (VOI) were taken for 3D histomorphometric evaluation, which was obtained by contouring. Morphing was done to create VOI for missing objects between two reference lines.

Vertebrae analyses

Five vertebrae were placed in a 20-mm tube for overall scanning and each vertebra was measured separately. The vertebrae were placed in the tube aligning through the foramen using a toothpick to position the bone. The empty space was covered with foam such that the vertebrae did not move within the tube during scanning. The vertebrae were arranged such that the interior facets were placed in the downward direction and the

superior facet is lined up, to match the line on the tube. The vertebrae thus, scanned were then analyzed for trabecular region. A single operator blinded to treatments, contoured the trabecular bone region within the vertebral body for CT slice. Details of the analyses are in Appendix B. The volume of interest (VOI) was thus identified in the trabecular region was subsequently analyzed. Relative bone volume (BV/TV), structural model index (SMI), physiological force (phy_fce), trabecular number (Tb.N), and separation (Tb.Sp) were calculated. Structural indices were assessed by three- dimensional (3D) techniques for trabecular bone.

Data generated by the scanner included the following. The mean and SD were calculated at each time point for trabecular bone structure. Bone volume, structural model index, physiological force, trabecular number and separation were generated. Bone volume (BV) is calculated using tetrahedron corresponding to the enclosed volume of the triangulated surface. Total volume (TV) of the sample was examined as a normalized index. Bone volume/total volume (BV/TV) was used to compare samples of varying size. Structural model Index (SMI) quantifies the plate versus rod-like nature of the cancellous bone such that structures that were purely rod-like have an SMI of three, whereas those that were purely plate-like have an SMI of zero.

Femur analyses

The right femur was placed in a 16-mm tube for overall scanning and the distal femur and midshaft were measured separately. The empty space was covered with foam such that the femur did not move within the tube during scanning. The femur was placed vertically such that the line on the tube was aligned with the anterior side of the femur patellar surface at the bottom of the tube and neck of the femur at the top of the tube. The

distal portion of the femur was scanned by identifying the growth plate, and from the growth plate 350 slices were taken for measurement. The distal femur thus, scanned was then analyzed for trabecular region. The midshaft of the femur was scanned for 34 slices by taking the average of the total femur length. The midshaft of the femur thus, scanned was then analyzed for cortical region by contouring the third and 32nd slice. The contours in between the slices were placed in a semi-automated fashion. Thus, the total number of cortical slices analyzed was always 30. Cortical thickness, cortical porosity, cortical area and medullary area were analyzed for cortical bone.

A single operator blinded to treatments, outlined the trabecular bone region within the distal femur for every 15 slices. Details of the procedure are in Appendix B. All the parameters were taken similar to the vertebrae for understanding the trabecular micro-architecture. Midshaft regions of all the femurs were analyzed by always contouring slice 30 through 1. Detailed descriptions of the μCT procedures are described in Appendix B.

Finite Element Analyses

Micro computed tomography images provide both geometric details and the information about the material properties of bone. This information is used to generate finite element models (142). Finite element analysis was performed by using specialized computer software in which the micro-computed tomography (μCT) histomorphometric data was used to simulate compression of a region of interest of a material. This enables one to determine the behavior of the material in response to the compression. Analyses were performed on the VOI previously identified in the fifth lumbar vertebrae and the distal femur. The data thus, obtained on micro-architecture was subjected to a high friction compression test in the z direction. This provides data on average strain, total

force, physiological force, stiffness, size independent stiffness, and average Von Mises stress of the trabecular bone. This data is used to determine the mechanical properties of the bone specimen. In this study the same scans used for architectural properties were used for FEM analyses. Detailed description of the FEM procedures are described in Appendix C.

Statistical Analyses

Data were analyzed using SAS (version 9.1, SAS Institute, Cary, NC). The completely randomized model was analyzed using the generalized linear model (GLM) procedure in SAS to analyze for effects of dietary iron on bone architecture and strength. Significance level was set at $P \leq 0.05$. Differences of means were tested by LS means.

CHAPTER IV

RESULTS AND DISCUSSION

Growing Rats

Results from bone analyses in growing female rats are presented in this chapter. Of the forty rats randomized to the growing treatment group, only those in diet groups 6, 35 and 150ppm were included in the present study. Only those rats received in the first shipment were included. Thus, bone analyses were conducted on five rats per diet group. The effect of dietary iron on body composition, nutritional adequacy indicators and hematological parameters for these rats are presented. The effects of dietary iron on micro-architectural properties, strength and quality of bones in growing rats are also discussed.

Body Composition

In our study the animals weighed an average of 76 grams initially and 226 grams at the end of the study. No significant differences were observed in either weight among the three diet groups (Table 4). Similar findings were reported in another study (207), in which the effects of marginal and excessive iron on body weight with no significant differences observed among the diet groups at the end of six week and 12 week feeding periods. In contrast to this study (207) and the findings of the present study, Medeiros et al. (11) reported a dramatic decrease in body weight and corresponding food intake in iron deficient rats (< 8mg Fe/kg diet).

TABLE 4

Effects of Dietary Iron on Body Composition and Indicators of Nutritional Adequacy in Growing Rats [1, 2]

Dietary Iron Concentration	Parameter				
	Initial Weight, *g*	Final weight, *g*	Urinary Hydroxyproline, *mmol/L/µmol urinary creatinine*	Serum Creatinine, *mmol/L*	Serum Albumin, *g/L*
6 ppm	82.0 ± 4.58	222.7 ± 6.03	0.004 ± 0.001	45 ± 4	39 ± 1
35 ppm	78.8 ± 4.58	239.4 ± 6.03	0.004 ± 0.001	48 ± 4	39 ± 1
150 ppm	67.4 ± 4.58	240.0 ± 6.03	0.005 ± 0.001	48 ± 4	37 ± 1
Diet	P = 0.0983	P = 0.1114	P = 0.7604	P = 0.8434	P = 0.5314

[1]Values within columns with different superscripts are significantly different ($P \leq 0.05$)
[2] Values in rows are LS means ± SE, n = 15

Although not significant, slight increase in the weight gain among excess fed iron fed rats was observed when compared to low iron fed rats that showed least weight gain. Similar findings were reported in two separate studies (208, 209). In the study of Beard et al. (208) rats were fed two levels of dietary iron, low (< 5 ppm) and adequate iron levels (50 ppm) for 6 weeks. The low iron level iron fed rats gained less weight and had lower final weights compared to iron adequate rats. Lowest body weights were observed in animals maintained on an iron deficient diet (9 ppm) in the study of Stangl and Kirchgessner (209) where rats were fed for 5 weeks. Observations from both the studies indicated lower body weights in male rats maintained on iron deficient diets and are in agreement with our findings.

Indicators of Nutritional Adequacy

We performed serum analyses in order to assess the nutritional status and liver function. No significant effect of dietary iron was observed in creatinine or albumin (Table 4). Although not significant, the albumin levels were lower in high iron fed groups when compared to low and adequate level iron fed groups. However, the albumin levels from all the three groups were lower compared to the normal albumin levels as provided by Harlan (personal communication). These differences could be due to the analytical methods employed for the assessment of albumin levels as other parameters indicate that the animals were growing normally and are fed adequately. Urinary hydroxyproline measured from a final 12 hr collection was corrected for urinary creatinine. Urinary hydroxyproline is an indicator of bone breakdown. Our results show no significant differences in urinary hydroxyproline among the dietary groups.

Hematology

Hematological indicators were used to assess the iron status in all the groups. Since our goal was to induce iron deficiency, excess and adequate iron levels and study their effect on bone micro-architecture it is of importance to ensure that this goal was achieved by examining the red blood cell count (RBC), hemoglobin (HB), hematocrit (HCT) and reticulocyte (RTC) counts. Significant results were observed in all the parameters of HCT, HB, RBC and RTC (Table 5). The rats fed with 6 ppm iron showed significantly lower levels of hemoglobin and HCT when compared to 35 and 150 ppm fed rats. However, no significant differences were observed between the 35 and 150 ppm groups. Besides low levels of hemoglobin and HCT, the 6 ppm fed rats exhibited significantly greater levels of RBC and RTC when compared to 35 ppm and 150 ppm iron fed groups (Table 5). Increased numbers of red blood cells and reticulocytes also confirms iron deficiency. Decreased oxygen carrying capacity is compensated by increased production of immature and mature RBC from the bone marrow. No differences were observed in the leukocyte counts due to dietary treatments, but all animals showed decreased level of WBC than the normal range (210, 211). Similar findings were reported in the study of Stangl and Kirchgessner (209) except for the levels of RBC. Though all the three groups showed an RBC within the normal range (210, 211), significant differences were observed among the groups (Table 5).

In the present study, we observed greater levels of RBC in lowest iron fed group whereas Stangl and Kirchgessner (209) observed the lower levels of RBC in low iron fed group. These differences could be due to the feeding duration as the rats in the current study were fed a longer period (18 weeks vs. 5 weeks) and also differences in dietary iron

TABLE 5

Effects of Dietary Iron on Hematological Status in Growing Rats [1, 2]

Treatment Group	Parameter				
	Hemoglobin, *g/L*	Hematocrit, %	Red Blood Corpuscles, $10^3/mm^3$	White Blood Corpuscles, $10^6/mm^3$	Reticulocytes, $10^6/mm^3$
6 ppm	112 ± 0.5[a]	29 ± 1[a]	9.34 ± 0.33[a]	3.17 ± 0.93	0.433 ± 0.034[a]
35 ppm	143 ± 0.4[b]	38 ± 1[b]	7.27 ± 0.29[b]	3.28 ± 0.83	0.190 ± 0.034[b]
150 ppm	152 ± 0.4[b]	40 ± 1[b]	7.70 ± 0.29[b]	3.70 ± 0.83	0.204 ± 0.030[b]
Reference range	110-180[3, 4]	36-48[3, 4]	7-10 [3,4]	6-17[3]	-
Diet	P = 0.0002	P = 0.0002	P = 0.0016	P = 0.9007	P = 0.0007

[1]Values within columns with different superscripts are significantly different ($P \leq 0.05$)

[2] Values in rows are LS means ± SE, n = 15

[3] Hrapkiewicz, et al. 1998

[4] Young, 1990

concentration because in the present study rats were given 6 ppm as against to 9 ppm in their study (209). The method of counting cells also could have contributed for this difference. We have used the automated instrument for counting cells including reticulocytes, and, therefore, our cell counts may be more reliable as compared to their measurement with coulter counter and hemoglobinometer (209). Conversely, our study findings are similar to two separate studies (212, 213) despite the differences in study duration and gender of animals used in this study. Dallman et al. (212) observed the differences in hematocrit whereas Siimes et al. (213) observed differences in both hematocrit and hemoglobin levels. Both studies have suggested that Sprague-Dawley rats fed very low dietary iron, 2 and 6 ppm iron (212), 7 ppm (213) showed decreased hemoglobin and HCT values.

Our findings on nutritional adequacy indicators as well as hematological indicators suggest that rats were adequately fed for growth and that iron deficiency was induced. No significant differences were observed in weights and albumin level, and the lowest iron fed group was made iron deficient as indicated by HB, HCT, RBC and RTC number. Hence, our goal was met to produce iron deficiency without affecting growth.

Bone Micro-architecture

Bone micro-architecture or the structural arrangement of bone is strongly related to bone strength. Since it is not enough to predict the quality of bone with bone mass, bone micro-architecture assessed by micro-CT is used in this study to observe the effects of dietary iron on bone microstructure and the corresponding changes in biomechanical parameters. This section presents data on fifth lumbar vertebrae, distal femur and cortical data on midshaft of right femur.

Fifth Lumbar Vertebrae

Vertebral trabecular bone parameters varied in growing rats with changes in dietary iron (Table 6). There were no significant differences between groups for bone volume/total volume (BV/TV), Connectivity density (Conn. D), trabecular thickness (Tb.Th) and degree of anisotropy (DA).

Similar results were observed in the structural model index (SMI) of growing rats fed with different levels of dietary iron (Table 6). The SMI describes the three-dimensional trabecular bone properties (8). The trabecular bone can be plate-like, rod-like or true sphere. Hilderbrand et al. (6) suggested that negative SMI values are derived from very dense samples resulting in a concave plate-like structure, also referred to as a spherical void. It is also reported that SMI values can be negative when the trabecular bone is dense and possess concave like structure with over 30% of BV/TV (109). In our study all the dietary groups showed BV/TV greater than 30%. This proposes a strong relation between SMI and BV/TV.

Hildrebrand et al. (6) proposed a negative correlation between SMI and BV/TV. However, a recent study Van Ruijven et al. (112) suggested that as bone volume fraction decreases, the number of plates also decreases. This decrease would be associated with a 40 % reduction in their thickness with an increase in number of rods. The authors concluded that the effect of bone loss on plate-like trabeculae was opposite to its effect on rod-like trabeculae. In our study, we did not see any significant reduction in bone volume fraction and trabecular thickness due to dietary treatment. Also the trabeculae were concave in structure indicating better bone quality and supporting the conclusions of the above study (112).

TABLE 6

Effects of Dietary Iron on L_5 and Distal Femur Bone Architecture in Growing Rats [1, 2]

Parameter		Dietary Iron Concentration 6 ppm	35 ppm	150 ppm	P
Bone Volume Fraction					
	L_5	0.309 ± 0.017	0.353 ± 0.017	0.338 ± 0.017	0.2031
	Femur	0.235 ± 0.026	0.288 ± 0.026	0.284 ± 0.026	0.3130
Connectivity Density, *1/mm*^{3}					
	L_5	52.83 ± 2.98	60.53 ± 2.98	61.40 ± 2.98	0.1235
	Femur	115.54 ± 7.82	108.50 ± 7.82	114.06 ± 7.82	0.8019
Structural Model Index					
	L_5	(-) 0.38 ± 0.209	(-) 0.72 ± 0.209	(-) 0.53 ± 0.209	0.5448
	Femur	1.27 ± 0.207	0.844 ± 0.207	0.864 ± 0.207	0.2972
Trabecular Number, *1/mm*					
	L_5	3.56 ± 0.104^a	3.90 ± 0.104^b	3.96 ± 0.104^b	0.0390
	Femur	4.05 ± 0.273	4.25 ± 0.273	4.51 ± 0.273	0.5160
Trabecular Thickness, *mm*					
	L_5	0.082 ± 0.002	0.085 ± 0.002	0.083 ± 0.002	0.3689
	Femur	0.072 ± 0.004	0.084 ± 0.004	0.081 ± 0.004	0.1443
Trabecular Separation, *mm*					
	L_5	0.277 ± 0.008^a	0.248 ± 0.008^b	0.242 ± 0.008^b	0.0246
	Femur	0.246 ± 0.020	0.241 ± 0.020	0.217 ± 0.020	0.5725
Degree of Anisotropy					
	L_5	1.83 ± 0.024	1.86± 0.024	1.85 ± 0.024	0.7197
	Femur	1.42 ± 0.024^a	1.51 ± 0.024^b	1.50 ± 0.024^b	0.0303

[1]Values within rows with different superscripts are significantly different ($P \leq 0.05$)

[2] Values in columns are LS means ± SE, n = 5

In contrast to our findings on SMI (Table 6), Medeiros et al. (11) reported rod-like properties in iron deficient rats. Bones tend to become more rod-like than plate-like with aging (7, 8, 48). The rats used in the study of Medeiros et al. (11) were much younger (8 weeks of age) than our rats (18 weeks) and were fed only for 5 weeks. Their animals showed rod-like SMI which was suggested as dietary iron effect (11). Since rod-like properties were not observed in our iron deficient rats in spite of being older compared to the rats in Medeiros et al. (11) study, it is not clear if dietary iron affects the SMI. Although the feeding duration was different, rats from their (11) study and our study showed significant reduction in hematocrit levels indicating iron deficiency has been induced. Besides hematocrit number, other parameters we used to assess iron deficiency such as reticulocytes and RBC may be more reliable indicators than heart weight and graying of hair used as indicators by Medeiros et al. (11). Since the animals in the present study were older and were fed for a longer period on an iron-deficient diet, we would also expect rod-like properties in this study. The rats used in our study although fed for longer period are still growing and showed thick and concave trabeculae. Also, we did not see a significant effect of dietary iron on SMI. Hence, age and feeding duration cannot be considered as a factor for these differences. It is not clear if strain differences might have contributed for such difference. Therefore, we cannot offer a possible explanation.

Dietary iron did not show a significant effect on trabecular thickness (Table 6). In contrast to our findings, Medeiros et al. (11) reported significant decrease of trabecular thickness in L_3 vertebrae of iron deficient rats ($P < 0.05$).

In growing rats the trabecular number (Tb. N) increased as the level of dietary iron increased and the average separation or air space (Tb. Sp) decreased as the level of dietary iron increased (Table 6). This suggests that trabecular architecture deteriorates with iron deficiency in growing rats. No significant differences in the trabecular number or separation were observed between 35 ppm and 150 ppm iron fed rats. In these rats it appears that excessive iron was not harmful to bone. Our results are in agreement with the findings of Medeiros et al. (193). No significant changes were observed in other architectural parameters in lumbar vertebrae for connectivity density and degree of anisotropy (Table 6).

Distal Femur

The data on the trabecular bone in distal femur architectural parameters of bone volume fraction (BV/TV), SMI, connectivity density, trabecular number, trabecular thickness and trabecular separation showed no significant effect of dietary iron (Table 6). The trabecular volume varies depending upon the skeletal site. Besides, the amount of cancellous bone also differs in different parts of femur. It is well known that the femur has less trabecular volume and more cortical bone when compared to vertebral bodies (214). Also studies have been reported that loss of trabecular bone will primarily be seen first in the spine region or vertebral body (94). Therefore, this difference in the skeletal sites might have contributed to less dietary iron effect on the femur trabecular bone than vertebrae. Another contributing factor for this less significant effect of iron on femur could be due to the differences in the cancellous bone growth in different skeletal sites. Since the rats were in the growing age, even if there were some loss of trabeculae, the

trabeculae might have been replaced with new ones. The growth of cancellous bone varies in different parts of femur.

It has been reported that, from birth to an age of 6 months, the bones of rats grow rapidly in length and width. Also a progressive increase in the cancellous bone occurs in the metaphyses. This is also supported from the study findings of Osterman et al. (118), in which the rats that were given 14 C-labeled disodium clodronate subcutaneously showed highest activity in the primary sponigiosa of the distal femur metaphysis and in the cortical bone of the femoral diaphysis when compared to the other parts of femur (118).

On the other hand, a significant effect of dietary iron is observed on distal femur degree of anisotropy (Table 6). Degree of anisotropy (DA) describes the material properties of bone in different directions. It is considered that higher degree of anisotropy indicates poorer bone quality (151). However, it is not known what levels are considered detrimental. The degree of anisotropy increased as the dietary iron concentration increased and was significantly lower in rats fed 6 ppm diet than in the 35 and 150 ppm Fe groups. However no significant differences were observed in the distal femur of rats fed recommended level (35 ppm) and excess iron (150 ppm).

The significant effect on DA in femur but not on any other properties of trabecular bone also suggests the growth of cancellous bone in femur diaphysis might have contributed to the replacement of lost trabeculae with new ones. However, this loss of trabeculae might have contributed to changes in the trabecular orientation, thus, affecting the DA. These higher DA values in 35 ppm and 150 ppm iron fed rats suggests that the structure is more anisotropic, and, therefore, some of the trabeculae providing

resistance to stress in preferential directions might be deleted (150). The loss of the preferentially oriented trabeculae affects the mechanical properties of bone (111).

Dietary iron did not affect any architectural properties in femur but affected lumbar bone. Similarly, the architectural property that describes the mechanics of bone (DA) was observed only in femur but not in lumbar bone. Studies have suggested that, any effect due to disease or treatment on the bone would be first noticed in the vertebral trabecular bone (94). Findings on human bones also suggest that, the extra load applied on the vertebral bone would result in the removal of horizontal trabeculae, affecting the mechanical properties of bone as well as the architectural properties (113). However, in our study we observed architectural alterations in vertebrae but no changes in the DA compared to the changes observed in femur. This again proposes the differences between the tissue morphology between human and rat models. Rat, a quadruped animal during movement receives 'cantilever bending' load, therefore the lumbar bone may receive less load compared to femur bone (215). This supports the findings in our study that the horizontal trabeculae might be deleted due to the extra load applied in femur but not in vertebrae. The architectural changes observed in vertebrae but not in femur might be due to the trabecular amount as well as due to the growth observed in femur diaphyses. Greater growth in femoral diaphyses than other parts of the femur and lumbar bone was supported by another study (118).

Interesting effects were observed in the trabecular architecture of lumbar vertebrae and distal femur. Although there were significant differences in the trabecular number, no significant effects were observed in the DA of lumbar vertebrae. On the other hand, the femur showed an increase in DA values although no significant changes were

observed in other architectural parameters. These differences can be understood by the findings of Hing et al. (151) conducted for the bone graft market. They observed that the porous hydroxyapatites with anisotropic characteristics showed lower compressive moduli than the isotropic specimens with the same apparent densities. Probably, the trabeculae in vertebra are more isotropic than the ones in femur because the femur might have replaced the lost trabeculae with the new ones. Therefore, despite having higher density or the thick trabecular bone in femur, there is a possibility of poor quality due to anisotropy resulting in changes in the direction of trabeculae. Our findings on anisotropy are in agreement with the observations of Sugita et al. (143). The authors suggested that mechanical properties of cancellous bone changes with subsequent changes in the direction of load applied. It is also proposed that the anisotropy of trabecular bone is site specific (145-147).

Femur Midshaft

No significant effects were observed in the architectural parameters of cortical bone namely total volume (TV), bone volume (BV), cortical thickness, cortical porosity, cortical area and medullary area (Table 7). Several reasons may be attributed for this unchanged effect in cortical bone of all the three groups of rats fed different levels of dietary iron. When compared to humans, rats show higher cortical bone and lower trabecular bone. Also in contrast to human bones, rats show an evenly distributed cortical and trabecular bone in different parts of the femur. Rats through a process of 'modeling dependent periosteal apposition' have the ability to adjust the cortical thickness and increase inertia (216). Another contributing factor may be minimal Haversian remodeling in cortical bone of rats. The reduced rate of Haversian remodeling decreases cortical

TABLE 7

Effects of Dietary Iron on Femur Midshaft Cortical Bone Architecture in Growing Rats [1, 2]

Parameter	Dietary Iron Concentration			P
	6 ppm	35 ppm	150 ppm	
Total Volume, mm^3	2.37 ± 0.076	2.59 ± 0.076	2.58 ± 0.076	0.1044
Bone Volume, mm^3	2.35 ± 0.075	2.57 ± 0.075	2.55 ± 0.075	0.1069
Cortical Thickness, *mm*	0.615 ± 0.012	0.646 ± 0.012	0.629 ± 0.012	0.2292
Cortical Porosity, *%*	0.009 ± 0.001	0.008 ± 0.001	0.010 ± 0.001	0.3106
Cortical Area, mm^2	5.08 ± 0.162	5.56 ± 0.162	5.53 ± 0.162	0.1609
Medullary Area mm^2	0.044 ± 0.005	0.046 ± 0.005	0.059 ± 0.005	0.2138

[1]Values within rows with different superscripts are significantly different ($P \leq 0.05$)

[2] Values in columns are LS means ± SE, n = 5

porosity (186). Also cortical bone is more inert than trabecular bone. In contrast to our findings, reduced width and area of cortical bone was observed by Medeiros et al. (15) in another study conducted on iron deficient rats.

Biomechanical Testing

Fifth lumbar and distal femur

Finite element analyses take into account both geometrical and material properties in producing values for strength parameters. Therefore, we used finite element analyses to assess the mechanical properties of bone. The μCT data was used to generate finite element models and to determine the behavior of the material in response to compression. Both fifth lumbar and distal femur were analyzed for strength parameters of physiological force, average strain, stiffness, size independent stiffness, Von Mises stresses and average cross section area for understanding bone biomechanics.

Our findings on the mechanical properties of lumbar vertebrae showed significant influences of dietary iron (Table 8). As the level of dietary iron increased the amount of physiological force required to crush the bone increased. The iron deficient rats (6 ppm) required significantly less force for compressing and crushing bone than those fed the recommended (35 ppm) or high iron (150 ppm) diets. However no significant differences were observed between the rats fed recommended level of dietary iron and excess iron. A similar trend was also observed in other strength parameters of average strain, bone stiffness and size-adjusted stiffness. This indicates that as the concentration of dietary iron increased the bone showed increased ability to withstand stress and strain. The rats fed an iron deficient diet had the greatest Von Mises stress within L_5 when the force was applied, followed by rats fed recommended level of iron and excess level of dietary iron.

TABLE 8

Effects of Dietary Iron on L_5 and Distal Femur Strength in Growing Rats[1, 2]

Parameter		Dietary Iron Concentration 6 ppm	35 ppm	150 ppm	P
Physiological Force, *N*					
	L_5	14.94 ± 1.09^a	18.70 ± 1.09^b	19.94 ± 1.09^b	0.0177
	Distal femur	18.24 ± 4.86	27.70 ± 4.86	26.75 ± 4.86	0.3500
Average Strain					
	L_5	0.347 ± 0.012^a	0.389 ± 0.012^b	0.391 ± 0.012^b	0.0340
	Distal femur	0.241 ± 0.028	0.282 ± 0.028	0.281 ± 0.028	0.5230
Stiffness, *N/m x 10^4*					
	L_5	$121.9 \times 10^4 \pm 8.2^a$	$152.8 \times 10^4 \pm 8.2^b$	$162.3 \times 10^4 \pm 8.2^b$	0.0110
	Distal femur	$246.9 \times 10^4 \pm 65.8$	$374.9 \times 10^4 \pm 65.8$	$362.2 \times 10^4 \pm 65.8$	0.3499
Size independent Stiffness, *N/m*					
	L_5	1110 ± 69^a	1432 ± 69^b	1377 ± 69^b	0.0143
	Distal femur	620 ± 150	906 ± 150	840 ± 150	0.3989
Von Mises, *Mpa*					
	L_5	36.28 ± 1.54^a	31.44 ± 1.54^b	29.57 ± 1.54^b	0.0252
	Distal femur	13.61 ± 1.73	10.58 ± 1.73	9.32 ± 1.73	0.2373
Average Cross Section Area, *mm^2*					
	L_5	4.49 ± 0.250	4.36 ± 0.250	4.86 ± 0.250	0.3693
	Distal femur	9.79 ± 0.270	9.98 ± 0.270	10.61 ± 0.270	0.1212

[1]Values within rows with different superscripts are significantly different ($P \leq 0.05$)

[2] Values in columns are LS means ± SE, n = 5

The rats fed with 35 ppm and 150 ppm showed lower stress suggesting better integrity and structural compensations. No significant differences were observed among recommended and excess iron fed groups (Table 8). Our findings were similar to the study of Medeiros et al. (11) despite the differences in the duration of the study and their lack of an excess iron fed group. Their study (11) showed the significant effect of iron deficiency on bone strength even when rats were fed only for 5 weeks.

In contrast to our findings on lumbar vertebrae distal femur showed no statistically significant effects on any of the mechanical properties of bone (Table 8). Several factors might have contributed for less vertebral strength when compared to femur. Findings of Guo et al. (108) suggest that the trabecular tissue is 20-30 % less stiff than cortical bone tissue. Their experiments on fatigue resistance of trabecular and cortical bone suggested that cortical bone tissue has higher fatigue resistance than trabecular bone tissue. The authors proposed that these differences could be due to the differences in tissue morphology (108). In another study, loads on the rat femoral neck showed more withstanding ability due to cortical bone than cancellous bone (124). Besides, rats differ in the microstructure such as minimal Haversian systems contributing to less bone remodeling (184, 185). The vertebral body and femur of rat receive different loads and stress when compared to humans, as rats are quadrupeds.

In summary, the trabecular bone architecture was affected by dietary iron. However, changes were seen more consistently in lumbar bone than in distal femur metaphyses, and none were seen in cortical mid-diaphyses region. Earlier studies have suggested that the amount of trabecular bone differs from site to site. The neck of the femur contains 25 % trabecular bone, whereas in a vertebral body the percentage ranges

from 66% to 90% (94). Therefore, loss of trabecular bone will primarily be seen first in the spine region or vertebral body. Consequently in our study changes were also observed more significantly in the trabecular region of lumbar bone than in femur. At the age of 6 months in rats the distal femur metaphyses shows progressive growth in cancellous bone. Therefore, the loss of trabeculae or deterioration of trabeculae might have been prevented by the growth activity. Conversely, the DA of distal femur indicated that dietary iron has influenced the trabecular direction but not in lumbar bone. This could be due to the greater load applied on femur than lumbar bone during locomotion. No significant alterations were observed in the cortical bone architecture. In the lumbar bone, iron deficiency appears to be detrimental for trabecular bone architecture.

The findings in our study on both lumbar and femur trabecular architectural parameters (Table 6) suggest poor trabecular bone quality in lumbar bone but not in femur in iron deficient rats. This is because vertebral bone is composed of more trabecular bone than femur. The strength analysis performed by μCT using FEM involves only the use of trabecular bone. Therefore, we would expect to see better and greater strength in femur but less strength in lumbar bone as suggested by trabecular micro-architecture. Our data on strength analysis (Table 8) also confirms the same as evidenced by trabecular architecture (Table 6). Stress and strain were observed to be higher in 6 ppm diet group. The physiological force was less in low iron fed group. However no significant differences were observed between adequate and high iron fed groups. This indicates that the strength parameters are affected by dietary iron in lumbar bone but not femoral bone and that iron deficiency is detrimental to lumbar bone. With no differences found for any of these variables between the recommended iron level (35 ppm) and high

iron level, we do not see detrimental effects of high iron intakes during periods of rapid growth in female rats.

CHAPTER V

RESULTS AND DISCUSSION

Sham-operated and Ovariectomized Rats

In this section, results on sham-operated and ovariectomized rats fed different levels of dietary iron are presented. Out of one hundred twenty-four female Sprague Dawley rats, forty rats or forty-four were randomly assigned to two groups: sham-operated and ovariectomized, respectively, and were fed with one of four levels of dietary iron (6 ppm, 12 ppm, 35 ppm and 150 ppm). However, for this study the analyses were performed only on bones of those rats that were received from the first shipment and three dietary regimens (6 ppm, 35 ppm and 150 ppm). Thus, five samples were analyzed from each group except for 6 and 150 ppm OVX where the total number of rats analyzed was four. The effect of dietary iron on body composition, nutritional adequacy indicators and hematological parameters are discussed. Also effects of dietary iron on micro-architectural properties, strength and quality of sham-operated and ovariectomized rats are presented.

Body Composition

Animals in both the surgical treatments (sham-operated and OVX) initially weighed an average of 75 grams (Table 9). No differences were observed due to diet, treatment or interaction. However a tendency towards diet effect on initial body weight ($p = 0.0882$) that was actually due to randomization was observed (Table 9). Weight gain by the end of the experiment showed significant differences between the groups. On

TABLE 9

Effects of Dietary Iron, Treatment, Diet and Treatment Interactions on Body Composition, Indicators of Nutritional Adequacy in Sham and Ovariectomized Rats [1, 2]

Treatment Group	Parameters				
	Initial Weight, *g*	Final weight, *g*	Urinary Hydroxyproline, *mmol/L/12hours*	Serum Creatinine, *mmol/L*	Serum Albumin, *g/L*
Sham-operated					
6 ppm	70.42 ± 3.60	257.28 ± 6.92	0.006 ± 0.001	52 ± 4	41 ± 1
35 ppm	71.54 ± 3.00	256.62 ± 6.92	0.004 ± 0.001	45 ± 4	42 ± 1
150 ppm	79.42 ± 3.00	246.18 ± 6.92	0.007 ± 0.001	50 ± 4	43 ± 1
Ovariectomized					
6 ppm	71.65 ± 2.74	266.32 ± 6.32	0.007 ± 0.001	49 ± 3	37 ± 1
35 ppm	77.20 ± 2.10	266.30 ± 6.92	0.004 ± 0.001	49 ± 4	37 ± 1
150 ppm	76.24 ± 2.10	280.18 ± 6.92	0.006 ± 0.001	48 ± 4	39 ± 1
Trt	P = 0.6130	P = 0.0042	P = 0.2138	P = 0.9220	P = 0.0002
Diet	P = 0.0882	P = 0.9658	P = 0.1399	P = 0.5865	P = 0.3253
Diet * Trt	P = 0.3529	P = 0.1378	P = 0.4670	P = 0.5993	P = 0.9875

[1]Values within columns with different superscripts are significantly different ($P \leq 0.05$)

[2] Values in rows are LS means ± SE, n = 31

average the sham-operated rats gained 179 grams with a final weight of 253 grams. Whereas, the ovariectomized rats gained 196 grams on average during the study and weighed on an average of 270 grams by the end of the study. These weight differences were due to significant effect of treatment (Table 9). No significant diet effects were observed on weight gain or final weight. In contrast to our findings, Stangl and Kirchgessner (209) observed lowest weight gain in the lowest dietary iron fed OVX rats.

Indicators of Nutritional Adequacy

Serum analyses were performed in both sham-operated and OVX animals to assess the nutritional status and liver function. No significant effects of dietary iron or diet × treatment interactions were observed for creatinine or albumin (Table 9). However, treatment effects were observed for serum albumin levels. Serum albumin levels were normal in sham. However, in OVX rats all the three iron groups showed a decrease in albumin levels. Studies have reported reduction in serum albumin levels after ovariectomy (71, 74, 172). This reduction in serum albumin levels may be associated with inflammation (72-74). Estrogen deficiency increases the production of pro-inflammatory cytokines IL-1, IL-6 and TNF-α (69, 70). Therefore, increased pro-inflammatory cytokines may result in lowered albumin levels. The lowered albumin levels observed in the OVX animals in the present study might be due to the estrogen deficiency. No significant effect of diet, treatment or interaction was observed for urinary hydroxyproline.

Hematology

Hematological indicators were used to assess the effect of diet, treatment and interactions in both sham-operated and ovariectomized animals. Although not significant,

a tendency towards diet effect ($P<0.07$) was observed on hemoglobin levels in both the experimental groups and in different iron concentrations (Table 10). The lowest hemoglobin levels were observed in 6 ppm groups (Table 10). However, all the three groups showed hemoglobin levels within the reference range (210). Our findings on hemoglobin levels at different iron concentrations were also supported by the findings of Shah and Belonje (207). Both male and female rats were used in the study but were fed with marginal (25 ppm), adequate (47 ppm) high (1260 ppm) or excessive iron for 6 and 12 weeks. Despite the normal levels of hemoglobin reported in our study and theirs (207), animals receiving lowest dietary iron concentration exhibited lower levels of hemoglobin. Reticulocyte counts also tended ($P = 0.095$) to be higher in the 6 ppm groups (Table 10). The combined hemoglobin concentrations and reticulocyte counts suggest that the iron deficiency achieved in the low iron groups was maintained even with the loss of ovarian hormone function (Table 10).

A treatment effect was observed on the hematocrit and WBC (Table 10). Lowest hematocrit levels were observed in sham-operated animals. Similarly, leukocyte counts were affected by treatment but not by diet or interaction (Table 10). Lower leukocyte values were observed in sham-operated animals. Furthermore, leukocyte counts in both treatment groups were below the reference range. Elevated levels of leukocytes have previously been found following ovariectomy (217, 218, 210). Similar findings were reported on WBC count among different dietary groups by Stangl and Kirchgessner (209).

In summary, all the nutrition indicators suggest that both the sham-operated and and OVX animals were fed adequately. No differences in weight gain due to diet was

TABLE 10

Effects of Dietary Iron, Treatment, Diet and Treatment Interactions on Hematological Status in Sham and Ovariectomized Rats [1, 2]

Treatment Group	Parameter Hemoglobin, *g/L*	Hematocrit, %	Red Blood Corpuscles, $10^3/mm^3$	White Blood Corpuscles, $10^6/mm^3$	Reticulocytes, $10^6/mm^3$
Sham-operated					
6 ppm	136 ± 0	36.78 ± 0.86	8.04 ± 0.30	3.08 ± 0.74	0.308 ± 0.030
35 ppm	147 ± 0	38.92 ± 0.96	7.65 ± 0.34	2.35 ± 1.17	0.206 ± 0.034
150 ppm	144 ± 0	38.12 ± 0.96	7.56 ± 0.34	2.82 ± 0.83	0.221 ± 0.039
Ovariectomized					
6 ppm	143 ± 0	38.72 ± 0.96	8.29 ± 0.34	4.77 ± 0.83	0.258 ± 0.034
35 ppm	151 ± 0	40.17 ± 1.11	7.42 ± 0.39	7.20 ± 0.95	0.216 ± 0.039
150 ppm	149 ± 0	40.52 ± 0.96	7.55 ± 0.34	4.05 ± 0.83	0.215 ± 0.034
Trt	P = 0.1148	P = 0.0310	P = 0.9980	P = 0.0029	P = 0.5999
Diet	P = 0.0683	P = 0.1487	P = 0.1197	P = 0.3968	P = 0.0950
Diet * Trt	P = 0.8969	P = 0.8468	P = 0.7718	P = 0.1693	P = 0.6716

[1]Values within columns with different superscripts are significantly different ($P \leq 0.05$)

[2] Values in rows are LS means ± SE, n = 31

observed in OVX animals. Also, the all the three diet groups in OVX showed a decrease in albumin levels. This reduction in albumin levels in OVX might be due to the estrogen deficiency, but may not be due to dietary changes, since we observed only treatment effect in reducing the albumin levels significantly. Several studies have supported that reduction in serum albumin levels is associated with inflammation (72-74) and that estrogen deficiency increases pro-inflammatory cytokines, IL-1, IL-6 and TNF-α production (69, 70). Thus, our findings on nutritional adequacy indicators suggest that were adequately fed although changes were observed in some of these parameters due to treatment effect. Iron deficiency was maintained in the 6 ppm rats as indicated by hematological parameters.

Bone Micro-architecture

Fifth Lumbar Vertebrae

Significant differences were observed in the vertebra of both sham and ovariectomized rats. The effect of treatment and also an interaction between diet and treatment was observed in the trabecular region of vertebrae (Table 11). The effect of treatment showed a statistically significant effect on BV/TV, SMI, Tb.N, and DA. No significant differences due to treatment were observed in the trabecular thickness, trabecular separation and connectivity density. Sham-operated rats showed greater bone volume and greater trabecular number compared to ovariectomized (OVX) rats. Higher Tb.N and also higher BV/TV in sham indicate better quality of bone. The lower Tb.N and lower BV/TV in OVX indicating poor bone quality may be due to erosion of trabeculae by osteoclasts. The structural model index in sham-operated rats showed negative values indicating more concave trabeculae whereas the SMI of OVX rats indicated more rod-

TABLE 11

Effects of Dietary Iron, Treatment, Diet and Treatment Interactions on L5 Bone Architecture in Sham and Ovariectomized Rats[1, 2]

Treatment Group	Architectural Parameter						
	BV/TV	Conn. D, *1/mm3*	SMI	Tb. N, *1/mm*	Tb.Th, *mm*	Tb.Sp, *mm*	DA
Sham-operated							
6 ppm	0.354 ± 0.021	40.48 ± 4.56[a]	(-) 0.940 ± 0.212	3.68 ± 0.15	0.092 ± 0.003	0.266 ± 0.014	1.73 ± 0.03
35 ppm	0.377± 0.021	48.65 ± 4.56[a]	(-) 1.108 ± 0.212	3.94 ± 0.15	0.091± 0.003	0.245 ± 0.014	1.84 ± 0.03
150 ppm	0.336 ± 0.021	62.96 ± 4.56[b]	(-) 0.484 ± 0.212	3.91 ± 0.15	0.084 ± 0.003	0.246 ± 0.014	1.80 ± 0.03
Ovariectomized							
6 ppm	0.288 ± 0.021	51.38 ± 4.56[ab]	0.068 ± 0.212	3.38 ± 0.15	0.085 ± 0.003	0.288 ± 0.014	1.80 ± 0.03
35 ppm	0.257± 0.024	49.37 ± 5.10[a]	0.448 ± 0.237	3.20 ± 0.17	0.084 ± 0.003	0.306 ± 0.015	1.82± 0.03
150 ppm	0.288 ± 0.024	45.52 ± 5.10[a]	0.159 ± 0.237	3.26 ± 0.17	0.089 ± 0.003	0.294 ± 0.015	1.84 ± 0.03
Trt	P = 0.0003	P = 0.6223	P = 0.0001	P = 0.0002	P = 0.2350	P = 0.2350	P = 0.0011
Diet	P = 0.9237	P = 0.2283	P = 0.4676	P = 0.9287	P = 0.8454	P = 0.8747	P = 0.0884
Diet * Trt	P = 0.2712	P = 0.0214	P = 0.1474	P = 0.3391	P = 0.1321	P = 0.3589	P = 0.3377

[1]Values within columns with different superscripts are significantly different ($P \leq 0.05$)

[2] Values in rows are LS means ± SE, sham 6, 35, 150 ppm and OVX 6 ppm n = 5, OVX 35 and 150 ppm n = 4

like than the sham. This suggests that plate-like trabeculae decreased along with a decrease in bone volume fraction. This is also supported by other studies (112, 219). Hildrebrand et al. (6) proposed a negative correlation between SMI and BV/TV. However, a recent study Van Ruijven et al. (112) suggested that as bone volume fraction decreases, the number of plates also decreases. This bone volume fraction decrease would also be associated with a 40 % reduction in the thickness of trabeculae with an increase in the number of rods. The authors concluded that the effect of bone loss on plate-like trabeculae was opposite to its effect on rod-like trabeculae.

Further, the DA was significantly affected by treatment. Higher DA values were observed in OVX when compared to sham. This indicates that OVX rats show poorer bone quality than sham (151, 152). These higher DA values suggests that the structure is more anisotropic, and, therefore, some of the trabeculae providing resistance to stress in preferential directions might be deleted (150). The loss of the preferentially oriented trabeculae results in lower quality bone (150). The loss of trabeculae in preferential direction affects the mechanical properties of bone (111). Similar to the findings in the current study, earlier studies have established that estrogen deficiency is detrimental to bone architecture (76-79).

No significant dietary iron effects were observed for any L_5 bone architecture variables (Table 11). Nevertheless, a trend towards a significant effect of iron on DA ($P = 0.0884$) was observed. The trend supported the iron deficient state (6 ppm) was less anisotropic than the other diets. The presence of rod-like properties exhibited by trabeculae in OVX and the trend observed in DA due to diet indicates poorer bone quality

in the recommended and high iron diets. Nonetheless, other indicators of architectural properties were not affected by dietary iron.

On the other hand, diet and treatment interactions exhibited a significant effect on connectivity density (Table 11). The connectivity density increased in sham-operated rats with an increase in dietary iron concentration. Greater connectivity density may be good if other architectural properties are in agreement with connectivity density. However, when lower bone volume fraction and greater DA are observed, greater connectivity density may also indicate poor bone quality. Greater connectivity density observed in the 150 ppm sham in spite of poor architectural properties suggest that the connections between trabeculae may be numerously broken. These broken trabeculae might have contributed for greater amount of trabeculae per millimeter when counted numerically. In the present study, significant increase in connectivity density was observed in sham150 ppm iron group when compared to 6 ppm and 35 ppm sham and 35 and 150 ppm OVX. This suggests that excess iron is detrimental to sham-operated rats and that deficiency or adequate levels of iron may be beneficial. Also the connectivity density in 150 ppm sham was significantly higher than 150 ppm OVX suggesting that ovarian hormone presence along with high iron after rapid growth achievement is not protective. There were no differences found between sham 150 ppm and 6 ppm OVX. No significant diet and treatment interactions were observed in other architectural parameters.

Distal Femur

Treatment showed a significant effect on the micro-architectural properties in distal femur (Table 12). The BV/TV, connectivity density, SMI and trabecular number were significantly greater with less trabecular separation in sham-operated rats than

TABLE 12

Effects of Dietary Iron, Treatment, Diet and Treatment Interactions on Distal Femur Bone Architecture in Sham and Ovariectomized Rats [1, 2]

Treatment Group	Architectural Parameter						
	BV/TV	Conn. D, *1/mm3*	SMI	Tb. N, *1/mm*	Tb. Th, *mm*	Tb. Sp, *mm*	DA
Sham-operated							
6 ppm	0.256 ± 0.022	95.30 ± 8.36	0.976 ± 0.149	4.09 ± 0.22	0.077 ± 0.003	0.241 ± 0.045	1.39 ± 0.026
35 ppm	0.246 ± 0.022	100.19 ± 8.36	1.074 ± 0.149	4.11 ± 0.22	0.073 ± 0.003	0.238 ± 0.045	1.43 ± 0.026
150 ppm	0.247± 0.022	119.47 ± 8.36	1.166 ± 0.149	4.42 ± 0.22	0.071 ± 0.003	0.218 ± 0.045	1.44 ± 0.026
Ovariectomized							
6 ppm	0.130 ± 0.022	43.39 ± 8.36	1.837 ± 0.149	1.77 ± 0.22	0.077 ± 0.003	0.651 ± 0.045	1.45 ± 0.026
35 ppm	0.110 ± 0.025	35.50 ± 9.35	2.08 ± 0.166	1.46 ± 0.24	0.080 ± 0.004	0.733 ± 0.050	1.45 ± 0.029
150 ppm	0.133 ± 0.025	38.82 ± 9.35	1.785 ± 0.166	1.66 ± 0.24	0.080 ± 0.004	0.640 ± 0.050	1.51 ± 0.029
Trt	P < 0.0001	P < 0.0001	P < 0.0001	P < 0.0001	P = 0.0922	P < 0.0001	P = 0.0378
Diet	P = 0.7877	P = 0.3952	P = 0.5476	P = 0.5473	P = 0.9522	P = 0.4889	P = 0.1357
Diet * Trt	P = 0.9035	P = 0.2703	P = 0.4758	P = 0.5885	P = 0.3994	P = 0.6214	P = 0.5263

[1]Values within columns with different superscripts are significantly different ($P \leq 0.05$)

[2] Values in rows are LS means ± SE, sham 6, 35, 150 ppm and OVX 6 ppm n = 5, OVX 35 and 150 ppm n = 4

OVX. A trend towards significant effect was observed in trabecular thickness. The SMI of sham-operated rats exhibited more plate-like properties than OVX rats indicating poorer trabecular properties in OVX. The distal femur DA of OVX was also greater indicating poorer bone structure. No significant diet effects or diet and treatment interactions were observed in distal femur (Table 12). Based on these architectural variables BV/TV, connectivity density, SMI, trabecular number, trabecular separation and DA, it can be concluded that estrogen deficiency is detrimental to trabecular bone architecture in the femur as confirmed by several studies (76-79). The sham-operated rats showed better bone quality than ovariectomized rats, which could be due to the inhibition of osteoclasts by the estrogen present in sham-operated rats preventing bone resorption. It is reported that estrogen inhibits the bone resorbing cells by inducing apoptosis (66).

Femur Midshaft

The treatment effect on cortical bone of femur showed no significant effect on total volume, bone volume, cortical thickness, cortical porosity, cortical area and medullary area (Table 13). No significant differences were observed in rats fed with different dietary iron concentrations (Table 13). Similarly, no significant differences were observed in diet and treatment interactions on any of the micro-architectural parameters (Table 13). These results suggest that cortical bone is less sensitive to ovariectomy and dietary iron due to the slower remodeling rate of cortical bone as compared to trabecular bone (94). This slower remodeling rate of cortical bone may be due to several contributing factors. Cortical bone has less remodeling surface than trabecular bone (108). Also cortical bones possess fewer number of bone remodeling cells when compared to trabecular bone. More importantly, cortical bone has less blood supply than

TABLE 13

Effects of Dietary Iron, Treatment, Diet and Treatment Interactions on Femur Midshaft Cortical Bone Architecture in Sham and Ovariectomized Rats[1, 2]

Treatment Group	Architectural Parameter					
	TV, mm^3	BV, mm^3	Co. Th, *mm*	Co. P, *%*	Co. Area, mm^2	M. Area, mm^2
Sham-operated						
6 ppm	2.70 ± 0.11	2.68 ± 0.11	0.699 ± 0.018	0.008 ± 0.001	5.81 ± 0.230	0.050 ± 0.004
35 ppm	2.85 ± 0.11	2.82 ± 0.11	0.693 ± 0.018	0.009 ± 0.001	6.11 ± 0.230	0.059 ± 0.004
150 ppm	2.60 ± 0.11	2.57 ± 0.11	0.651 ± 0.018	0.010 ± 0.001	5.57 ± 0.230	0.053 ± 0.004
Ovariectomized						
6 ppm	2.77 ± 0.11	2.75 ± 0.11	0.663 ± 0.018	0.008 ± 0.001	5.94 ± 0.230	0.048 ± 0.004
35 ppm	2.78 ± 0.12	2.75 ± 0.12	0.691 ± 0.020	0.009 ± 0.001	5.96 ± 0.258	0.055 ± 0.004
150 ppm	2.91 ± 0.12	2.89 ± 0.12	0.689 ± 0.020	0.010 ± 0.001	6.23 ± 0.258	0.060 ± 0.004
Trt	P = 0.2859	P = 0.2852	P = 0.9903	P = 0.6896	P = 0.2852	P = 0.8462
Diet	P = 0.7630	P = 0.7749	P = 0.5149	P = 0.1437	P = 0.7749	P = 0.1028
Diet * Trt	P = 0.2500	P = 0.2551	P = 0.1561	P = 0.9668	P = 0.2551	P = 0.4638

[1]Values within columns with different superscripts are significantly different ($P \leq 0.05$)

[2] Values in rows are LS means ± SE, sham 6, 35, 150 ppm and OVX 6 ppm n = 5, OVX 35 and 150 ppm n = 4

trabecular bone. This makes it possible for less exposure to hormones and systemic factors that affect bone remodeling. In addition, minimal Haversian systems in rat cortical bone (186) also might have contributed for lack of cortical bone response towards diet or treatment or both.

Biomechanical Testing

Biomechanical properties of bone were assessed using finite element modeling. Finite element models were generated using the μCT analyses and the material properties of the bone in response to compression were predicted. Both fifth lumbar vertebrae and distal femora were analyzed for strength parameters of physiological force, average strain, stiffness, size independent stiffness, Von Mises stresses and average cross section area.

Fifth Lumbar Strength

Our findings on the mechanical properties of lumbar vertebrae showed significant influence of treatment (Table 14). The physiological force required for compression of vertebra were significantly greater in sham compared to OVX. Similarly, average strain, stiffness, and size independent stiffness were also greater in sham compared to OVX. Yet no significant differences were observed in average cross section area of sham and OVX rats. This suggests that the size of the bone was not changed due to ovariectomy. No significant diet effects were observed in the biomechanical indicators of physiological force, strain, stiffness, average cross section area except Von Mises stresses in sham-operated and OVX rats. The Von Mises stresses were significantly lower in 150ppm group when compared to 6 and 35 ppm iron levels. However, no significant differences were observed between 6 and 35 ppm groups. Similarly, the diet and treatment

TABLE 14

Effects of Dietary Iron, Treatment, Diet and Treatment Interactions on L5 Strength in Sham and Ovariectomized Rats[1, 2]

Treatment Group	Strength Parameter					
	Physiological Force, *N*	Average Strain	Stiffness, *N/m x 10* ^{4}	Size independent Stiffness, *N/m*	Von Mises, *Mpa*	Average Cross Section Area, mm^2
Sham-operated						
6 ppm	18.90 ± 2.03	0.341 ± 0.021	147.6 x 10^4 ± 14.8	1263.5 ± 135.9	17.05 ± 1.64^{ac}	4.98 ± 0.18
35 ppm	21.35 ± 2.03	0.383 ± 0.021	161 x 10^4 ± 14.8	1503.7 ± 135.9	16.85 ± 1.64^{ac}	4.72 ± 0.18
150 ppm	18.22 ± 2.03	0.363 ± 0.021	139.5 x 10^4 ± 14.8	1280.9 ± 135.9	18.96 ± 1.64^{a}	4.71 ± 0.18
Ovariectomized						
6 ppm	14.62 ± 2.03	0.307 ± 0.021	107.2 x 10^4± 14.8	935.3 ± 135.9	21.16 ± 1.64^{a}	5.20 ± 0.18
35 ppm	12.11 ± 2.03	0.316 ± 0.021	89.6 x 10^4± 14.8	801.4 ± 135.9	25.88 ± 1.64^{b}	4.75 ± 0.18
150 ppm	15.12 ± 2.62	0.341 ± 0.027	111 x 10^4 ± 19.2	1013.4 ± 175.4	12.52 ± 2.12^{c}	4.96 ± 0.23
Trt	P = 0.0044	P = 0.0338	P = 0.0014	P = 0.0013	P = 0.1293	P = 0.2833
Diet	P = 0.9992	P = 0.3752	P = 0.9871	P = 0.9143	P = 0.0161	P = 0.1494
Diet * Trt	P = 0.3207	P = 0.5869	P = 0.3817	P = 0.2677	P = 0.0010	P = 0.8206

[1]Values within columns with different superscripts are significantly different ($P \leq 0.05$)

[2] Values in rows are LS means ± SE, sham 6, 35, 150 ppm and OVX 6 ppm n = 5, OVX 35 and 150 ppm n = 4

interactions affected Von Mises stresses significantly.

Von Mises stresses, an indicator of the amount of stress within a bone when a force is applied. Diet and treatment interactions showed significant effects such that the 35 ppm OVX showed significantly greater stress than any other diet and treatment group. The 150 ppm OVX showed the lowest stress compared to the 6 and 35 ppm OVX and the 150 ppm sham. This suggests that, with the increase in iron levels, stress with in the bone also increased in sham-operated rats, thus altering the internal structure of the bone. The findings on sham mechanical properties are in agreement with the architectural properties. However, the OVX rats showed lower stress in high iron group indicating lower stress and internal structural compensations. In contrast the architectural properties of OVX (connectivity density, DA and SMI) suggest that high iron was detrimental. This suggests that with estrogen deficiency, structural compensations occur internally, thereby, reducing the stress in bone. Although, 35 ppm OVX showed greater stress and 150 ppm OVX lower stress than other groups, other architectural properties suggest no significant differences in both the groups (BV/TV, DA and connectivity density). Studies have suggested that a bone with greater BV/TV, distributes stress uniformly. Uniform distribution of stress damages the tissue uniformly rather than at one specific point. Also, unevenness of the stress occurs if there is a decrease in the connectivity and BV/TV (219). In our study, we observed deceased connectivity density and lower BV/TV in 150ppm and 35 ppm OVX animals. However, the present study did not determine the stress distribution in the vertebral bone. Nonetheless, studies have suggested that lower stress can cause loss of cortical bone and more specifically the trabecular bone and thereby, affecting the homeostasis of normal bone mass maintenance (220). In the present

study, we observed greater loss of trabecular bone and lower stress in 150 ppm OVX when compared to other groups. This suggests that, Von Mises stresses alone cannot be considered as an indicator of the over all bone quality. Because, all the architectural parameters and strength parameters indicate that, OVX had poor bone quality when compared to sham and that greater levels of iron was detrimental to sham and OVX.

Distal Femur Strength

Treatment showed significant effect on the strength of distal femur (Table 15). The physiological force was significant due to treatment. Greater force was required to compress or crush the bone of sham compared to OVX indicating poor bone quality in OVX. Similarly, the strain and size adjusted stiffness required to deform the bone in sham is greater as compared to OVX. But the Von Mises stress is lower in sham compared to OVX. This again confirms the poor bone quality in OVX than sham. However, no significant changes were observed in the average cross section area indicating that the size of the bone was not altered.

Although, treatment showed a significant effect on the strength of distal femur, the effect of diet and diet by treatment interactions on distal femur was not significant. However, lumbar vertebrae showed significant effect due to diet and diet by treatment interactions. This suggests that effect of diet and diet by treatment interactions will be more prominently observed with high amounts of trabecular region. Studies have suggested that vertebral bodies have greater trabecular region when compared to femoral neck and distal femur. And the loss of trabecular bone will primarily be seen first in the spine region or vertebral body (94). Therefore, this difference in the skeletal sites might

TABLE 15

Effects of Dietary Iron, Treatment, Diet and Treatment Interactions on Distal Femur Strength in Sham and Ovariectomized Rats[1, 2]

Treatment Group	Strength Parameter					
	Physiological Force, *N*	Average Strain	Stiffness, *N/m x 10*^{4}	Size independent Stiffness, *N/m*	Von Mises, *Mpa*	Average Cross Section Area, *mm*^{2}
Sham-operated						
6 ppm	18.65 ± 4.94	0.227± 0.031	258.5 x 10^4 ± 69.3	602.8 ± 134.6	6.26 ± 1.13	9.90 ± 0.50
35 ppm	25.24 ± 4.94	0.273 ± 0.031	352.3 x 10^4± 69.3	761.7 ± 134.6	5.78 ± 1.13	10.87 ± 0.50
150 ppm	25.44 ± 4.94	0.278 ± 0.031	344.4 x 10^4 ± 69.3	770.3 ± 134.6	6.14 ± 1.13	10.67 ± 0.50
Ovariectomized						
6 ppm	7.14 ± 4.94	0.148 ± 0.031	96.7 x 10^4 ± 69.3	210.5 ± 134.6	12.07 ± 1.13	11.12 ± 0.50
35 ppm	3.96 ± 5.52	0.104 ± 0.035	53.6 x 10^4 ± 77.4	121.6 ± 150.5	14.81 ± 1.27	10.94 ± 0.56
150 ppm	8.28 ± 5.52	0.163 ± 0.035	112.1 x 10^4 ± 77.4	285.5 ± 150.5	11.28 ± 1.27	10.13 ± 0.56
Trt	P = 0.0007	P = 0.0002	P = 0.0007	P = 0.0002	P < 0.0001	P = 0.5563
Diet	P = 0.7413	P = 0.5336	P = 0.7792	P = 0.6765	P = 0.4095	P = 0.6057
Diet * Trt	P = 0.6331	P = 0.3926	P = 0.6369	P = 0.6729	P = 0.2441	P = 0.2375

[1]Values within columns with different superscripts are significantly different ($P \leq 0.05$)

[2] Values in rows are LS means ± SE, sham 6, 35, 150 ppm and OVX 6 ppm n = 5, OVX 35 and 150 ppm n = 4

have contributed to less dietary iron effect on the femur trabecular bone than vertebrae. Besides, several factors might have contributed for less vertebral strength when compared to femur. Findings of Guo et al. (108) suggest that the trabecular tissue is 20-30 % less stiff than cortical bone tissue. Their experiments on fatigue resistance of trabecular and cortical bone suggested that cortical bone tissue has higher fatigue resistance than trabecular bone tissue. The authors proposed that these differences could be due to the differences in tissue morphology (108). In another study, loads on the rat femoral neck showed more withstanding ability due to cortical bone than cancellous bone (124). Besides, rats differ in the microstructure such as minimal Haversian systems contributing to less bone remodeling (184, 185). The vertebral body and femur of rat receive different loads and stress when compared to humans, as rats are quadrupeds.

The effect of treatment on the architectural parameters in L_5 bone on BV/TV, Tb.N, and DA suggests that sham-operated rats had better bone quality than OVX. Poor bone quality in OVX may be due to erosion of trabeculae by osteoclasts. The SMI of OVX rats indicated more rod-like properties than the sham. This suggests that plate-like trabeculae decreased along with a decrease in bone volume fraction. No significant changes were observed in connectivity density due to treatment. However diet and treatment interactions influenced connectivity density. Although, greater connectivity density was observed in sham-operated rats with an increase in dietary iron concentration, other architectural parameters suggested high iron was detrimental. This suggests that the greater connectivity density might be due to the numerously broken trabeculae. These broken trabeculae might have contributed for more amounts of trabeculae per millimeter when counted numerically. This is also confirmed by the

increase in trabecular number and less bone volume fraction in high iron groups. Similarly, the trend in DA ($P = 0.0884$) due to diet effect also suggested that with increase in iron levels anisotropy increased. This higher DA values suggests that some of the trabeculae might be deleted in preferential directions affecting the mechanical properties of bone (150). Findings on human bones also suggest that, the extra load applied on the vertebral bone would result in the removal of horizontal trabeculae, affecting the mechanical properties of bone as well as the architectural properties (113).

Similar findings due to treatment were observed in distal femur but no diet or diet by treatment interactions were observed. The treatment effects on architectural as well as strength parameters indicated better bone quality in sham-operated rats than ovariectomized rats. This could be due to the inhibition of osteoclasts by the estrogen present in sham-operated rats and thus, preventing bone. Based on these findings it can be concluded that estrogen deficiency is detrimental to trabecular bone architecture. This is also supported by several studies (76-79). No treatment or diet or diet × treatment effects were observed in the architectural properties of cortical bone. This suggests that cortical bone may be less affected by dietary iron or treatment.

However, the diet as well as diet by treatment interactions on mechanical stress of bone (Von Mises stresses) showed greater stress with increase in iron levels in sham-operated rats although no significant differences were observed between 6 and 35 ppm sham. This suggests that with the increase in iron levels, stress with in the bone also increased in sham-operated rats, thus altering the internal structure of the bone. In contrast, the OVX showed greater stress in 35 ppm and lower stress in 150 ppm groups. In spite of the differences in the stresses the architectural parameters suggest no

significant differences between 35 and 150 ppm OVX groups. The present study observed decrease in connectivity and bone volume fraction in 35 and 150 pm OVX animals. This might have contributed for a variation in stress (219). Studies have also suggested that lower stress can cause loss of cortical bone and more specifically the trabecular bone and thereby affecting the homeostasis of normal bone mass maintenance (220). In the present study, we observed greater loss of trabecular bone and lower stress in 150 ppm OVX when compared to other groups. The findings of this study suggest that sham had better bone quality than OVX in terms of architectural parameters and strength parameters. The study also suggests that greater levels of iron (35 and 150 ppm) was detrimental to sham and OVX. However, in the growing rats 6 ppm was detrimental. Therefore, dietary iron restriction in sham operated or ovariectomized rats would be beneficial for trabecular bone, since we found significant effects in lumbar bone where greater trabecular bone is present compared to distal femur that has lower trabecular bone.

CHAPTER VI

SUMMARY AND CONCLUSIONS

Summary

One hundred twenty-four female Sprague Dawley rats were fed diets of varying levels of dietary iron to examine the effect of iron during growth and following ovariectomy on bone micro-architecture and strength. Forty or forty four rats were randomized to the growing, sham or OVX groups; only those in the first shipment and in diet groups 6, 35 and 150 ppm were included in this study.

Our findings in the rapidly growing rats on nutritional adequacy indicators as well as hematological indicators suggest that rats were adequately fed for growth and that iron deficiency was induced in the 6 ppm fed rats. No significant differences were observed in weights and albumin level, and the lowest iron fed group was made iron deficient as indicated by HB, HCT, RBC and RTC number. Hence, our goal to produce iron deficiency without affecting growth was met.

In summary, the trabecular bone architecture of growing rats was affected by dietary iron. The findings in our study on both lumbar and femur trabecular architectural parameters (Table 6) suggest poor trabecular bone quality in iron deficient rats. However, changes were seen more consistently in lumbar bone than in distal femur metaphyses, and none were seen in cortical mid-diaphyses region. Earlier studies have suggested that the amount of trabecular bone differs from site to site. The neck of the femur contains 25 %

trabecular bone, whereas in a vertebral body the percentage ranges from 66% to 90% (94). Therefore, loss of trabecular bone will primarily be seen first in the spine region or vertebral body**.** Consequently in our study changes were also observed more significantly in the trabecular region of lumbar bone than in femur. Another contributing factor for less significant effect in femur could be due to the growth observed in distal femur metaphyses. Studies have suggested that rats show progressive growth in cancellous bone at the age of six months or 24 weeks. Since our rats were 18 weeks old we would expect growth in the region, and, therefore, the loss of trabeculae or deterioration of trabeculae might have been prevented by the growth activity. Conversely, the DA of distal femur indicated that dietary iron has influenced the trabecular direction but not in lumbar bone. This could be due to the greater load applied on femur than lumbar bone during locomotion. No significant alterations were observed in the cortical bone architecture. In the lumbar bone as well as femur iron deficiency appears to be detrimental for trabecular bone architecture and trabecular orientation respectively.

The strength analyses in growing rats, significantly affected the lumbar bone but not femur. This is because vertebral bone is composed of more trabecular bone than femur. The strength analysis performed by μCT using FEM involves only the use of trabecular bone. Therefore, we would expect to see better and greater strength in femur but less strength in lumbar bone as suggested by trabecular micro-architecture. Our data on strength analysis (Table 8) also confirms the same as evidenced by trabecular architecture (Table 6). Stress and strain were observed to be higher in 6 ppm diet group indicating the structural modifications of bone internally. The physiological force at which a bone completely breaks was less in low iron fed group indicating poor strength.

However no significant differences were observed between adequate and high iron fed groups. This indicates that the strength parameters are affected by dietary iron in lumbar bone but not femoral bone and that iron deficiency is detrimental to lumbar bone. With no differences found for any of these variables between the recommended iron level (35 ppm) and high iron level, we do not see detrimental effects of high iron intakes during periods of rapid growth in female rats.

In the sham-operated and ovariectomized rats the nutrition indicators suggest that both the sham-operated and OVX animals were fed adequately (Table 9). No significant differences in weight gain due to diet were observed. Treatment significantly affected final weights. However, in all the three diet groups in OVX albumin concentrations were lower than shams. This lower albumin levels in OVX might be due to the estrogen deficiency but may not be due to dietary changes (69-71, 74, 172). Thus, our findings on nutritional adequacy indicators suggest that rats were adequately fed although changes were observed in some of these parameters due to treatment effect. There was a diet trend for both hemoglobin and reticulocyte counts suggesting that the 6 ppm fed rats were iron deficient (Table 10). Thus, we conclude that the iron deficiency produced during growth was not reversed due to ovariectomy and time.

Treatment effects on the architectural parameters in L_5 bone suggest that sham-operated rats had better bone quality than OVX. The SMI of OVX rats indicated more rod-like properties than the sham. This suggests that plate-like trabeculae decreased along with a decrease in bone volume fraction. No significant changes were observed in connectivity density due to treatment. However diet and treatment interactions influenced connectivity density. Although, greater connectivity density was observed in sham-

operated rats with an increase in dietary iron concentration, other architectural parameters suggested high iron was detrimental. This suggests that the greater connectivity density might be due to the numerously broken trabeculae. These broken trabeculae might have contributed for more amounts of trabeculae per millimeter when counted numerically. This is also confirmed by the increase in trabecular number and less bone volume fraction in high iron groups. Similarly, the trend in DA ($P = 0.0884$) due to diet effect also suggested that with increase in iron levels anisotropy increased. This higher DA values suggests that some of the trabeculae might be deleted in preferential directions affecting the mechanical properties of bone (150). Findings on human bones also suggest that, the extra load applied on the vertebral bone would result in the removal of horizontal trabeculae, affecting the mechanical properties of bone as well as the architectural properties (113).

Similar findings due to treatment were observed in distal femur but no diet or diet by treatment interactions were observed. The treatment effects on architectural as well as strength parameters indicated better bone quality in sham-operated rats than ovariectomized rats. This could be due to the inhibition of osteoclasts by the estrogen present in sham-operated rats and thus, preventing bone. Based on these findings it can be concluded that estrogen deficiency is detrimental to trabecular bone architecture. This is also supported by several studies (76-79). No treatment or diet or diet × treatment effects were observed in the architectural properties of cortical bone. This suggests that cortical bone may be less affected by dietary iron or treatment.

However, the diet as well as diet by treatment interactions on mechanical stress of bone (Von Mises stresses) showed greater stress with increase in iron levels in sham-

operated rats although no significant differences were observed between 6 and 35 ppm sham. This suggests that with the increase in iron levels, stress with in the bone also increased in sham-operated rats, thus altering the internal structure of the bone. In contrast, the OVX showed greater stress in 35 ppm and lower stress in 150 ppm groups. In spite of the differences in the stresses the architectural parameters suggest no significant differences between 35 and 150 ppm OVX groups. The present study observed a decrease in connectivity and bone volume fraction in 35 and 150 pm OVX animals. This might have contributed for a variation in stress (219). Studies have also suggested that lower stress can cause loss of cortical bone and, more specifically, the trabecular bone and, thereby, affecting the homeostasis of normal bone mass maintenance (220). In the present study, we observed greater loss of trabecular bone and lower stress in 150 ppm OVX when compared to other groups. The findings of this study suggest that sham had better bone quality than OVX in terms of architectural parameters and strength parameters. The study also suggests that greater levels of iron (35 and 150 ppm) was detrimental to sham and OVX.

The cortical bone architecture in growing rats as well as sham and ovariectomized rats did not show any effect due to diet (Tables 7 and 13). This suggests that cortical bone is less metabolically active than trabecular bone. Similarly no effects due to treatment or diet by treatment interactions were observed in sham-operated and ovariectomized rats.

These results suggest that cortical bone is less sensitive to ovariectomy and dietary iron due to the slower remodeling rate of cortical bone as compared to trabecular bone (94). This slower remodeling rate of cortical bone may be due to several contributing factors. Cortical bone has less remodeling surface than trabecular bone

(108). Also cortical bones possess fewer number of bone remodeling cells when compared to trabecular bone. More importantly, cortical bone has less blood supply than trabecular bone. This makes it possible for less exposure to hormones and systemic factors that affect bone remodeling. In addition, minimal Haversian systems in rat cortical bone (186) also might have contributed for lack of cortical bone response towards diet or treatment or both.

Results of Hypotheses Testing

This study proceeds with the following hypotheses:

1. There will be no statistically significant differences in L_5 trabecular architecture.
    a. There will be no statistically significant effect of iron in growing rats.

    Hypothesis 1a was rejected because the L_5 architectural parameters showed that 6 ppm iron fed animals showed poor bone quality when compared to 35 ppm and 150 ppm iron fed animals. No significant differences were observed between 35 ppm and 150 ppm iron fed animals (Table 6).

    b. There will be no statistically significant effect of iron in sham-operated or ovariectomized rats.

    Hypothesis 1b was not rejected because the L_5 architectural parameters showed that there were no significant differences due to diet in the older animals, sham-operated or ovariectomized groups (Table 11).

    c. There will be no statistically significant differences between sham-operated and ovariectomized rats.

    Hypothesis 1c was rejected because the L_5 architectural parameters showed that BV/TV, SMI, Tb.N. and DA were significantly affected. Sham-

operated animals exhibited better bone quality than ovariectomized animals. However, no significant differences were observed in Conn. D, Tb.Th and Tb.Sp (Table 11).

d. There will be no statistically significant diet by treatment interactions in sham-operated and ovariectomized rats.

Hypothesis 1d was rejected because there were significant interactions in connectivity density. The 150 ppm in sham was significantly greater than 6 ppm and 35 ppm sham and 35 and150 ppm OVX. No significant differences were observed between 6 ppm and 35 ppm iron fed OVX animals (Table 11).

2. There will be no statistically significant differences in distal femur trabecular architecture.

a. There will be no statistically significant effect of iron in growing rats.

Hypothesis 2a was rejected because dietary iron significantly affected DA in distal femur. The DA was significantly greater in 35 ppm and 150 ppm when compare to 6 ppm iron fed animals. No significant differences were observed in 35 ppm and 150 ppm iron fed animals. All other architectural parameters were not affected by dietary iron (Table 6).

b. There will be no statistically significant effect of iron in sham-operated or ovariectomized rats.

Hypothesis 2b was not rejected because the distal femur showed no significant differences in any of the dietary iron groups (Table 12).

c. There will be no statistically significant differences between sham-operated and ovariectomized rats on distal femur trabecular architecture.

Hypothesis 2c was rejected because the distal femur on BV/TV, Conn.D, SMI, Tb.N, Tb.Sp, and DA were significantly affected. No significant effect was observed in Tb.Th. architectural parameters. Sham-operated animals exhibited better bone quality than ovariectomized animals (Table 12).

d. There will be no statistically significant diet by treatment interactions in sham-operated and ovariectomized rats.

Hypothesis 1d was not rejected because the distal femur showed no significant interactions between any of the dietary iron and treatment groups (Table 12).

3. There will be no statistically significant differences in femur cortical bone architecture.

a. There will be no statistically significant effect of iron in growing rats.

Hypothesis 3a was not rejected because the architectural parameters in femur midshaft cortical bone showed no differences between in any of the dietary iron groups (Table 7).

b. There will be no statistically significant effect of iron in sham-operated or ovariectomized rats.

Hypothesis 3b was not rejected because the architectural parameters in femur midshaft cortical bone showed no significant differences in any of the dietary iron groups and also between sham-operated and ovariectomized animals (Table 13).

c. There will be no statistically significant differences between sham-operated or ovariectomized rats.

Hypothesis 3c was not rejected because the architectural parameters in femur midshaft cortical bone showed no significant differences (Table 13).

d. There will be no statistically significant diet by treatment interactions in sham-operated or ovariectomized rats.

Hypothesis 3d was not rejected because the architectural parameters in femur midshaft cortical bone showed no significant differences (Table 13).

4. There will be no statistically significant differences in L_5 strength.

a. There will be no statistically significant effect of iron in growing rats.

Hypothesis 4a was rejected because the architectural parameters showed significant effect of iron on bone strength. The strength of bone in 6 ppm iron fed animals was significantly lower than 35 ppm and 150 ppm iron fed animals. No significant differences were observed between 35 ppm and 150 ppm iron fed animals (Table 8).

b. There will be no statistically significant effect of iron in sham-operated or ovariectomized rats.

Hypothesis 4b was rejected because the Von Mises Stresses were significantly greater in 150 ppm sham than 35 ppm and 6 ppm sham and also 150 ppm OVX. No significant differences were observed between 35 ppm and 150 ppm. All the three dietary iron concentrations in OVX are significantly different. However low stress was observed in 150 ppm OVX. No significant changes were observed in average cross section area (Table 14).

c. There will be no statistically significant differences between sham-operated and ovariectomized rats.

Hypothesis 4c was rejected because all the strength parameters showed significant differences except Von Mises stresses and average cross section area. Sham showed better bone strength when compared to OVX (Table 14).

d. There will be no statistically significant diet by treatment interactions in sham-operated or ovariectomized rats.

Hypothesis 1d was rejected because the Von Mises Stresses were significantly greater in 35 ppm OVX than 6, 35 ppm 150 ppm sham and 6, 150 ppm OVX. No significant differences were observed among all the three dietary iron levels in sham. All the three dietary iron concentrations in OVX are significantly different. However low stress was observed in 150 ppm OVX due to diet and treatment interactions. No significant changes were observed in average cross section area (Table 14).

5. There will be no statistically significant differences in distal femur strength.

a. There will be no statistically significant effect of iron in growing rats.

Hypothesis 5a was not rejected because the distal femur strength analyses indicated no significant differences in all the dietary iron concentrations (Table 8).

b. There will be no statistically significant effect of iron in sham-operated and ovariectomized rats.

Hypothesis 5b was not rejected because the distal femur strength analyses indicated no significant differences in all the dietary iron concentrations (Table 15).

c. There will be no statistically significant differences between sham-operated or ovariectomized rats.

Hypothesis 5c was rejected because all the architectural parameters on strength analyses except the average cross section area indicated significant effect of treatment. Sham-operated animals exhibited better bone strength than ovariectomized animals (Table 15).

d. There will be no statistically significant diet by treatment interactions in sham-operated or ovariectomized rats.

Hypothesis 5d was not rejected because the distal femur strength analyses indicated no significant differences in diet by treatment interactions (Table 15).

Conclusion

In conclusion, the trabecular architecture and strength properties of this study suggests that iron deficiency is detrimental to growing rats and that adequate or high iron levels may be beneficial during rapid growth periods. On the other hand, sham-operated and ovariectomized animals showed better bone quality with iron deficiency. Adequate or high iron level appears to be detrimental to sham-operated or ovariectomized rats. This suggests that after rapid growth is achieved and when estrogen levels are lowered, iron deficiency may be beneficial and adequate or excess levels of iron may be harmful to bone. Our findings also suggest that the effect of iron changes with skeletal site since we found significant effects in lumbar bone but not on distal femur or midshaft.

Recommendations

Recommendations for further research include the following changes in the experiment. The results of animal studies are limited, as they cannot be applied to

humans. Therefore, studies on pre and postmenopausal women might be ideal to explore the effects of adequate, inadequate and excess intake of iron on bone micro-architecture. Bone tissue biopsies can be taken for assessing the micro-architecture.

The rats could be fed ad libitum with normal diet excepting iron. All the animals can be fed the amount of those eating the least ad libitum that would equalize protein, energy, vitamin and mineral except for iron. Iron could be given by gavage.

Literature Cited

1. Rodgers, M. M. & Cavanagh, P. R. Glossary of biomechanical terms, concepts, and units. Available at http://lob.incubadora.fapesp.br/portal/t/glossary. Accessed on November 10, 2005.

2. Evans, G. F. (1973) Mechanical properties of bone. Charles C. Thomas Pubisher, Springfield, Illinois; 1973. p. 57-60.

3. Cotton, J. R., Zioupos, P., Winwood, K. & Taylor, M. (2003) Analysis of creep strain during tensile fatigue of cortical bone. J Biomech. 36: 943-949.

4. Burr, D. B. & Turner, C. H. Biomechanics of bone. In: Primer on the metabolic bone diseases and disorders of mineral metabolism. American Society for Bone and Mineral Research, Washington, D.C; 2003. p. 58-64.

5. Turner, C. H. & Burr, D. B. (1993) Basic biomechanical measurements of bone: a tutorial. Bone 14: 595-608.

6. Hildebrand, T., Laib, A., Muller, R., Dequeker, J. & Ruegsegger, P. (1999) Direct three-dimensional morphometric analysis of human cancellous bone: microstructural data from spine, femur, iliac crest, and calcaneus. J Bone Miner. Res 14: 1167-1174.

7. Halloran, B. P., Ferguson, V. L., Simske, S. J., Burghardt, A., Venton, L. L. & Majumdar, S. (2002) Changes in bone structure and mass with advancing age in the male C57BL/6J mouse. J Bone Miner. Res 17: 1044-1050.

8. Ding, M. & Hvid, I. (2000) Quantification of age-related changes in the structure model type and trabecular thickness of human tibial cancellous bone. Bone 26: 291-295.

9. Lane, N. E., Kumer, J. L., Majumdar, S., Khan, M., Lotz, J., Stevens, R. E., Klein, R. & Phelps, K. V. (2002) The effects of synthetic conjugated estrogens, a (cenestin) on trabecular bone structure and strength in the ovariectomized rat model. Osteoporos. Int. 13: 816-823.

10. Smit, T. H., Odgaard, A. & Schneider, E. (1997) Structure and function of vertebral trabecular bone. Spine 22: 2823-2833.

11. Medeiros, D. M., Stoecker, B., Plattner, A., Jennings, D. & Haub, M. (2004) Iron deficiency negatively affects vertebrae and femurs of rats independently of energy intake and body weight. J. Nutr. 134: 3061-3067.

12. Qin, L., Raggatt, L. J. & Partridge, N. C. (2004) Parathyroid hormone: a double-edged sword for bone metabolism. Trends Endocrinol. Metab 15: 60-65.

13. Boivin, G. Y., Chavassieux, P. M., Santora, A. C., Yates, J. & Meunier, P. J. (2000) Alendronate increases bone strength by increasing the mean degree of mineralization of bone tissue in osteoporotic women. Bone 27: 687-694.

14. Boivin, G. & Meunie, P. J. (2001) Changes in bone remodeling rate influence the degree of mineralization of bone which is a determinant of bone strength: therapeutic implications. Adv. Exp. Med. Biol. 496: 123-127.

15. Medeiros, D. M., Plattner, A., Jennings, D. & Stoecker, B. (2002) Bone morphology, strength and density are compromised in iron-deficient rats and exacerbated by calcium restriction. J. Nutr. 132: 3135-3141.

16. Rattanakul, C., Lenbury, Y., Krishnamara, N. & Wollkind, D. J. (2003) Modeling of bone formation and resorption mediated by parathyroid hormone: response to estrogen/PTH therapy. Biosystems 70: 55-72.

17. Vural, F., Vural, B., Yucesoy, I. & Badur, S. (2005) Ovarian aging and bone metabolism in menstruating women aged 35-50 years. Maturitas 52: 147-153.

18. Christenson, R. H. (1997) Biochemical markers of bone metabolism: an overview. Clin. Biochem. 30: 573-593.

19. Angus, R. M., Sambrook, P. N., Pocock, N. A. & Eisman, J. A. (1988) Dietary intake and bone mineral density. Bone Miner. 4: 265-277.

20. West, C. E. (1996) Strategies to control nutritional anemia. Am. J. Clin. Nutr. 64: 789-790.

21. O'Dell, B. L. (1981) Roles for iron and copper in connective tissue biosynthesis. Philos. Trans. R. Soc. Lond B Biol. Sci. 294: 91-104.

22. Jaecques, S. V., Van Oosterwyck, H., Muraru, L., Van Cleynenbreugel, T., De Smet, E., Wevers, M., Naert, I. & Vander, S. J. (2004) Individualised, micro CT-based finite element modelling as a tool for biomechanical analysis related to tissue engineering of bone. Biomaterials 25: 1683-1696.

23. Baron, R. General principles of bone biology. In: Primer on the metabolic bone diseases and disorders of mineral metabolism. The American Society for Bone and Mineral Research; 2003. p.1-8.

24. Jilka, R. L. (1998) Cytokines, bone remodeling, and estrogen deficiency: a 1998 update. Bone 23: 75-81.

25. de Crombrugghe, B., Lefebvre, V. & Nakashima, K. (2001) Regulatory mechanisms in the pathways of cartilage and bone formation. Curr. Opin. Cell

Biol. 13: 721-727.

26. Matkovic, V., Landoll, J. D., Badenhop-Stevens, N. E., Ha, E. Y., Crncevic-Orlic, Z., Li, B. & Goel, P. (2004) Nutrition influences skeletal development from childhood to adulthood: a study of hip, spine, and forearm in adolescent females. J. Nutr. 134: 701S-705S.

27. Gilsanz, V., Gibbens, D. T., Carlson, M., Boechat, M. I., Cann, C. E. & Schulz, E. E. (1988) Peak trabecular vertebral density: a comparison of adolescent and adult females. Calcif. Tissue Int. 43: 260-262.

28. Meunier, P. J. & Boivin, G. (1997) Bone mineral density reflects bone mass but also the degree of mineralization of bone: therapeutic implications. Bone 21: 373-377.

29. Karsenty, G. (2001) When developmental biology meets human pathology. Proc. Natl. Acad. Sci. U. S. A 98: 5385-5386.

30. Karsenty, G. (2000) The central regulation of bone remodeling. Trends Endocrinol. Metab 11: 437-439.

31. Frost, H. M. (1969) Tetracycline-based histological analysis of bone remodeling. Calcif. Tissue Res. 3: 211-237.

32. Watkins, B. A., Lippman, H. E., Le Bouteiller, L., Li, Y. & Seifert, M. F. (2001) Bioactive fatty acids: role in bone biology and bone cell function. Prog. Lipid Res. 40: 125-148.

33. Heaney, R. P. (1996) Pathophysiology of osteoporosis. Am. J. Med. Sci. 312: 251-256.

34. Bord, S., Vedi, S., Beavan, S. R., Horner, A. & Compston, J. E. (2000) Megakaryocyte population in human bone marrow increases with estrogen treatment: a role in bone remodeling? Bone 27: 397-401.

35. van der Linden, J. C., Birkenhager-Frenkel, D. H., Verhaar, J. A. & Weinans, H. (2001) Trabecular bone's mechanical properties are affected by its non-uniform mineral distribution. J. Biomech. 34: 1573-1580.

36. Matkovic, V. (1996) Skeletal development and bone turnover revisited. J. Clin. Endocrinol. Metab 81: 2013-2016.

37. Saggese, G., Baroncelli, G. I. & Bertelloni, S. (2002) Puberty and bone development. Best. Pract. Res. Clin. Endocrinol. Metab 16: 53-64.

38. Seeman, E. & Eisman, J. A. (2004) 7: Treatment of osteoporosis: why, whom, when and how to treat. Med. J. Aust. 180: 298-303.

39. Banu, J. & Kalu, D. N. (2002) Effects of cerivastatin and parathyroid hormone on the lumbar vertebra of aging male Sprague-Dawley rats. Bone 31: 173-179.

40. Bailey, D. A. (1997) The Saskatchewan Pediatric Bone Mineral Accrual Study: bone mineral acquisition during the growing years. Int. J. Sports Med. 18 Suppl 3: S191-S194.

41. Koletzko, B., Aggett, P. J., Bindels, J. G., Bung, P., Ferre, P., Gil, A., Lentze, M. J., Roberfroid, M. & Strobel, S. (1998) Growth, development and differentiation: a functional food science approach. Br. J. Nutr. 80 Suppl 1: S5-S45.

42. Murray, R. D., Columb, B., Adams, J. E. & Shalet, S. M. (2004) Low bone mass is an infrequent feature of the adult growth hormone deficiency syndrome in middle-age adults and the elderly. J. Clin. Endocrinol. Metab 89: 1124-1130.

43. Overton, T. R. & Basu, T. K. (1999) Longitudinal changes in radial bone density in older men. Eur. J. Clin. Nutr. 53: 211-215.

44. Feik, S. A., Thomas, C. D. & Clement, J. G. (1997) Age-related changes in cortical porosity of the midshaft of the human femur. J. Anat. 191 (Pt 3): 407-416.

45. McCalden, R. W., McGeough, J. A., Barker, M. B. & Court-Brown CM (1993) Age-related changes in the tensile properties of cortical bone. The relative importance of changes in porosity, mineralization, and microstructure. J. Bone Joint Surg. Am. 75: 1193-1205.

46. Yeni, Y. N., Brown, C. U. & Norman, T. L. (1998) Influence of bone composition and apparent density on fracture toughness of the human femur and tibia. Bone 22: 79-84.

47. Burr, D. B., Forwood, M. R., Fyhrie, D. P., Martin, R. B., Schaffler, M. B. & Turner, C. H. (1997) Bone microdamage and skeletal fragility in osteoporotic and stress fractures. J Bone Miner. Res 12: 6-15.

48. Laib, A., Kumer, J. L., Majumdar, S. & Lane, N. E. (2001) The temporal changes of trabecular architecture in ovariectomized rats assessed by MicroCT. Osteoporos. Int. 12: 936-941.

49. Riggs, B. L., Wahner, H. W., Melton, L. J., III, Richelson, L. S., Judd, H. L. & Offord, K. P. (1986) Rates of bone loss in the appendicular and axial skeletons of women. Evidence of substantial vertebral bone loss before menopause. J. Clin. Invest 77: 1487-1491.

50. Recker, R., Lappe, J., Davies, K. M. & Heaney, R. (2004) Bone remodeling increases substantially in the years after menopause and remains increased in older osteoporosis patients. J. Bone Miner. Res. 19: 1628-1633.

51. Ahlborg, H. G., Johnell, O., Nilsson, B. E., Jeppsson, S., Rannevik, G. & Karlsson, M. K. (2001) Bone loss in relation to menopause: a prospective study during 16 years. Bone 28: 327-331.

52. Riggs, B. L., Khosla, S. & Melton, L. J., III (1998) A unitary model for involutional osteoporosis: estrogen deficiency causes both type I and type II osteoporosis in postmenopausal women and contributes to bone loss in aging men. J. Bone Miner. Res. 13: 763-773.

53. Mosekilde, L. (1990) Consequences of the remodelling process for vertebral trabecular bone structure: a scanning electron microscopy study (uncoupling of unloaded structures). Bone Miner. 10: 13-35.

54. Eriksen, E. F., Hodgson, S. F., Eastell, R., Cedel, S. L., O'Fallon, W. M. & Riggs, B. L. (1990) Cancellous bone remodeling in type I (postmenopausal) osteoporosis: quantitative assessment of rates of formation, resorption, and bone loss at tissue and cellular levels. J. Bone Miner. Res. 5: 311-319.

55. Silva, M. J. & Gibson, L. J. (1997) Modeling the mechanical behavior of vertebral trabecular bone: effects of age-related changes in microstructure. Bone 21: 191-199.

56. Bell, K. L., Loveridge, N., Power, J., Garrahan, N., Stanton, M., Lunt, M., Meggitt, B. F. & Reeve, J. (1999) Structure of the femoral neck in hip fracture: cortical bone loss in the inferoanterior to superoposterior axis. J Bone Miner. Res 14: 111-119.

57. Stein, M. S., Feik, S. A., Thomas, C. D., Clement, J. G. & Wark, J. D. (1999) An automated analysis of intracortical porosity in human femoral bone across age. J Bone Miner. Res 14: 624-632.

58. Liang, C. T., Barnes, J., Seedor, J. G., Quartuccio, H. A., Bolander, M., Jeffrey, J. J. & Rodan, G. A. (1992) Impaired bone activity in aged rats: alterations at the cellular and molecular levels. Bone 13: 435-441.

59. Kiebzak, G. M., Smith, R., Gundberg, C. C., Howe, J. C. & Sacktor, B. (1988) Bone status of senescent male rats: chemical, morphometric, and mechanical analysis. J Bone Miner. Res 3: 37-45.

60. Nilsson, A., Ohlsson, C., Isaksson, O. G., Lindahl, A. & Isgaard, J. (1994) Hormonal regulation of longitudinal bone growth. Eur. J. Clin. Nutr. 48 Suppl 1: S150-S158.

61. Kream, B. E., Petersen, D. N. & Raisz, L. G. (1990) Parathyroid hormone blocks the stimulatory effect of insulin-like growth factor-I on collagen synthesis in cultured 21-day fetal rat calvariae. Bone 11: 411-415.

62. Klaushofer, K., Hoffmann, O., Gleispach, H., Leis, H. J., Czerwenka, E., Koller,

K. & Peterlik, M. (1989) Bone-resorbing activity of thyroid hormones is related to prostaglandin production in cultured neonatal mouse calvaria. J. Bone Miner. Res. 4: 305-312.

63. Vaananen, H. K. & Harkonen, P. L. (1996) Estrogen and bone metabolism. Maturitas 23 Suppl: S65-S69.

64. Ikeda, S., Tsurukami, H., Ito, M., Sakai, A., Sakata, T., Nishida, S., Takeda, S., Shiraishi, A. & Nakamura, T. (2001) Effect of trabecular bone contour on ultimate strength of lumbar vertebra after bilateral ovariectomy in rats. Bone 28: 625-633.

65. Parfitt, A. M., Mathews, C. H., Villanueva, A. R., Kleerekoper, M., Frame, B. & Rao, D. S. (1983) Relationships between surface, volume, and thickness of iliac trabecular bone in aging and in osteoporosis. Implications for the microanatomic and cellular mechanisms of bone loss. J. Clin. Invest 72: 1396-1409.

66. Kameda, T., Mano, H., Yuasa, T., Mori, Y., Miyazawa, K., Shiokawa, M., Nakamaru, Y., Hiroi, E., Hiura, K. et al. (1997) Estrogen inhibits bone resorption by directly inducing apoptosis of the bone-resorbing osteoclasts. J. Exp. Med. 186: 489-495.

67. Li, M., Shen, Y. & Wronski, T. J. (1997) Time course of femoral neck osteopenia in ovariectomized rats. Bone 20: 55-61.

68. Bagi, C. M., DeLeon, E., Ammann, P., Rizzoli, R. & Miller, S. C. (1996) Histo-anatomy of the proximal femur in rats: impact of ovariectomy on bone mass, structure, and stiffness. Anat. Rec. 245: 633-644.

69. Pfeilschifter, J., Koditz, R., Pfohl, M. & Schatz, H. (2002) Changes in proinflammatory cytokine activity after menopause. Endocr. Rev. 23: 90-119.

70. Speyer, C. L., Rancilio, N. J., McClintock, S. D., Crawford, J. D., Gao, H., Sarma, J. V. & Ward, P. A. (2005) Regulatory effects of estrogen on acute lung inflammation in mice. Am. J. Physiol Cell Physiol 288: C881-C890.

71. Kurabayashi, T., Fujimaki, T., Yasuda, M., Yamamoto, Y. & Tanaka, K. (1993) Time-course of vertebral and femoral bone loss in rats administered gonadotrophin-releasing hormone agonist. J. Endocrinol. 138: 115-125.

72. Kaysen, G. A., Yeun, J. & Depner, T. (1997) Albumin synthesis, catabolism and distribution in dialysis patients. Miner. Electrolyte Metab 23: 218-224.

73. Marusic, A., Kos, K., Stavljenic, A. & Vukicevic, S. (1990) Talc granulomatosis in the rat. Involvement of bone in the acute-phase response. Inflammation 14: 205-216.

74. Tanizawa, T., Yamaguchi, A., Uchiyama, Y., Miyaura, C., Ikeda, T., Ejiri, S.,

Nagal, Y., Yamato, H., Murayama, H. et al. (2000) Reduction in bone formation and elevated bone resorption in ovariectomized rats with special reference to acute inflammation. Bone 26: 43-53.

75. Dick, I. M., St John, A., Heal, S. & Prince, R. L. (1996) The effect of estrogen deficiency on bone mineral density, renal calcium and phosphorus handling and calcitropic hormones in the rat. Calcif. Tissue Int. 59: 174-178.

76. Bagi, C. M., Ammann, P., Rizzoli, R. & Miller, S. C. (1997) Effect of estrogen deficiency on cancellous and cortical bone structure and strength of the femoral neck in rats. Calcif. Tissue Int. 61: 336-344.

77. Turner, R. T., Vandersteenhoven, J. J. & Bell, N. H. (1987) The effects of ovariectomy and 17 beta-estradiol on cortical bone histomorphometry in growing rats. J. Bone Miner. Res. 2: 115-122.

78. Wronski, T. J., Lowry, P. L., Walsh, C. C. & Ignaszewski, L. A. (1985) Skeletal alterations in ovariectomized rats. Calcif. Tissue Int. 37: 324-328.

79. Wronski, T. J., Dann, L. M., Scott, K. S. & Cintron, M. (1989) Long-term effects of ovariectomy and aging on the rat skeleton. Calcif. Tissue Int. 45: 360-366.

80. Banu, J., Wang, L. & Kalu, D. N. (2002) Age-related changes in bone mineral content and density in intact male F344 rats. Bone 30: 125-130.

81. Kanis, J. A. & Gluer, C. C. (2000) An update on the diagnosis and assessment of osteoporosis with densitometry. Committee of Scientific Advisors, International Osteoporosis Foundation. Osteoporos. Int. 11: 192-202.

82. Felsenberg, D. & Boonen, S. (2005) The bone quality framework: determinants of bone strength and their interrelationships, and implications for osteoporosis management. Clin. Ther. 27: 1-11.

83. Marshall, D., Johnell, O. & Wedel, H. (1996) Meta-analysis of how well measures of bone mineral density predict occurrence of osteoporotic fractures. BMJ 312: 1254-1259.

84. Kanis, J. A. (2002) Diagnosis of osteoporosis and assessment of fracture risk. Lancet 359: 1929-1936.

85. Bouxsein, M. L. (2003) Mechanisms of osteoporosis therapy: a bone strength perspective. Clin. Cornerstone. Suppl 2: S13-S21.

86. Bouxsein, M. L. (2003) Bone quality: where do we go from here? Osteoporos. Int. 14 Suppl 5: 118-127.

87. Currey, J. D. (2003) Role of collagen and other organics in the mechanical properties of bone. Osteoporos. Int. 14: 29-36.

88. Jepsen, K. J. (2003) The aging cortex: to crack or not to crack. Osteoporos. Int. 14 Suppl 5: 57-66.

89. Turner, C. H. (2002) Biomechanics of bone: determinants of skeletal fragility and bone quality. Osteoporos. Int. 13: 97-104.

90. Van Rietbergen, B., Weinans, H., Huiskes, R. & Odgaard, A. (1995) A new method to determine trabecular bone elastic properties and loading using micromechanical finite-element models. J. Biomech. 28: 69-81.

91. Kishimoto, H. (2005) [Change in the definition of osteoporosis especially on bone quality]. Clin. Calcium 15: 736-740. (Abs.) Article in Japanese.

92. Hanson, N. A. & Bagi, C. M. (2004) Alternative approach to assessment of bone quality using micro-computed tomography. Bone 35: 326-333.

93. Akkus, O., Adar, F. & Schaffler, M. B. (2004) Age-related changes in physicochemical properties of mineral crystals are related to impaired mechanical function of cortical bone. Bone 34: 443-453.

94. Einhorn, T. A. (1992) Bone strength: the bottom line. Calcif. Tissue Int. 51: 333-339.

95. Crabtree, N. J., Kroger, H., Martin, A., Pols, H. A., Lorenc, R., Nijs, J., Stepan, J. J., Falch, J. A., Miazgowski, T. et al. (2002) Improving risk assessment: hip geometry, bone mineral distribution and bone strength in hip fracture cases and controls. The EPOS study. European Prospective Osteoporosis Study. Osteoporos. Int. 13: 48-54.

96. Biology-online. org. Definition on ultimate strength. Available at http://www.biology-online.org/dictionary/ultimate_strength. Accessed on October 10, 2005.

97. Zebaze, R. M., Jones, A., Welsh, F., Knackstedt, M. & Seeman, E. (2005) Femoral neck shape and the spatial distribution of its mineral mass varies with its size: Clinical and biomechanical implications. Bone 37: 243-252.

98. Beck, T. (2003) Measuring the structural strength of bones with dual-energy X-ray absorptiometry: principles, technical limitations, and future possibilities. Osteoporos. Int. 14 Suppl 5: 81-88.

99. Seeman, E. (2003) Bone quality. Osteoporos. Int. 14 Suppl 5: 3-7.

100. Lu, P. W., Cowell, C. T., LLoyd-Jones, S. A., Briody, J. N. & Howman-Giles, R. (1996) Volumetric bone mineral density in normal subjects, aged 5-27 years. J Clin. Endocrinol. Metab 81: 1586-1590.

101. Andreassen, T. T., Jorgensen, P. H., Flyvbjerg, A., Orskov, H. & Oxlund, H.

(1995) Growth hormone stimulates bone formation and strength of cortical bone in aged rats. J Bone Miner. Res 10: 1057-1067.

102. Bono, C. M. & Einhorn, T. A. (2003) Overview of osteoporosis: pathophysiology and determinants of bone strength. Eur. Spine J 12 Suppl 2: S90-S96.

103. Seeman, E. (2001) Clinical review 137: Sexual dimorphism in skeletal size, density, and strength. J Clin. Endocrinol. Metab 86: 4576-4584.

104. Seeman, E. (2002) Pathogenesis of bone fragility in women and men. Lancet 359: 1841-1850.

105. Nieves, J. W., Formica, C., Ruffing, J., Zion, M., Garrett, P., Lindsay, R. & Cosman, F. (2005) Males have larger skeletal size and bone mass than females, despite comparable body size. J Bone Miner. Res 20: 529-535.

106. Duan, Y., Parfitt, A. & Seeman, E. (1999) Vertebral bone mass, size, and volumetric density in women with spinal fractures. J Bone Miner. Res 14: 1796-1802.

107. Dalle, C. L. & Giannini, S. (2004) Bone microarchitecture as an important determinant of bone strength. J. Endocrinol. Invest 27: 99-105.

108. Guo, E. X. & Goldstein, S. A. (1997) Is Trabecular bone tissue different from cortical bone tissue. Forma 12: 185-196.

109. Ito, M., Nishida, A., Koga, A., Ikeda, S., Shiraishi, A., Uetani, M., Hayashi, K. & Nakamura, T. (2002) Contribution of trabecular and cortical components to the mechanical properties of bone and their regulating parameters. Bone 31: 351-358.

110. Kleerekoper, M., Villanueva, A. R., Stanciu, J., Rao, D. S. & Parfitt, A. M. (1985) The role of three-dimensional trabecular microstructure in the pathogenesis of vertebral compression fractures. Calcif. Tissue Int. 37: 594-597.

111. Kothari, M., Keaveny, T. M., Lin, J. C., Newitt, D. C. & Majumdar, S. (1999) Measurement of intraspecimen variations in vertebral cancellous bone architecture. Bone 25: 245-250.

112. van Ruijven, L. J., Giesen, E. B., Mulder, L., Farella, M. & van Eijden, T. M. (2005) The effect of bone loss on rod-like and plate-like trabeculae in the cancellous bone of the mandibular condyle. Bone 36: 1078-1085.

113. Thomsen, J. S., Ebbesen, E. N. & Mosekilde, L. I. (2002) Age-related differences between thinning of horizontal and vertical trabeculae in human lumbar bone as assessed by a new computerized method. Bone 31: 136-142.

114. Aaron, J. E., Shore, P. A., Shore, R. C., Beneton, M. & Kanis, J. A. (2000) Trabecular architecture in women and men of similar bone mass with and without

vertebral fracture: II. Three-dimensional histology. Bone 27: 277-282.

115. Parfitt, A. M. (1992) Implications of architecture for the pathogenesis and prevention of vertebral fracture. Bone 13 Suppl 2: S41-S47.

116. Simpson, E. K., Parkinson, I. H., Manthey, B. & Fazzalari, N. L. (2001) Intervertebral disc disorganization is related to trabecular bone architecture in the lumbar spine. J. Bone Miner. Res. 16: 681-687.

117. Amling, M., Posl, M., Ritzel, H., Hahn, M., Vogel, M., Wening, V. J. & Delling, G. (1996) Architecture and distribution of cancellous bone yield vertebral fracture clues. A histomorphometric analysis of the complete spinal column from 40 autopsy specimens. Arch. Orthop. Trauma Surg. 115: 262-269.

118. Osterman, T., Virtamo, T., Kippo, K., Lauren, L., Pasanen, I., Hannuniemi, R. & Sellman, R. (1997) Distribution of clodronate in the bone of adult rats and its effects on trabecular and cortical bone. J Pharmacol. Exp. Ther. 280: 1051-1056.

119. Briggs, A. M., Greig, A. M., Wark, J. D., Fazzalari, N. L. & Bennell, K. L. (2004) A review of anatomical and mechanical factors affecting vertebral body integrity. Int. J. Med. Sci. 1: 170-180.

120. Bell, K. L., Loveridge, N., Jordan, G. R., Power, J., Constant, C. R. & Reeve, J. (2000) A novel mechanism for induction of increased cortical porosity in cases of intracapsular hip fracture. Bone 27: 297-304.

121. Bousson, V., Meunier, A., Bergot, C., Vicaut, E., Rocha, M. A., Morais, M. H., Laval-Jeantet, A. M. & Laredo, J. D. (2001) Distribution of intracortical porosity in human midfemoral cortex by age and gender. J. Bone Miner. Res. 16: 1308-1317.

122. Tabensky, A., Duan, Y., Edmonds, J. & Seeman, E. (2001) The contribution of reduced peak accrual of bone and age-related bone loss to osteoporosis at the spine and hip: insights from the daughters of women with vertebral or hip fractures. J. Bone Miner. Res. 16: 1101-1107.

123. Yeh, O. C. & Keaveny, T. M. (2001) Relative roles of microdamage and microfracture in the mechanical behavior of trabecular bone. J. Orthop. Res. 19: 1001-1007.

124. Peng, Z., Tuukkanen, J., Zhang, H., Jamsa, T. & Vaananen, H. K. (1994) The mechanical strength of bone in different rat models of experimental osteoporosis. Bone 15: 523-532.

125. Follet, H., Boivin, G., Rumelhart, C. & Meunier, P. J. (2004) The degree of mineralization is a determinant of bone strength: a study on human calcanei. Bone 34: 783-789.

126. Borah, B., Ritman, E. L., Dufresne, T. E., Jorgensen, S. M., Liu, S., Sacha, J., Phipps, R. J. & Turner, R. T. (2005) The effect of risedronate on bone mineralization as measured by micro-computed tomography with synchrotron radiation: correlation to histomorphometric indices of turnover. Bone 37: 1-9.

127. Ciarelli, T. E., Fyhrie, D. P. & Parfitt, A. M. (2003) Effects of vertebral bone fragility and bone formation rate on the mineralization levels of cancellous bone from white females. Bone 32: 311-315.

128. Forslind, K., Keller, C., Svensson, B. & Hafstrom, I. (2003) Reduced bone mineral density in early rheumatoid arthritis is associated with radiological joint damage at baseline and after 2 years in women. J Rheumatol. 30: 2590-2596.

129. Oxlund, H., Mosekilde, L. & Ortoft, G. (1996) Reduced concentration of collagen reducible cross links in human trabecular bone with respect to age and osteoporosis. Bone 19: 479-484.

130. Liebschner, M. A. (2004) Biomechanical considerations of animal models used in tissue engineering of bone. Biomaterials 25: 1697-1714.

131. Linde, F., Hvid, I. & Pongsoipetch, B. (1989) Energy absorptive properties of human trabecular bone specimens during axial compression. J Orthop. Res 7: 432-439.

132. Muller, R. & Ruegsegger, P. (1995) Three-dimensional finite element modelling of non-invasively assessed trabecular bone structures. Med Eng Phys. 17: 126-133.

133. Newitt, D. C., Majumdar, S., Van Rietbergen, B., von Ingersleben, G., Harris, S. T., Genant, H. K., Chesnut, C., Garnero, P. & MacDonald, B. (2002) In vivo assessment of architecture and micro-finite element analysis derived indices of mechanical properties of trabecular bone in the radius. Osteoporos. Int. 13: 6-17.

134. Taddei, F., Pancanti, A. & Viceconti, M. (2004) An improved method for the automatic mapping of computed tomography numbers onto finite element models. Med Eng Phys. 26: 61-69.

135. Bourne, B. C. & Van Der Meulen, M. C. (2004) Finite element models predict cancellous apparent modulus when tissue modulus is scaled from specimen CT-attenuation. J Biomech. 37: 613-621.

136. Hollister, S. J., Brennan, J. M. & Kikuchi, N. (1994) A homogenization sampling procedure for calculating trabecular bone effective stiffness and tissue level stress. J Biomech. 27: 433-444.

137. Marks, L. W. & Gardner, T. N. (1993) The use of strain energy as a convergence criterion in the finite element modelling of bone and the effect of model geometry on stress convergence. J Biomed. Eng 15: 474-476.

138. Niebur, G. L., Feldstein, M. J., Yuen, J. C., Chen, T. J. & Keaveny, T. M. (2000) High-resolution finite element models with tissue strength asymmetry accurately predict failure of trabecular bone. J. Biomech. 33: 1575-1583.

139. Hou, F. J., Lang, S. M., Hoshaw, S. J., Reimann, D. A. & Fyhrie, D. P. (1998) Human vertebral body apparent and hard tissue stiffness. J Biomech. 31: 1009-1015.

140. Van Rietbergen, B., Odgaard, A., Kabel, J. & Huiskes, R. (1998) Relationships between bone morphology and bone elastic properties can be accurately quantified using high-resolution computer reconstructions. J Orthop. Res 16: 23-28.

141. Ladd, A. J., Kinney, J. H., Haupt, D. L. & Goldstein, S. A. (1998) Finite-element modeling of trabecular bone: comparison with mechanical testing and determination of tissue modulus. J Orthop. Res 16: 622-628.

142. Van Rietbergen, B. (2001) Micro-FE analyses of bone: state of the art. Adv. Exp. Med Biol. 496: 21-30.

143. Sugita, H., Oka, M., Toguchida, J., Nakamura, T., Ueo, T. & Hayami, T. (1999) Anisotropy of osteoporotic cancellous bone. Bone 24: 513-516.

144. Frost, H. M. (1987) The mechanostat: a proposed pathogenic mechanism of osteoporoses and the bone mass effects of mechanical and nonmechanical agents. Bone Miner. 2: 73-85.

145. Geraets, W. G., Van der Stelt, P. F., Netelenbos, C. J. & Elders, P. J. (1990) A new method for automatic recognition of the radiographic trabecular pattern. J Bone Miner. Res 5: 227-233.

146. Majumdar, S., Kothari, M., Augat, P., Newitt, D. C., Link, T. M., Lin, J. C., Lang, T., Lu, Y. & Genant, H. K. (1998) High-resolution magnetic resonance imaging: three-dimensional trabecular bone architecture and biomechanical properties. Bone 22: 445-454.

147. Chappard, C., Brunet-Imbault, B., Lemineur, G., Giraudeau, B., Basillais, A., Harba, R. & Benhamou, C. L. (2005) Anisotropy changes in post-menopausal osteoporosis: characterization by a new index applied to trabecular bone radiographic images. Osteoporos. Int.16: 1193-202.

148. Luo, G., Kinney, J. H., Kaufman, J. J., Haupt, D., Chiabrera, A. & Siffert, R. S. (1999) Relationship between plain radiographic patterns and three- dimensional trabecular architecture in the human calcaneus. Osteoporos. Int. 9: 339-345.

149. Odgaard, A. (1997) Three-dimensional methods for quantification of cancellous bone architecture. Bone 20: 315-328.

150. Brunet-Imbault, B., Lemineur, G., Chappard, C., Harba, R. & Benhamou, C. L. (2005) A new anisotropy index on trabecular bone radiographic images using the fast Fourier transform. BMC. Med. Imaging 5: 4.

151. Hing, K. A., Best, S. M., Tanner, K. E., Bonfield, W. & Revell, P. A. (2004) Mediation of bone ingrowth in porous hydroxyapatite bone graft substitutes. J Biomed. Mater. Res A 68: 187-200.

152. Homminga, J., Van-Rietbergen, B., Lochmuller, E. M., Weinans, H., Eckstein, F. & Huiskes, R. (2004) The osteoporotic vertebral structure is well adapted to the loads of daily life, but not to infrequent "error" loads. Bone 34: 510-516.

153. Jianhua, H., Liang, Z., Lilian, Z. & Gongyi, H. (2002) Effects of alendronate on structural properties of trabecular bone in dogs. Chin Med Sci. J 17: 210-214.

154. Rossi, L., Migliaccio, S., Corsi, A., Marzia, M., Bianco, P., Teti, A., Gambelli, L., Cianfarani, S., Paoletti, F. & Branca, F. (2001) Reduced growth and skeletal changes in zinc-deficient growing rats are due to impaired growth plate activity and inanition. J. Nutr. 131: 1142-1146.

155. Lerner, A. L., Kuhn, J. L. & Hollister, S. J. (1998) Are regional variations in bone growth related to mechanical stress and strain parameters? J. Biomech. 31: 327-335.

156. Bonadio, J., Jepsen, K. J., Mansoura, M. K., Jaenisch, R., Kuhn, J. L. & Goldstein, S. A. (1993) A murine skeletal adaptation that significantly increases cortical bone mechanical properties. Implications for human skeletal fragility. J. Clin. Invest 92: 1697-1705.

157. Jepsen, K. J., Schaffler, M. B., Kuhn, J. L., Goulet, R. W., Bonadio, J. & Goldstein, S. A. (1997) Type I collagen mutation alters the strength and fatigue behavior of Mov13 cortical tissue. J. Biomech. 30: 1141-1147.

158. David, V., Laroche, N., Boudignon, B., Lafage-Proust, M. H., Alexandre, C., Ruegsegger, P. & Vico, L. (2003) Noninvasive in vivo monitoring of bone architecture alterations in hindlimb-unloaded female rats using novel three-dimensional microcomputed tomography. J. Bone Miner. Res. 18: 1622-1631.

159. Burr, D. B., Forwood, M. R., Fyhrie, D. P., Martin, R. B., Schaffler, M. B. & Turner, C. H. (1997) Bone microdamage and skeletal fragility in osteoporotic and stress fractures. J. Bone Miner. Res. 12: 6-15.

160. Barlet, J. P., Coxam, V., Davicco, M. J. & Gaumet, N. (1994) [Animal models of post-menopausal osteoporosis]. Reprod. Nutr. Dev. 34: 221-236.(Abs.) Article in French.

161. Chachra, D., Lee, J. M., Kasra, M. & Grynpas, M. D. (2000) Differential effects of ovariectomy on the mechanical properties of cortical and cancellous bone in rat

femora and vertebrae. Biomed. Sci. Instrum. 36: 123-128.

162. Goldstein, S. A., Goulet, R. & McCubbrey, D. (1993) Measurement and significance of three-dimensional architecture to the mechanical integrity of trabecular bone. Calcif. Tissue Int. 53 Suppl 1: S127-S132.

163. Compston, J. E. (1994) Connectivity of cancellous bone: assessment and mechanical implications. Bone 15: 463-466.

164. Jensen, K. S., Mosekilde, L. & Mosekilde, L. (1990) A model of vertebral trabecular bone architecture and its mechanical properties. Bone 11: 417-423.

165. Ulrich, D., Van Rietbergen, B., Laib, A. & Ruegsegger, P. (1999) The ability of three-dimensional structural indices to reflect mechanical aspects of trabecular bone. Bone 25: 55-60.

166. Feldkamp, L. A., Goldstein, S. A., Parfitt, A. M., Jesion, G. & Kleerekoper, M. (1989) The direct examination of three-dimensional bone architecture in vitro by computed tomography. J. Bone Miner. Res. 4: 3-11.

167. Ruegsegger, P., Koller, B. & Muller, R. (1996) A microtomographic system for the nondestructive evaluation of bone architecture. Calcif. Tissue Int. 58: 24-29.

168. Aufdemorte, T. B., Boyan, B. D., Fox, W. C. & Miller, D. (1993) Diagnostic tools and biologic markers: animal models in the study of osteoporosis and oral bone loss. J. Bone Miner. Res. 8 Suppl 2: S529-S534.

169. Kalu, D. N. (1991) The ovariectomized rat model of postmenopausal bone loss. Bone Miner. 15: 175-191.

170. Rodgers, J. B., Monier-Faugere, M. C. & Malluche, H. (1993) Animal models for the study of bone loss after cessation of ovarian function. Bone 14: 369-377.

171. Davidson, M. K., Lindsey, J. R. & Davis, J. K. (1987) Requirements and selection of an animal model. Isr. J. Med. Sci. 23: 551-555.

172. Kalu, D. N., Liu, C. C., Hardin, R. R. & Hollis, B. W. (1989) The aged rat model of ovarian hormone deficiency bone loss. Endocrinology 124: 7-16.

173. Turner, R. T. & Spelsberg, T. C. (1991) Correlation between mRNA levels for bone cell proteins and bone formation in long bones of maturing rats. Am. J. Physiol 261: E348-E353.

174. Erben, R. G. (1996) Trabecular and endocortical bone surfaces in the rat: modeling or remodeling? Anat. Rec. 246: 39-46.

175. Martin, E. A., Ritman, E. L. & Turner, R. T. (2003) Time course of epiphyseal growth plate fusion in rat tibiae. Bone 32: 261-267.

176. Acheson, R. M., Macintyre, M. N. & Oldham, E. (1959) Techniques in longitudinal studies of the skeletal development of the rat. Br. J. Nutr. 13: 283-292.

177. Turner, R. T., Maran, A., Lotinun, S., Hefferan, T., Evans, G. L., Zhang, M. & Sibonga, J. D. (2001) Animal models for osteoporosis. Rev. Endocr. Metab Disord. 2: 117-127.

178. Hogan, H. A., Ruhmann, S. P. & Sampson, H. W. (2000) The mechanical properties of cancellous bone in the proximal tibia of ovariectomized rats. J. Bone Miner. Res. 15: 284-292.

179. O'Flaherty, E. J. (1991) Physiologically based models for bone-seeking elements. I. Rat skeletal and bone growth. Toxicol. Appl. Pharmacol. 111: 299-312.

180. Wang, L., Banu, J., McMahan, C. A. & Kalu, D. N. (2001) Male rodent model of age-related bone loss in men. Bone 29: 141-148.

181. Thorndike, E. A. & Turner, A. S. (1998) In search of an animal model for postmenopausal diseases. Front Biosci. 3: c17-c26.

182. Frost, H. M. & Jee, W. S. (1992) On the rat model of human osteopenias and osteoporoses. Bone Miner. 18: 227-236.

183. Grynpas, M. D., Chachra, D. & Lundon, K. (2000) Bone quality in animal models of osteoporosis. Drug Development Research 49: 146-158.

184. Tran, V. P., Vignery, A. & Baron, R. (1982) Cellular kinetics of the bone remodeling sequence in the rat. Anat. Rec. 202: 445-451.

185. Jee, W. S., Mori, S., Li, X. J. & Chan, S. (1990) Prostaglandin E2 enhances cortical bone mass and activates intracortical bone remodeling in intact and ovariectomized female rats. Bone 11: 253-266.

186. Sietsema, W. K. (1995) Animal models of cortical porosity. Bone 17: 297S-305S.

187. Reddy, M. B. & Cook, J. D. (1994) Absorption of nonheme iron in ascorbic acid-deficient rats. J. Nutr. 124: 882-887.

188. Tuderman, L., Myllyla, R. & Kivirikko, K. I. (1977) Mechanism of the prolyl hydroxylase reaction. 1. Role of co-substrates. Eur. J. Biochem. 80: 341-348.

189. Rothman, R. H., Klemek, J. S. & Toton, J. J. (1971) The effect of iron deficiency anemia on fracture healing. Clin. Orthop. Relat Res. 77: 276-283.

190. Heppenstall, R. B. & Brighton, C. T. (1977) Fracture healing in the presence of anemia. Clin. Orthop. Relat Res. 253-258.

191. Campos, M. S., Barrionuevo, M., Alferez, M. J., Gomez-Ayala, A. E., Rodriguez-Matas, M. C., Lopez, A., I & Lisbona, F. (1998) Interactions among iron, calcium, phosphorus and magnesium in the nutritionally iron-deficient rat. Exp. Physiol 83: 771-781.

192. Yokoi, K., Kimura, M. & Itokawa, Y. (1991) Effect of dietary iron deficiency on mineral levels in tissues of rats. Biol. Trace Elem. Res. 29: 257-265.

193. Medeiros, D. M., Ilich, J. Z., Ireton, J., Matkovic, V., Shiry, L. & Wildman, R. (1997) Femurs from rats fed diets deficient in copper or iron have decreased mechanical strength and altered mineral composition. J. Trace Elem. Exp. Med. 10: 197-203.

194. Schnitzler, C. M., Macphail, A. P., Shires, R., Schnaid, E., Mesquita, J. M. & Robson, H. J. (1994) Osteoporosis in African hemosiderosis: role of alcohol and iron. J Bone Miner. Res 9: 1865-1873.

195. Conte, D., Caraceni, M. P., Duriez, J., Mandelli, C., Corghi, E., Cesana, M., Ortolani, S. & Bianchi, P. A. (1989) Bone involvement in primary hemochromatosis and alcoholic cirrhosis. Am. J. Gastroenterol. 84: 1231-1234.

196. de Vernejoul, M. C., Pointillart, A., Golenzer, C. C., Morieux, C., Bielakoff, J., Modrowski, D. & Miravet, L. (1984) Effects of iron overload on bone remodeling in pigs. Am. J. Pathol. 116: 377-384.

197. Diamond, T., Stiel, D. & Posen, S. (1989) Osteoporosis in hemochromatosis: iron excess, gonadal deficiency, or other factors? Ann. Intern. Med. 110: 430-436.

198. Diamond, T., Pojer, R., Stiel, D., Alfrey, A. & Posen, S. (1991) Does iron affect osteoblast function? Studies in vitro and in patients with chronic liver disease. Calcif. Tissue Int. 48: 373-379.

199. Duquenne, M., Rohmer, V., Legrand, E., Chappard, D., Wion, B. N., Basle, M. F., Audran, M. & Bigorgne, J. C. (1996) Spontaneous multiple vertebral fractures revealed primary haemochromatosis. Osteoporos. Int. 6: 338-340.

200. Storey, M. L. & Greger, J. L. (1987) Iron, zinc and copper interactions: chronic versus acute responses of rats. J Nutr. 117: 1434-1442.

201. Kipp, D., Pinero, D. & Beard, J. L. (1998) Low bone mass and volume in iron-deficient rats. FASEB J 12: A508 (abs.).

202. Kipp, D. E., Beard, J. L. & Lees, C. J. (2002) Mild iron deficiency results in altered bone mass and histomorphometry in growing female rats. FASEB J 16: A273 (abs.).

203. Ilich-Ernst, J. Z., McKenna, A. A., Badenhop, N. E., Clairmont, A. C., Andon, M. B., Nahhas, R. W., Goel, P. & Matkovic, V. (1998) Iron status, menarche, and

calcium supplementation in adolescent girls. Am. J. Clin. Nutr. 68: 880-887.

204. Harris, M. M., Houtkooper, L. B., Stanford, V. A., Parkhill, C., Weber, J. L., Flint-Wagner, H., Weiss, L., Going, S. B. & Lohman, T. G. (2003) Dietary iron is associated with bone mineral density in healthy postmenopausal women. J. Nutr. 133: 3598-3602.

205. Maurer, J., Harris, M. M., Stanford, V. A., Lohman, T. G., Cussler, E., Going, S. B. & Houtkooper, L. B. (2005) Dietary iron positively influences bone mineral density in postmenopausal women on hormone replacement therapy. J. Nutr. 135: 863-869.

206. Reeves, P. G., Rossow, K. L. & Lindlauf, J. (1993) Development and testing of the AIN-93 purified diets for rodents: results on growth, kidney calcification and bone mineralization in rats and mice. J Nutr. 123: 1923-1931.

207. Shah, B. G. & Belonje, B. (1991) Marginal or excess dietary iron and rat tissue trace element levels. Trace Elem Med. 8: 143-148.

208. Beard, J. L., Zhan, C. S. & Brigham, D. E. (1995) Growth in iron-deficient rats. Proc. Soc. Exp. Biol. Med 209: 65-72.

209. Stangl, G. I. & Kirchgessner, M. (1998) Effect of different degrees of moderate iron deficiency on the activities of tricarboxylic acid cycle enzymes, and the cytochrome oxidase, and the iron, copper, and zinc concentrations in rat tissues. Z. Ernahrungswiss. 37: 260-268.

210. Hrapkiewicz, K., Medina, L. & Holmes, D. (1998) Clinical Laboratory Animal Medicine., 2nd ed., Iowa State University Press, Ames, IA.

211. Young, D. S. (1990) Implementation of SI units for clinical laboratory data: style specifications and conversion tables. J Nutr. Biochem. 1: 599-613.

212. Dallman, P. R., Refino, C. & Yland, M. J. (1982) Sequence of development of iron deficiency in the rat. Am. J Clin. Nutr. 35: 671-677.

213. Siimes, M. A., Refino, C. & Dallman, P. R. (1980) Manifestation of iron deficiency at various levels of dietary iron intake. Am. J Clin. Nutr. 33: 570-574.

214. Duan, Y., De, L., V & Seeman, E. (1999) Parathyroid hormone deficiency and excess: similar effects on trabecular bone but differing effects on cortical bone. J Clin. Endocrinol. Metab 84: 718-722.

215. Hou, J. C., Salem, G. J., Zernicke, R. F. & Barnard, R. J. (1990) Structural and mechanical adaptations of immature trabecular bone to strenuous exercise. J. Appl. Physiol 69: 1309-1314.

216. Bagi, C. M., Wilkie, D., Georgelos, K., Williams, D. & Bertolini, D. (1997)

Morphological and structural characteristics of the proximal femur in human and rat. Bone 21: 261-267.

217. Soung, D. Y., Khalil, D. A., Arquitt, A. B., Smith, B. J., Hammond, L. J., Droke, E. A., Lucas, E. A., Devareddy, L. & Arjmandi, B. H. (2004) Soy isoflavones prevent the ovarian hormone deficiency-associated rise in leukocytes in rats. Phytomedicine. 11: 303-308.

218. Kuhn, G., Hardegg, W., Noack, S. & Trunk, H. (1991) Long-term effects of hysterectomy and bilateral oophorectomy on lymphoid tissue in female Lewis rats. Vet. Immunol. Immunopathol. 29: 353-363.

219. Yeni, Y. N., Hou, F. J., Vashishth, D. & Fyhrie, D. P. (2001) Trabecular shear stress in human vertebral cancellous bone: intra- and inter-individual variations. J. Biomech. 34: 1341-1346.

220. Be'ery-Lipperman, M. & Gefen, A. (2005) Contribution of muscular weakness to osteoporosis: computational and animal models. Clin. Biomech. (Bristol, Avon) 20: 984-997.

APPENDICES

APPENDIX A
INSTITUTIONAL ANIMAL CARE AND USE COMMITTEE PROTOCOL APPROVAL

OKLAHOMA STATE UNIVERSITY

OSU

College of Veterinary Medicine
Laboratory Animal Resources Unit
Stillwater, Oklahoma 74078-2002
405-744-7631

Memorandum

DATE: February 3, 1998

TO: Dr. Andrea Arquitt
Nutritional Sciences

FROM: Dr. K. Vargas
IACUC Veterinarian

SUBJECT: Protocol Approval

Your protocol, #709, entitled "Effects of Iron on Bone in Growing and in Mature Rats", has been approved for 108 rats by the Institutional Animal Care and Use Committee. The protocol is approved through January 31, 2001.

A modification must be submitted to the committee for approval prior to any changes in the protocol.

Institutional Assurance number A3722-01

OKLAHOMA STATE UNIVERSITY

OSU

College of Veterinary Medicine
Laboratory Animal Resources Unit
Stillwater, Oklahoma 74078-2002
405-744-7631

Memorandum

DATE: August 21, 1998

TO: Dr. Andrea Arquitt
Nutritional Sciences

FROM: Dr. Archie Clutter
IACUC Chairman

SUBJECT: Modification Approval

The modification to protocol, #709, entitled "Effects of Iron on Bone in Growing and in Mature Rats", for addition of 12 rats has been approved by the Institutional Animal Care and Use Committee.

dgm

APPENDIX B

PROCEDURES FOR MICRO-COMPUTED TOMOGRAPHY ANALYSES

APPENDIX B

PROCEDURES FOR MICRO-COMPUTED TOMOGRAPHY ANALYSES

Procedures for Bone Scanning

Fifth Lumbar Vertebrae

The previously cleaned fifth lumbar vertebrae were removed from-20^{o}C freezer and placed in a 20mm tube for scanning in micro-CT. The following procedure was used for scanning the bone using micro-CT. Use an appropriate sized tube based on the largest vertebrae. Use the same tube for all analyses.

1. Place five vertebrae in the tube aligning through the foramen using a toothpick to position the bone. Vertebral processes will be in the natural direction.
2. The empty space inside the tube should be covered with foam by wrapping the column of vertebrae in foam such that the vertebrae do not move within the tube during scanning.
3. Place vertebrae in the tube such that the interior facets are placed in the downward direction and the superior facet is lined up, to match the line on the tube. Place tube in micro-CT and close the door.
4. Scan bones using the computer connected to the micro-CT.
5. The monitor in the computer shows three screens: operator name/uct40, session's manager and dec term.
6. Register the operator name for the first time, using the operator name/uct40 screen. The same operator name can be used later while working with micro-CT

for scanning and analyzing the bones.

7. Enter sample name and number by clicking the first button in the operator name/uct40 screen. Save the data after entering the sample name. Note down the sample number and instrument number in a lab notebook.
8. Click the second button in the operator name/uct40 screen.
9. Enter the sample number of rat.
10. Click 'rat vertebrae L4 20mm'. Although a different vertebra may be analyzed the program name remains the same.
11. Click 'scout view' twice.
12. Click 'reference line'. Use shift for adjusting the region of reference line.
13. Place the reference line such that one vertebra in the tube was in between the two lines of the reference line. Then click on the image.
14. Click 'save scout' and then 'batch measurement'.
15. Press 'other' in the main screen and enter again the sample number for the next vertebrae scanning (measurement). Then repeat the procedure from step 12.
16. Complete selecting and saving scout of all vertebrae in the tube and then close the window so that the machine starts scanning.
17. For every 300 slices it takes approximately one hour 30 minutes to scan.
18. After completing the scanning the bones were analyzed for trabecular region

Distal Femur Metaphyses

The right femur was removed from -20^{o}C freezer and placed in a 16mm tube for scanning in micro-CT. Unlike vertebra, each femur was scanned separately. Both the metaphyses and cortical mid-diaphyses were measured separately while scanning.

1. Similar to vertebrae, the right femur should be placed vertically such that the line on the tube was aligned with the anterior side of the femur patellar surface at the bottom of the tube and neck of the femur at the top of the tube.
2. The empty space was covered with foam by wrapping the bone prior to insertion such that the femur does not move within the tube during scanning.
3. Enter the operator name in the operator name/uct40 screen.
4. Enter sample name and number by clicking the first button in the operator name/uct40 screen. Save the data after entering the sample name. Note down the sample number and instrument number in a lab notebook.
5. Click the second button in the operator name/uct40 screen.
6. Enter the sample number of rat.
7. Click rat femur 16mm.
8. Click scout view twice.
9. Click reference line. Use shift for adjusting the region of reference line.
10. Identify the distal growth plate.
11. Place the reference line such that the bottom line matches with the growth plate.
12. From the growth plate measure proximally 350 slices using reference line.
13. Click save scout and then batch measurement.
14. Now start the procedure for scanning mid-diaphyses.
15. If mid-cortical shaft analyses will be done, proceed to the next section before beginning analyses.

Femur Cortical Mid-diaphyses

Femur mid-diaphyses measurement should be taken on the same scout view that was used to measure distal femur metaphyses. The same sample number should be used. However, the machine automatically generates a different measurement number for mid-diaphyses.

1. Click reference line.
2. Calculate the length of the bone. Use reference line to the top end of the bone and note down the number.
3. Move the reference line to the bottom end of the scout view picture such that the bottom line of the reference line matches with lower end of the bone. Note down the number on bottom end of the bone.
4. Calculate the average of the top and bottom end of the bone. Note down all the values in a lab notebook.
5. Move the reference line to find the center of the bone based on the average number calculated.
6. Find the distance in millimeters for 17 slices by using the reference line.
7. Subtract the distance of 17 slices from the average number that was calculated and take the measurement at this number. (This enables to take the measurement exactly at the midpoint such that 17 slices would be above and 17 slices below the mid-point).
8. Using shift adjust reference line for 34 slices.

9. Click save scout and then batch measurement. Now close the window and the machine starts scanning for both metaphyseal and mid-diaphyseal region of right femur.
10. After completing the scanning the bones were analyzed for trabecular and cortical region of the metaphyseal and mid-diaphyseal region of the bone respectively.

Procedure for Bone Analyses

1. Go to the operator name/uct40 screen and click third button.
2. A small window will pop-up. Click the sample number of the bone in the sample column.
3. Select the measurement number on the right hand side of the screen based on the type of bone that needs to be analyzed. (For example: trabecular or cortical bone needs to be selected while analyzing femur bone). This step allows opening a window that shows the images of the bone scanned.
4. Click on the first image and then go to the task bar to select zoom. Click zoom 2x or 3x. This step allows magnifying the first image that was selected previously.
5. Identify the growth plate and start contouring the slices as described below for each bone separately.

Fifth Lumbar Vertebrae Analyses

1. The trabecular region was analyzed by identifying the growth plate from both the cranial and caudal regions.
2. The analyses were done starting from the cranial to the caudal region of the growth plates.

3. The start slice was taken as growth plate plus 25 slices from the cranial region and stop slice was taken as growth plate minus 25 slices from the caudal region.
4. Beginning from the start slice to every 15th slice, the slices were contoured. The slices between the first and each 15th slice were morphed in a semi-automated fashion.
5. Contour (draw a line) the first slice in anti-clock wise direction with the help of the mouse such that all the trabecular area was included. Care should be taken that no cortical bone was included while analyzing for trabecular region.
6. After contouring the first slice, click on to go to the 15th slice and repeat contouring similar to the first slice.
7. Select range and morph on the small window located on the right hand bottom corner.
8. Repeat the procedure for every 15th slices and click morph for every 15th slice.
9. After contouring the stop slice click cancel on the small window located on the right hand bottom corner. Then select click evaluation 3D, select default VOI and then click start evaluation. (The machine will automatically evaluate the trabecular region of the bone and generates the print out. Save these printouts in a folder).
10. Go to file, click exit and start again with new sample analyses.

Distal Femur Metaphyses Anlayses

1. The trabecular region was analyzed by identifying the growth plate.
2. Contours were then placed in a semi-automated fashion to produce a trabecular core.

3. The metaphyseal trabecular region was analyzed by identifying the growth plate from the distal part of the femur and included all distal trabecular bone.
4. The start slice was taken as the 25th slice proximal to the distal femur growth plate.
5. The stop slice was taken as the distal growth plate plus 150 slices towards the proximal femur.
6. Analyses of the distal femur trabecular region were performed from the start slice to the stop slice.
7. The procedure from step five in vertebra analysis was followed to analyze the distal femur trabecular region.
8. The trabecular region was prepared for analysis by drawing contours for the first slice and every 15 slices to produce a trabecular core.
9. The slices between the first and the15th slice were morphed in a semi-automated fashion.

Cortical Mid-diaphyses Analyses

1. Before starting for the cortical mid-diaphyses analyses, go to the "dec term" screen.
2. Type in decterm, "eval_Midshaft."
3. This step allows a small window to pop-up in which the sample number and measurement number should be selected.
4. Click on the third slice for cortical mid-diaphyses analyses.
5. Contour the outer edge of the slice selected using mouse in anti-clock wise selection.

6. Again contour the inner part of the bone in clock-wise direction.
7. Care should be taken that all the cortical bone is included.
8. Select the 32nd slice. Contour the slice similar to the third slice.
9. After contouring the third and 32nd slice click on "contouring" on the small window located on the right hand bottom corner.
10. Click on "range."
11. Click on "iterate backwards."
12. Once the iteration is complete, click "cancel."
13. Click on "evaluation 3D"
14. Click on "start evaluation."
    a. The machine will automatically evaluate the cortical region of the bone and generates the print out.
    b. Save these printouts in a folder.
    c. Check the print outs for the symbol "~" in front of the values reported. This symbol indicates that only cortical region was evaluated by machine.
15. Go to file, click exit and start again with new sample analyses.

Data Generation

1. Go to dec term
2. Type "uct_list"
3. Press enter key
4. Enter measurement number from '_____'(The measurement number of the sample whichever is the first one in the analyses need to be entered).

5. Press enter key
6. Enter measurement number to '_____'(The measurement number of the sample whichever is the first one in the analyses need to be entered).
7. Press enter key.
8. The machine will start processing the measurement numbers for data generation.
9. Once the symbol '$' is generated, go to the normal computer that has WSFTP/Smart FTP program for micro-CT data.
10. Open the micro-CT scratch file using WSFTP/Smart FTP program and save the data. (The data generated will be saved in a note pad by default).
11. Import the data from notepad into an excel sheet.
12. Save data in the excel sheet.

APPENDIX C

PROCEDURES FOR FINITE ELEMENT ANALYSES

APPENDIX C

PROCEDURES FOR FINITE ELEMENT ANALYSES

Fifth Lumbar Vertebrae and Distal Femur Metaphyses

The trabecular region of both lumbar vertebrae and distal femur metaphyses were used to assess the bone mechanical properties using finite element models generated through micro-CT. The following procedures were adopted for generating the data through FE models.

1. Analyze the trabecular region of the bone.
2. Go to the sessions manager screen and click views.
3. Click micro-CT data.
4. Search instrument number of the sample that needs to be analyzed for FEM
5. Highlight the latest "seg aim" file on the sessions manager screen.
6. Go to the dec term screen and type "fem " (Type one 'space' after fem)
7. Right click the mouse in the dec term to paste the "seg aim" file
8. Press enter key.
9. Note down the entry number in the lab book.

This procedure enables the machine to generate the FEM data. Approximately it takes one day to complete the data generation for one bone. To check if the FEM is completed the following procedure should be followed.

10. Go to dec term
11. Type "que" and then press "enter" key

12. Check if the “que” generated has the entry number. If the number is not found then the FEM is completed.

    After the FEM is completed, the FEM data should be saved. The following procedure should be used to save the FEM data.

13. Go the screen sessions manager.
14. Click views.
15. Click micro-CT
16. Search for instrument number and then sample number
17. Double click the file post list (This step allows one to see the data generated in a separate window. This data should be saved as a text file. The procedure is as follows).
18. In the window, click on edit. Click “select all.”
19. Again click on edit. Click “copy.”
20. Go to file and click exit.
21. Now go to the screen sessions manager and click on the button “applications.” Select note pad (This step allows one to paste the data copied from the window).
22. In the note pad, click on “file” and select “save as.” This step generates a small window. Delete the existing file in this small window. Do not close the window.
23. After deleting the existing file go to sessions manager, click on views, click on “micro-CT scratch.” Highlight the file name on the task bar and paste this file on the small window generated from the notepad (step 22). Next to the copied file type the study name and rat number. Click “ok” and close the note pad.

24. The file will be saved in scratch file of micro-CT. Using the WS FTP/Smart FTP program, the data from the micro-CT scratch can be imported. Print data from the scratch file and calculate all the strength parameters.

The following parameters are generated for the assessment of mechanical properties of bone. All these parameters should be inserted into excel sheet for automatic calculation of values. However, the data from the micro-CT pint outs should be manually entered into the excel sheet.

1. X dimension = generated from the machine
2. Y Dimension = generated from the machine
3. Z Dimension = generated from the machine
4. Voxel Size = generated from the machine
5. Total Voxels = generated from the machine
6. Total Elements = generated from the machine
7. Voxel Volume = generated from the machine
8. Number of Nodes = generated from the machine
9. Average strain = generated from the machine, correct entry for exponent
10. Apparent strain = generated from the machine
11. Average/Apparent Stress Ratio = calculated

    = Average strain/apparent strain

12. Displacement, mm (100%) = generated from the machine
13. Total Force, N = generated from the machine, correct entry for exponent
14. Extrinsic Stiffness, N/m = calculated

    = (Total force/displacement) x 1000

15. Physiological Force, N = calculated

= (Total force x 0.003)

16. Trabecular Core Volume, mm^3 = data taken from micro-CT print outs

17. Trabecular core height, mm = z dimension x voxel size

18. Average Cross Section Area, mm^2 = calculated

= Trabecular core volume/ Trabecular core height

19. Intrinsic stiffness, N/mm^2 or Size Independent Stiffness = calculated

= Total force/ Average cross sectional area

20. Average Von Mises Stresses = generated from the machine, correct entry for exponent

21. Von Mises Stresses, Standard Deviation = generated from the machine, correct entry for exponent

22. Minimum Von Mises = generated from the machine, correct entry for exponent

23. Maximum Von Mises = generated from the machine, correct entry for exponent

24. Skewness = generated from the machine, correct entry for exponent.

25. Curtosis = = generated from the machine, correct entry for exponent

26. Force Adjustment Constant = calculated

= (Lowest total force, a constant/ total force for each bone) ÷ 100

The constant is determined by taking the lowest mean value for the total force within the treatment group.

27. Corrected Von Mises Stresses, Average = calculated

= Force adjustment constant x Von Mises stresses for each bone

VITA

Kavitha Sankavaram

Candidate for the Degree of

Master of Science

Thesis: EFFECTS OF IRON ON BONE MICRO-ARCHITECTURE AND STRENGTH IN FEMALE RATS DURING RAPID GROWTH AND FOLLOWING OVARIECTOMY

Major Field: Nutritional Sciences

Biographical:

Personal Data: Born in Tirupathi, Andhra Pradesh, India, on January 1, 1977, the daughter of Mr. S.M. Shankar and Mrs. S. Krishnaveni

Education: Graduated from Rayalseema High School, Tirupathi, India in April 1994; received Bachelor of Science degree from Acharya N. G. Ranga Agriculture University, Bapatla, India in September 1998; Received Master of Science from S. V. University, Tirupathi, India in April 2001. Completed the requirements for the Master of Science degree with a major in Nutritional Sciences at Oklahoma State University in December 2005.

Experience: Employed by S. V. University, Department of Home Science, Tirupathi, India as graduate teaching assistant, June 2000 to March 2001, Worked as Project Co-coordinator, Community Development Society, Pulivendla, India, May 2001 to May 2002. Employed by S. V. University, Department of Home Science, Tirupathi, India as graduate teaching assistant, June 2002 to December 2002 Employed by S. V. University, Department of Home Science, Tirupathi, India as graduate teaching assistant, Jan 2003 to June 2003. Employed by Oklahoma State University, Department of Nutritional Sciences as a graduate research assistant, August 2003 to December 2005.

Professional Memberships:

Member, National Service Scheme of India
Secretary, Home science Association, S. V. University, Tirupathi, India, 1999 to 2000.
Vice-President, Home Science Association, S. V. University, Tirupathi, India, 2000 to 2001.
Member, Group Study Exchange (GSE) Team, Rotary International Dist. 3160, India, 2002 to 2003
Federation of American Societies of Experimental Biology

Awards and Honors:

Recipient of Dorothy M. Pearson Gold Medal, S. V.University, Tirupathi, India, 2001.

Recipient of Silver Jubilee Gold Medal, S.V. University, Tirupathi India, 2001

Recipient of Certificate of Commendation for Pulse Polio Immunization Drive

Name: Kavitha Sankavaram Date of Degree: December, 2005

Institution: Oklahoma State University Location: Stillwater, Oklahoma

Title of Study: EFFECTS OF IRON ON BONE STRENGTH AND MICRO-ARCHITECTURE IN FEMALE RATS DURING RAPID GROWTH AND FOLLOWING OVARIECTOMY

Pages in Study: 161 Candidate for the Degree of Master of Science

Major Field: Nutritional Sciences

Scope and Method of Study: This study investigated the effects of varying levels of dietary iron on bone micro-architecture and strength of female rats. Weanling rats were fed with one of three levels of dietary iron: 6 ppm, 35 ppm or 150 ppm. At 18 weeks of age growing rats were killed and bones were collected. Ovariectomy was performed to mimic menopause or sham-operated as controls at 18 weeks in the other two groups. After 30 weeks of age both sham-operated and ovariectomized rats were killed and bones were collected. Right femur and fifth lumbar (L_5) vertebrae were used for analyzing the bone micro-architecture and strength using micro-computed tomography (μCT-40, SCANCO MEDICAL AG, Zurich, SW).

Findings: Iron deficiency significantly decreased L_5 architecture (Tb.N, Tb.Sp) and strength (Phy_fce, Strain, Stiffness, SIS) and increased Von Mises in growing rats. Femur architecture indicated by degree of anisotropy (DA) but not strength was affected by diet. Sham L_5 architecture (BV.TV, Tb.N) was significantly greater and DA was lower indicating better quality bone than in OVX. A diet x treatment interaction was found for connectivity density with greater density in the 150 ppm sham rats. Shams had significantly greater L_5 strength (Phy_fce, Strain, Stiffness, SIS) with a diet x treatment interaction for Von Mises (35 ppm OVX greater than all others and 150 ppm OVX less than 6 and 35 ppm sham and OVX). No diet, treatment or interactions were found in any group in femur mid-shaft cortical architecture. Our findings suggest that dietary iron affects bone micro-architecture and strength in low iron fed growing animals but not in sham and OVX. The diet by treatment interactions suggests that high iron may be detrimental to some. However, it was not clear what levels of iron when combined with estrogen deficiency would be detrimental with aging. Our findings also suggest that the effect of iron changes with skeletal site since we found significant effects in lumbar bone but not on distal femur or midshaft.

ADVISER'S APPROVAL: Andrea B Arquitt